REINFORCED SOIL STRUCTURES

Volume II. Summary of Research and Systems Information

FACING PANEL

REINFORCEMENT

REINFORCED SOIL STRUCTURES

VOLUME II. SUMMARY OF RESEARCH AND SYSTEMS INFORMATION

BY

BARRY R. CHRISTOPHER
SAFDAR A. GILL
JEAN-PIERRE GIROUD
ILAN JURAN
JAMES K. MITCHELL
FRANCOIS SCHLOSSER
JOHN DUNNICLIFF

PREPARED FOR

Federal Highway Administration
Office of Engineering and Highway Operations
Research and Development
McLean, Virginia

BY

STS CONSULTANTS, LTD.
NORTHBROOK, ILLINOIS

1. REPORT NO. FHWA-RD-89-043	2. GOVERNMENT ACCESSION NO.	3. RECIPIENT'S CATALOG NO.
4. TITLE AND SUBTITLE REINFORCED SOIL STRUCTURES VOLUME II. SUMMARY OF RESERACH AND SYSTEMS INFORMATION		5. REPORT DATE November, 1989
		6. PERFORMING ORGANIZATION CODE
7. AUTHOR(S) Barry R. Christopher, Safdar Gill, Jean-Pierre Giroud, Ilan Juran, James K. Mitchell, Francois Schlosser and John Dunnicliff		8. PERFORMING ORGANIZATION REPORT NO.
9. PERFORMING ORGANIZATION NAME AND ADDRESS STS Consultants, Ltd. 111 Pfingsten Road Northbrook, Illinois 60062		10. WORK UNIT NO. NCP3E3b0022
		11. CONTRACT OR GRANT NO. DTFH61-84-C-00073
12. SPONSORING AGENCY NAME AND ADDRESS Office of Engineering and Highway Operations R&D Federal Highway Administration 6300 Georgetown Ave. McLean, Virginia 22101-2296		13. TYPE OF REPORT & PERIOD COVERED Final Report (9/84 through 10/88)
		14. SPONSORING AGENCY CODE

15. SUPPLEMENTARY NOTES

FHWA Contract Manager (COTR): A. F. DiMillio (HNR-30)
FHWA Technical Consultant: J.A. DiMaggio (HNG-31)

16. ABSTRACT
Volume II was essentially prepared as an Appendix of supporting information for Volume I.
This volume contains much of the supporting theory and a summary of the research used to
verify the design approach contained in Volume I, as well as general information
concerning proprietary reinforced soil systems. The information provided in this volume
is not required for design evaluation and as such Volume I can stand alone.

The basis for this volume was the NCHRP 290 report on "REINFORCEMENT OF EARTH
SLOPES AND EMBANKMENT" (Mitchell and Villet, 1987) and the research program performed
as part of the contract to develop the design guidelines contained in Volume I.
A summary of that research program is contained in the Introduction section of this
volume.

17. KEY WORDS Abutments, Construction, Design, Embankment, Instrumentation, Nailing, Reinforcement, Slopes, Soil Specifications, Stabilization, Walls	18. DISTRIBUTION STATEMENT No restrictions. This document is available to the public through the National Technical Information Service, Springfield, Virginia 22161		
19. SECURITY CLASSIF. Unclassified	20. SECURITY CLASSIF. Unclassified	21. NO. OF PAGES 158	22. PRICE

REINFORCED SOIL STRUCTURES
VOLUME II. SUMMARY OF RESEARCH AND SYSTEMS INFORMATION

TABLE OF CONTENTS

LIST OF FIGURES

LIST OF TABLES

INTRODUCTION

1.0 SCOPE AND ORGANIZATION

This volume of the Reinforced Soil Structures manual provides supporting information for the different types of soil reinforcement systems and the design approaches contained in volume I, Design and Construction Guidelines. Following a review of the contents of volume II, a brief summary of the research performed and primary conclusions will be provided. The remaining sections were prepared to coincide with the chapters in volume I for ease of reference. The Description of Systems section, which follows the Introduction section, provides additional information on the specific reinforced soil systems reviewed in chapter 1 of volume I. The next section, Pullout Resistance Evaluation, provides supporting information for determining pullout design parameters for specific reinforcement types using both empirical relations and pullout test results. The final three sections provide support information used to develop the design guidelines for the different reinforced soil systems, reinforced fill walls, reinforced engineered slopes and soil nailing for in-situ reinforcement, respectively.

2.0 SUMMARY OF RESEARCH

The "Behavior of Reinforced Soil" project sponsored by the Federal Highway Administration was performed to develop comprehensive guidelines for evaluating and using soil reinforcement techniques in the construction of retaining walls, cut slopes, and roadway embankments. The work encompassed a literature review, laboratory tests, full scale field tests, analytical evaluation, confirmation of design parameters and equations, and the preparation of construction procedures and practices.

The lab phase of the study included measuring reinforcement variables and stress distribution patterns, determining the types of materials suitable for soil reinforcement and developing the standard lab test procedures for obtaining the design parameters. This task was carried out by centrifuge tests at the University of California, Davis, reduced scale model tests at Ecole Nationale de Pont et Chaussees, France, and pullout, direct shear, and triaxial methods for evaluation of design parameters at STS Consultants, Ltd.

Centrifuge tests on small reinforced soil models using scaled down reinforcements based on similitude requirements were carried out to study the behavior of reinforced soil walls as it is affected by such factors as reinforcement extensibility, external loading, full height facing panels, and foundation compressibility. From centrifuge tests on 47 small models, it was learned that the behavior of walls reinforced with a wide variety of materials, both extensible and inextensible, is

similar at failure, and prior conventional design methods may be overly conservative.

Reduced scale model tests were performed on model reinforcements representing metal strips, plastic strips, plastic grids, woven and nonwoven geotextiles and anchors. The models were constructed using a step by step method similar to actual wall construction. Models were constructed to heights necessary to fail internally be breakage or deformation to qualitatively evaluate failure conditions. Some of the models were instrumented to evaluate the distribution of stress. The model test results were used to evaluate the location of the failure surface and the magnitude of lateral deformation for reinforcements of different extensibility and surface characteristics. The results indicated that only very extensible materials such as nonwoven geotextiles and highly deformable plastic truly acted as extensible reinforcement modeled by a Rankine stress distribution. All other "extensible" materials, woven geotextiles, plastic grids, and high tenacity plastic strips were found to behave more like inextensible reinforcement which is similar to the findings of the small scale centrifuge test program.

Pullout tests were conducted to evaluate soil reinforcement interaction for various types of reinforcement under varying normal load and soil conditions. Based on a literature review and tests in a small pullout box on model reinforcement, a relatively large (4.4 ft x 2.3 ft x 1.5 ft) pullout box was developed which significantly reduced some of the boundary influences of previous devices. Consistent test procedures were also developed that were subsequently used as a model to prepare an ASTM standard for pullout testing. The procedures were used to evaluate 12 different reinforcement materials, including metal and fiber strips, bar mats, wire mesh (both welded and woven), extruded and welded geogrids, slit film and coarse woven geotextiles and needle punches and heat bonded nonwoven geotextiles. Tests were also performed on epoxy coated reinforcement to evaluate the influence of epoxy on pullout resistance. Iterative strain measurements were made along the length of extensible reinforcement to evaluate in soil strain response and stress transfer. The results were used to develop more consistent pullout evaluation procedures for the various types of reinforcement, as was presented in chapter 2 of volume I. The approach uses a single pullout coefficient F* and a geometric factor α to evaluate pullout for any type of reinforcement. The procedures allow for continual updating of the interpretive procedures for the pullout factors as more data is developed without modifying the design approach. The determination of F* and α will be covered in detail in the Pullout Resistance Evaluation section of this volume.

Full scale field tests were constructed and monitored by STS Consultants, Ltd. The field tests include construction and monitoring of eight walls, each 35 ft long and 20 ft long and 20

ft high, and four slopes, 50 ft wide and 25 ft high. The field instrumentation program was developed to evaluate important internal stability design parameters. These include locating maximum stresses in the reinforcement, lateral stress distribution, lateral movement of the faces during and after construction, stress distribution from surcharge and footing loads, and stress relaxation. Inclinometers were installed in the active zone of all slopes and walls. The base was also optically surveyed. Stress in the reinforcement was evaluated through bonding resistant strain gages mounted on the reinforcement. Two pullout tests were also performed on each wall.

The field wall results are discussed in detail in the Reinforced Fill Wall section of this volume. In summary, they indicated that all reinforcement when designed using a unified approach behave in a similar predictable manner. When the density of reinforcement (amount of reinforcement per area of the reinforced section) is similar, the principal difference in performance can be attributed to the extensibility of the reinforcement. The construction of a wall to failure using the same design approach as was used for the other structures indicated the conservative nature of the current design procedures. Existing design methods for reinforced embankment slopes were similarly found to be conservative. However, all things considered, variability in construction procedures, fill and backfill, foundation material and construction control would suggest only moderate changes in current design procedures at this time. Rather, this information should be used to improve design consistency.

Five large centrifuge models (1:12 scale factors) were tested to model the behavior of four of the full scale instrumented walls built as a part of the project.[62] Good agreement was obtained between reinforcement tensions developed in the centrifuge models and those in the prototypes. This agreement adds credibility to the centrifuge modeling technique for study of reinforced soil structure. The results showed that the maximum tensions developed in the reinforcements at working stress levels depend both on the reinforcement stiffness and the relative movement between the soil and reinforcement. Finite element analyses gave good predictions of the reinforcement tensions in the five different large model walls.

A discrete finite element program, SSCOMP, was used to conduct a parametric study of reinforced soil walls. The effects of variations in structure geometry, loading, foundation soil type, wall facing type, and soil compaction on internal stresses and deformations were determined. The computer program was used with some confidence, because it was successfully used to predict the stress in reinforcements of a number of full scale walls for which measured values were available and in a number of large centrifuge test models that were tested during another phase of this project.

3

The results of the finite element program are discussed in detail in the Reinforced Fill Wall section of this volume. Among the most significant findings from these analyses were that: (1) prior design methods may underpredict reinforcement tensions when there is significant compaction of the backfill during construction; (2) predictions by FEM and conventional analysis methods do not always give comparable results, especially for nonstandard wall conditions; and (3) wall face deformations can be significantly changed through variations in reinforcement length and spacing.

The results of the parametric study provided insights and understanding that were helpful in the development of the design method and recommendations presented in chapter 3, volume I.

In addition to the finite element method parametric study, a simplified analytical method was developed for estimating the lateral earth pressure coefficient in reinforced soil structures as a function of the reinforcement stiffness, the soil stiffness, and the shear transfer between the soil and the reinforcement.[1] Computer program SSCOMP was evaluated for prediction of stresses and deformations in reinforced soil structures when a more complete analysis is needed than can be obtained by using the simplified method.

The simplified analytical method successfully predicted the reinforcement tensions in eleven full scale reinforced soil walls and agreed with the results obtained using the finite element method. Good FEM predictions were made of the reinforcement tensions developed in the full scale instrumented walls built as part of the FHWA project. Predictions of deformations were less successful.

The final task was to use the research to verify and unify existing design methods and incorporate them into the Design and Construction Guidelines volume. As will be discussed in more detail in the Reinforced Fill Wall section of this manual, the research found that external design could be modified by inclining the thrust at the back of the wall, at least for inextensible reinforcement. Insufficient data was available to justify this approach for extensible reinforcement. This modification will allow for shorter base widths in the reinforced zone. For internal stability, a simplified approach was developed around the stiffness of the reinforced zone. The approach allows the influence of extensibility and density of reinforcement to be directly analyzed while decreasing the complexity of some of the previous models in terms of the distribution of stress in the reinforced zone. Finally, a first order approximation method of the anticipated lateral deformation in the wall was developed empirically based on the extensibility of the reinforcement and the reinforcement length to height ratio. A simple method with a good experimental base was not previously available. The proposed deformation response method

could later be theoretically improved by incorporating stiffness factor into the analysis. These procedures were incorporated into a step by step design approach.

As will be reviewed in the Reinforced Engineering Slope section of this volume, the research substantiated the use of a limit equilibrium approach for design of reinforced engineered slopes. A step by step method is given based on classical rotationally stability analysis with a chart procedure used for a rapid check of the results.

The information used to develop the method for evaluating nailed soil retaining structures contained in chapter 6 of volume I was developed in a separate FHWA project.[50] Comments and supporting information pertaining to the design recommendations in volume I are included in the Soil Nailing section of this volume.

CHAPTER 1

DESCRIPTION OF SYSTEMS

1.0 INTRODUCTION

Reinforced soil systems can be classified in three categories:
placed soil reinforced systems, in-situ reinforced systems, and
multianchored systems. Systems belonging to these categories are
described below in section 2, 3, and 4, respectively. Many of
the systems of reinforced soil walls are patented or proprietary.
Many companies provide a complete package of services including
design, preparation of plans and specifications for the structure
and supply of the manufactured wall components. They may also
provide erection assistance to the contractor during start up of
construction.

The various systems which are being offered have different
performance histories, and this sometimes creates difficult in
adequate technical evaluation. Methods for handling the matter
of specification and obtaining the most cost competitive and
technologically acceptable system are covered in the Manual.
Nevertheless, it should be recognized that some systems are more
suitable for low walls, and some are applicable for remote areas,
while others are more suited for urban areas with more rigid
requirements.

Brief descriptions of the various proprietary systems under each
category are included herein. Systems that are not discussed for
the reasons given in chapter 1 of Volume I are succinctly
described in section 5 devoted to alternative systems.

2.0 PLACED SOIL REINFORCED SYSTEMS

Reinforced fill structures embody three basic components, namely:
engineered fill, also called engineered fill (reinforced soil
volume, or backfill), reinforcement and facing elements which
prevent surface erosion and give an aesthetically pleasing face
(figure 1). There are a variety of systems marketed by different
specialty companies which use different types of reinforcements
and facing elements. In practically every case, a granular
material is used within the reinforced soil volume with little
variation in its specified quality or gradation. The mechanism
of stress transfer between the reinforcement and the backfill is
another variable in the different systems; for example, by
friction or by passive resistance or combinations thereof. Some
systems are similar in principle but different in reinforcement
materials used; for example, steel strips and plastic strips.
Descriptions of the presently available and commonly known
systems and materials are given below. Table 1 provides a
summary of the various systems.

Reinforced Soil Volume

Finished Grade

Facing

Random Backfill

Original Ground Surface

Limits of Construction Excavation

Levelling Pad or Footing

Reinforcing Strips
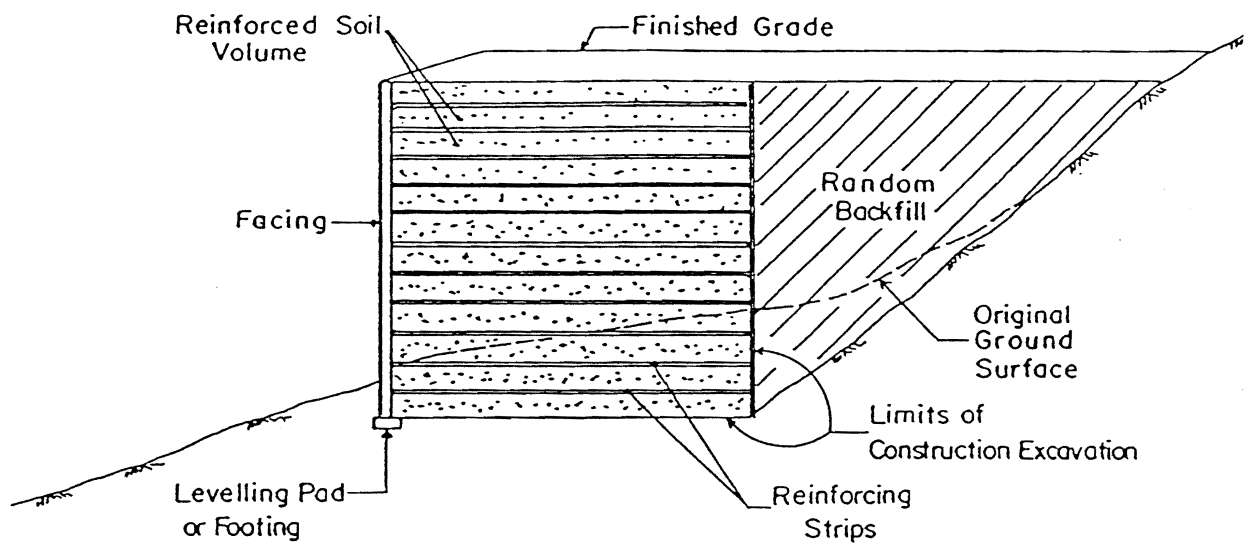
Figure 1. Principal elements of reinforced fill walls.

Table 1. Summary of reinforcement and face panel details for
various reinforced soil systems.

System Name	Reinforcement Detail	Typical Face Panel Detail[1]
Reinforced Earth: (The Reinforced Earth Company 1700 N. Moore St. Arlington, VA 22209-1960)	Galvanized Ribbed Steel Strips: 0.16 in (4 mm) thick; 2 in (50 mm) wide. Epoxy coated strips also	Facing panels are cruciform shaped precast concrete 4.9 ft x 4.9 ft x 5.5 in (1.5 m x 1.5 m x 14 cm). Half size panels used at top and bottom.
VSL Retained Earth (VSL Corporation, 101 Albright Way, Los Gatos, CA 95030)	Rectangular grid of W11 or W20 plain steel bars, 24 in x 6 in (61 cm x 15 cm) grid. Each mesh may have 4, 5 or 6 longitudinal bars. Epoxy coated meshes also available.	Precast concrete panel. Hexagon shaped, (59-1/2 in high, 68-3/8 in wide between apex points, 6.5 in thick (1.5 m x 1.75 m x 16.5 cm).
Mechanically Stabilized Embankment. (Dept. of Transportation, Div. of Engineering Services, 5900 Folsom Blvd., PO Box 19128 Sacramento, CA 95819).	Rectangular grid, nine 3/8 in (9.5 mm) diameter plain steel bars on 24 in x 6 in (61 cm x 15 cm) grid. Two bar mats per panel. (connected to the panel at four points).	Precast concrete; rectangular 12.5 ft (3.81 m) long, 2 ft (61 cm) high and 8 in (20 cm) thick.
Georgia Stabilized Embankment (Dept. of Transportation, State of Georgia, No. 2 Capitol Square Atlanta, GA 30334-1002) Arlington, VA 22209-1960	Rectangular grid of five 3/8 in diameter (9.5 mm) plain steel bars on 24 in x 6 in (61 cm x 15 cm) grid 4 bar mats per panel	Precast concrete panel; rectangular 6 ft (1.83 m) wide, 4 ft (1.22 m) high with offsets for interlocking.
Hilfiker Retaining Wall: (Hilfiker Retaining Walls, PO Drawer L Eureka, CA 95501)	Welded wire mesh, 2 in x 6 in grid (5 cm x 15 cm) of W4.5 x W3.5 (.24 in x .21 in diameter), W7 x W3.5 (.3 in x .21 in), W9.5 x W4 (.34 in x .23 in), and W12 x W5 (.39 in x .25 in) in 8 ft wide mats.	Welded wire mesh, wrap around with additional backing mat and 1.4 in (6.35 mm) wire screen at the soil face (with geotextile or shotcrete, if desired).
Reinforced Soil Embankment (The Hilfiker Company 3900 Broadway Eureka, CA 95501)	6 in x 24 in (15 cm x 61 cm) welded wire mesh: W9.5 to W20 - .34 in to .505 in (8.8 mm to 12.8 mm) diameter.	Precast concrete unit 12 ft 6 in (3.8 m) long, 2 ft (61 cm) high. Cast in place concrete facing also used.
Websol: (Soil Structures International, Ltd.) 58 Highgate High St. London N65HX England)	5.3 in (135 mm) wide Paraweb: made from high tenacity polyester fibers by Imperial Chemical Industries.	T-shaped precast concrete panel 34.4 sq. ft. (3.2 m²) area, 6.3 in (160 mm) thick.
York Method: (Transport and Road Research Laboratory, Crowthorne, Berkshire, England)	Galvanized mild steel or stainless steel or glass fiber reinforced plastic or Paraweb or Terram.	Hexagonal; glass fiber reinforced cement; 24 in (600 m) across the flat; 9 in (225 m) deep.
Anda Augmented Soils (Anda Augmented Soils Ltd. Oaklands House, Solarton Road, Farnborough Hants GU14 7QL England)	Fibretain straps (pultruded fiberglas reinforced plastic strip, developed by Pilkington Brothers, 1.6, 3.1 or 6.3 in wide, .08, 0.10 or .16 in thick (40, 80, or 160 mm wide 2, 2.5 or 4 mm thick).	Precast concrete crib units with 12 in (30 cm high) headers 4 ft (1.2 m) apart.
Tensar Geogrid System (The Tensar Corporation 1210 Citizens Parkway, Morrow, GA 30260)	Non-metallic polymeric grid mat made from high density polyethylene of polypropylene	Non-metallic polymeric grid mat (wrap around of the soil reinforcement grid with shotcrete finish, if desired), precast concrete units.
Miragrid System (Mirafi, Inc. PO Box 240967 Charlotte, NC 28224)	Non-metallic polymeric grid made of polyester multifilament yarns coated with latex acrylic.	Precast concrete units or grid wrap around soil.
Maccaferri Terramesh System (Maccaferri Gabions, Inc. 43A Governor Lane Blvd. Williamsport, MD 21795	Continuous sheets of galvanized double twisted woven wire mesh with PVC coating.	Rock filled gabion baskets laced to reinforcement.

[1]Many other facing types as compared to those listed, are possible with any specific system.

a.   Reinforced Earth

Reinforced Earth is a registered trademark of The Reinforced
Earth Company.

Reinforced Earth, which uses metal strip reinforcement, has been
by far the most widely used to date. The Reinforced Earth
Company is headquartered in the United States in Arlington,
Virginia and markets, designs and supports construction through
regional offices around the United States.

Facing panels for the early Reinforced Earth Walls consisted of
metallic half cylinders of a semielliptic section, fabricated
from galvanized steel sheets. A typical facing element had a
length of 33 ft (10 m), an effective height of 13.1 in (33.3 cm)
and a thickness of 0.12 in (3 mm). Each element weights 253 lb
(115 kilograms). Reinforcing strips are connected to the unit by
bolts passing through the strip and the interlocking
(overlapping) edges of the facing units. Shorter units and
specials are supplied to form corners and bends.

The metal facing unit has now been largely superseded by a
precast concrete unit which is cross shape (cruciform) in front
elevation (figures 2a and 2b). A standard unit weighs lighter
0.8 or 1.1 tons and is 4.9 ft (1.5 m) wide 4.9 ft (1.5 m) high
with total thickness of 7.1 in (18 cm) or 5.5 in (14 cm). All
edges of the unit are rebated to prevent any straight through
joints. These rebates also facilitate visual alignment of the
units during construction. A further aid to alignment is in the
form of a dowel bar extending from the upper and lower edges of
one arm of the cross element. These dowels are also used as
pivot points for the construction of curved walls. A
compressible material is placed in horizontal joints between the
panels and it allows vertical deformation. Each panel contains
lifting anchors to facilitate handling and placing.

Each unit is furnished with embedded connector tables, called tie
strips, cast in place during manufacture. These tie strips which
are usually 2.5 ft (0.75 m) apart horizontally and 2.5 ft (0.75
m)(connection with the steel strip reinforcement. Other special
types of panels which are used to obtain desired overall geometry
are also available. These include half panels for use at the
base and special panels with varying heights in 8 in (20 cm)
increments for use at the top of the wall to give an upper line
of the facing any desired inclination. Angle elements for
changes in directions are also available.

(a)

2nd course of
full-panels

1st course of
half-panels

1st course of
full-panels

(b)

TIE STRIP

1 1/2"
MIN.

3 1/2"

1/2" Ø A325 BOLT

FRONT

BACK FACE
OF PANEL
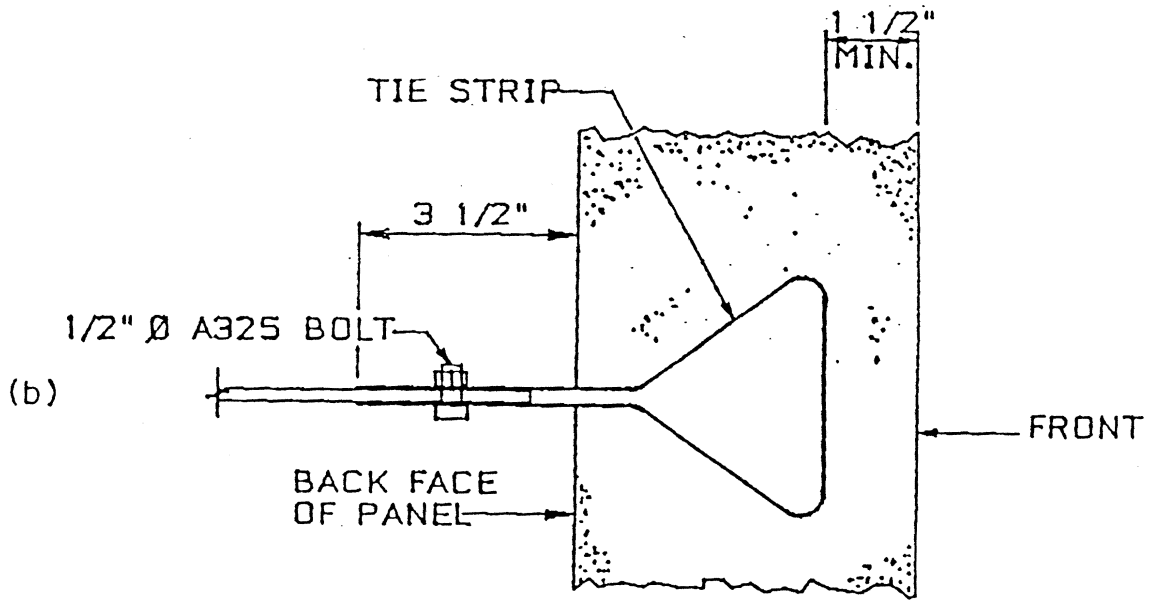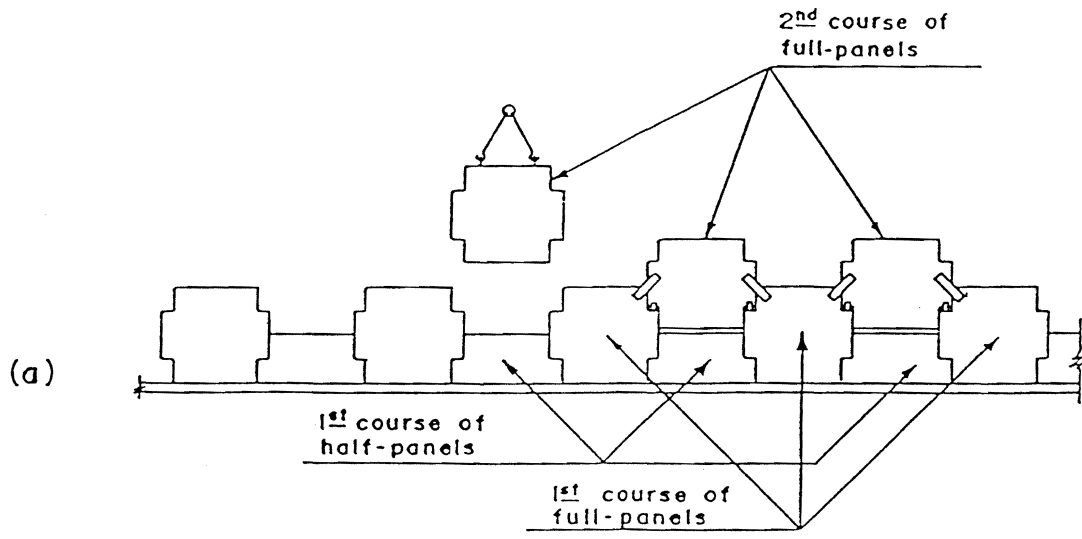
CONNECTION DETAIL
NO SCALE

Figure 2. Segmented facing panels used for
Reinforced Earth walls.

10

The reinforcement used in the Reinforced Earth walls is exclusively metal, usually galvanized steel strips. The strips are generally 0.157 in (4 mm) thick and 2 in (50 mm) in width. Until about 1975 plain strips were in common use. Now the surface of the strips is ribbed in order to improve the apparent friction. The ribbed strips are called "High Adherence Reinforcement." Epoxy coated ribs are also used.

A free draining, nonplastic soil fill is required for the Reinforced Earth structure in order to achieve the necessary interaction between the fill and the reinforcing strips. The following gradation limits are usually specified:

Particle Size	Percent Passing
6 in (250 mm)	100
3 in (76 mm)	100 - 75
No. 200 (75 μm)	15 max.

The Reinforced Earth system is subject to patents owned by its inventory, Henry Vidal. The Reinforced Earth Company of Arlington, Virginia is the exclusive licensee for this system in the United States.

b. Hilfiker Retaining Wall

This system, also called Welded Wire Wall (WWW) and Reinforced Soil Embankment (RSE) is manufactured and marketed by Hilfiker Retaining Walls of Eureka, California.

Welded Wire Wall (WWW) Description: This system employees a welded wire mesh grid within the backfill to serve as reinforcement for the soil. The face end of each mesh is bent upward to provide the facing and then attached to the facing of the next upper layer (figure 3). The mesh is fabricated to ASTM 185 Standards and is fabricated in 8 ft (2.44 m) wide mats of varying lengths and can be ordered according to project requirements. The mats are placed in alternating layers with compacted backfill to produce a composite structure. The thickness of compacted material between the reinforcing mats is generally 18 in (46 cm). The mats initially used were 9 gauge (W1.7) wire laid in 2 in by 6 in (5 cm x 15 cm) mesh oriented such that the wires spaced at 2 in (5 cm) are perpendicular to the wall face. (The W size is the area of the wire in hundreths of square inches, i.e., the area of W1.7 = 0.017 in^2). Presently, heavier wire mesh W4.5 x W3.5, W7 x W3.5, W9.5 x W4 and W12 x W5 is used for wall heights up to 51 ft (16 m). Vertical spacing between the reinforcing mesh is 18 in (46 cm) or 9 in (23 cm.). Backing mats are installed behind the bent up face portion of each reinforcing mat during construction. The backing mats which are made of 2 in x 6 in W1.7 x W1.7 welded wire mesh are oriented to reduce the openings between the mesh wire to serve as additional support for the 1/4 in (6.35 mm) wire screen or geotextile fabric, this serves as protection against

11

BACKING MAT · CAP · ROADWAY
PRONGLESS TRAY
SOIL FILL
FACE OF STANDARD TRAYS
GRAVEL FILL
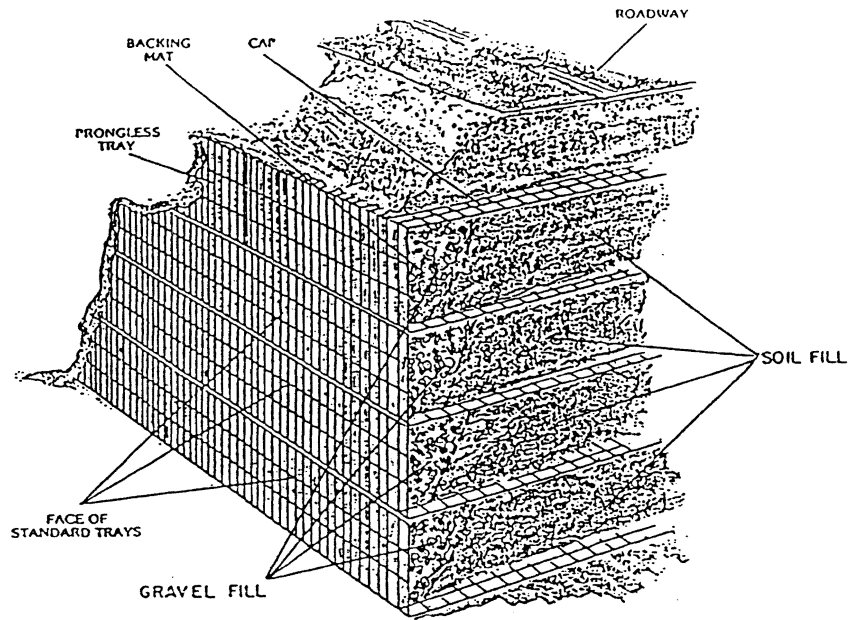
The Gridcote system is interlocking. A backing mat is attached to the tray facing for reinforcement, while a steel screen prevents the loss of backfill materials.

CAP
¼" MESH SCREEN
PRONGLESS TRAY
¼" MESH SCREEN
STANDARD TRAY
BACKING MAT

CAP
BACKING MAT
PRONGLESS TRAY
BACKING MAT
STANDARD TRAY
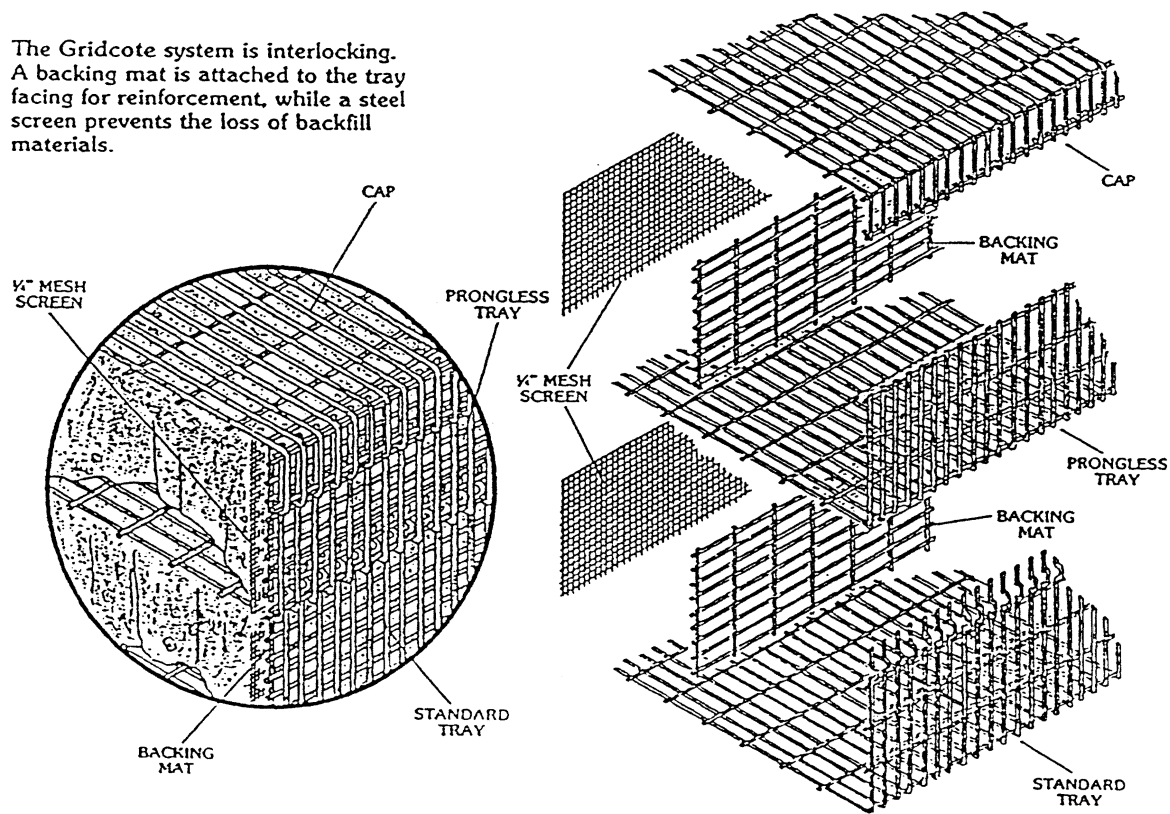
Figure 3. Hilfiker Welded Wire Wall system.

fallout of soil particles through the face. The durability is estimated using sacrificial steel.

Structure backfill for Welded Wire Wall is generally specified to be free from stones or lumps exceeding 6 in in greatest dimension, organic material, or other unsuitable material, as determined by the Engineer. In addition, backfill material shall have a "Plasticity Index" not exceeding 10, as determined by California Test 204.

This system is patented by Hilfiker Retaining Walls of Eureka, California. Patent #4,117,686, #4,329,089 and #4,505,621.

Reinforced Soil Embankment (RSE):

The RSE system, also developed by Hilfiker Retaining Walls of Eureka, California, uses either precast panels or a cast in place concrete face.

For the precast panel system, the reinforcement is in the form of heavy gauge welded wire mesh in a 6 in by 24 in (15 cm by 61 cm) grid with the 6 in (15 cm) spacing oriented perpendicular to the wall face. Vertical spacing between the reinforcing mats is 24 in (61 cm). Each reinforcing mat has a steel strip riveted to its head which fits into slots in the top and bottom of the prefabricated concrete facing panels to anchor the reinforcement to both the top and the bottom facing panels (figure 4). The RSE has a prefabricated leveling pad placed directly on the foundation to which the first layer of the wire mesh is attached. The wire sizes range from W9.5 (0.348 inch, 9 mm, diameter) to W20 (0.505 in, 13 mm, diameter). Fill requirements are the same as for the Welded Wire Wall.

The RSE system with precast panels is patented by Hilfiker Retaining Walls. Patent #243,697, #243,613, #4,260,296, #4,324,508 and #4,343,572.

The soil reinforcements for the cast in place system are similar to the RSE with panels. The mat is bent up to provide the vertical reinforcement for concrete face. A temporary face and geotextile fabric are used to hold the backfill until the wall facing is cast in place. Fill requirements are the same as for the Welded Wire Wall.

c.   VSL RETAINED EARTH System

The RETAINED EARTH system is a composite soil reinforcement system developed by VSL Corporation of Los Gatos, California. It employs welded wire mesh to reinforce soil placed as fill.

This system employs a hexagonal reinforced precast concrete facing panel 59 1/4 in (1.5 m) high and 68 3/8 in (1.75 m) wide between the apex points and 6.5 in (16.5 cm) thick (figure 5). Half panels are used at the bottom and top. Reinforcement of the soil is by welded wire mesh (bar mats), which consist of either

Facing Panel

Reinforcement

Precast Concrete
Facing Panel

Reinforcing
Welded Wire
Mesh
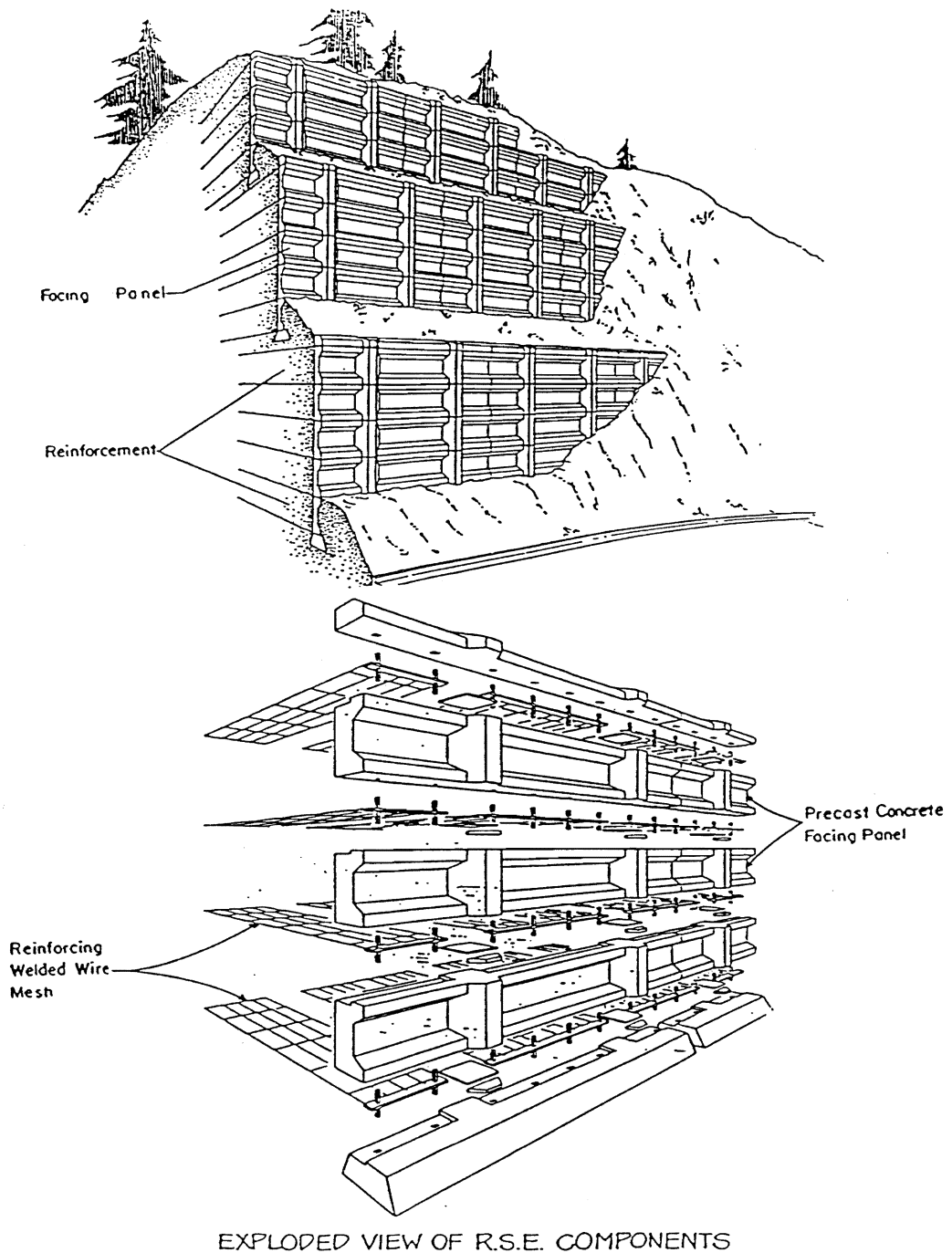
EXPLODED VIEW OF R.S.E. COMPONENTS

Figure 4. Hilfiker's Reinforced Soil Embankment Wall system.

14

FRONT VIEW

SCHEMATIC

Coping

Facing Panel

Reinforcing Mesh

Leveling Pad

Granular Backfill

68 3/8"

8 7/32 8 7/8 34 3/16" 8 7/8 8 7/32

14 5/8"

59 1/4"

30"

14 5/8"

SWIFT LIFT

5/8" DIA. BAR

1" DIA. HOLE 8" DEEP

TYPICAL PANEL
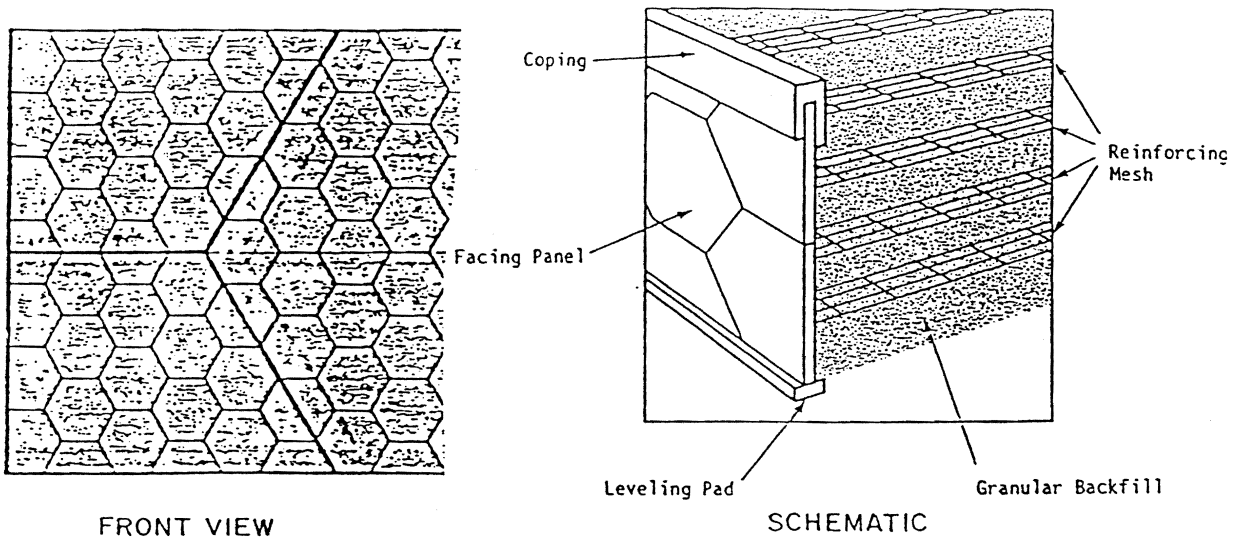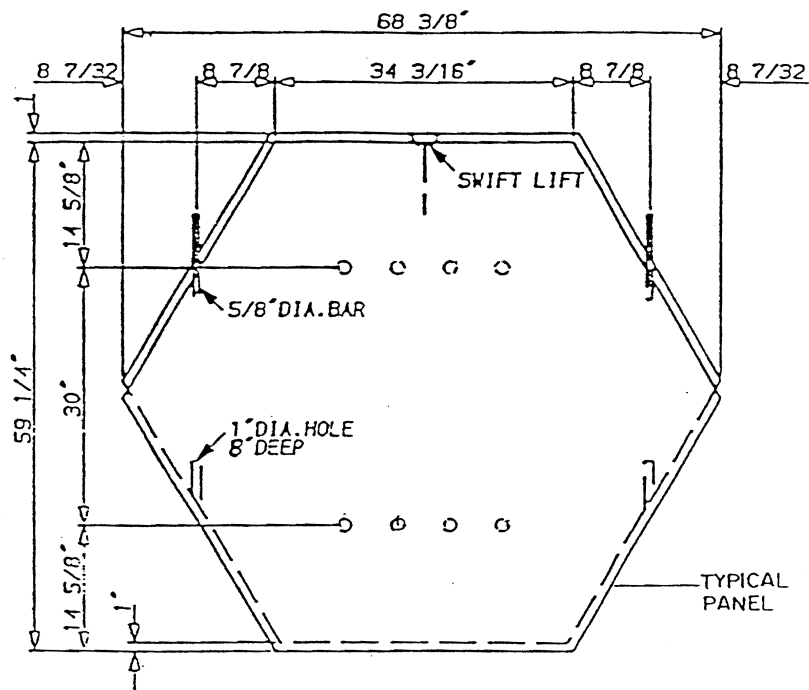
Figure 5. VSL RETAINED EARTH WALL system.

W11 or W20 plain steel bars placed in a rectangular grid with longitudinal and transverse bar spacings of 6 in (15 cm) and 24 in (61 cm), respectively. Each mesh may have 4, 5 or 6 longitudinal bars, depending on the design requirements. Epoxy coated meshes are also available. The overall length of the mats depends on the geometry of the site, external loading and physical properties of both the backfill and the earth to be retained.

The longitudinal elements of the bar mats are looped at one end which allows attachment to the concrete face panels by means of a metal rod slipped through the loop and loops embedded in the panel.

The VSL RETAINED EARTH system is licensed under a Reinforced Earth Company patent, although it has a patent of its own on the bottom head connection used to fasten the reinforcing mesh to the precast facing panel. The system is marketed in the United States by the VSL Corporation of Los Gatos, California.

   d.   Mechanically Stabilized Embankment (MSE)

This system was developed by the California Department of Transportation based on a series of tests performed in 1973-75 to determine pullout resistance of various arrangements of reinforcements. The first wall using this system was built near Dunsmuir, California in 1975.

The facing panels are precast concrete, rectangular in shape, 12.5 ft (3.81 m) long, 2 ft (61 cm) high, 8 in (20 cm) thick to the VSL system. Four bar mats can be connected to each panel. The mats have horizontal spacing of 75 in (1.91 m), center to center, and vertical spacing of 12 in (30 cm). Bar mats on this system are normally not galvanized. The bar mats are attached to the facing elements by insertion of the two bar yoke through precast holes in the facing panels. The prethreaded bars are bolted into positions and subsequently field epoxy coated to eliminate corrosion at the critical threaded sections (figure 6).

   e.   Georgia Stabilized Embankment (GASE)

The GASE system was developed by the Georgia Department of Transportation in its search for a nonproprietary and more competitive reinforced soil wall other than the ones offered by vendors of the several proprietary systems.

This system consists of a precast concrete faced wall stabilized with welded wire mesh. The wire mesh used is similar to the one described for the VSL RETAINED EARTH system. The facing panels are 6 ft (1.83 m) wide by 4 ft (1.22 m) high as shown in figure 7. Four reinforcement mats are attached to each panel, at two levels with horizontal center to center spacing of 2 ft 8 in (81 cm) and a vertical spacing of 24 in (61 cm).

A high quality granular backfill is used for the reinforced structure. Fill requirements conform to FHWA specifications.

Full Strecher —| |— Planter Blockout Top
Half Strecher —| Center of Each Panel

                                         |← 6'-3" →|← 6'-3" →|
                                    |←8"→|

2'-1/8"

2'-1/8"

                          └─ 1/2" Expansion Joint

Shear Key ─┐

                    ─ 1/2"X1'-8 1/2" Bolts

                 ↖ 6 1/2" to 8"
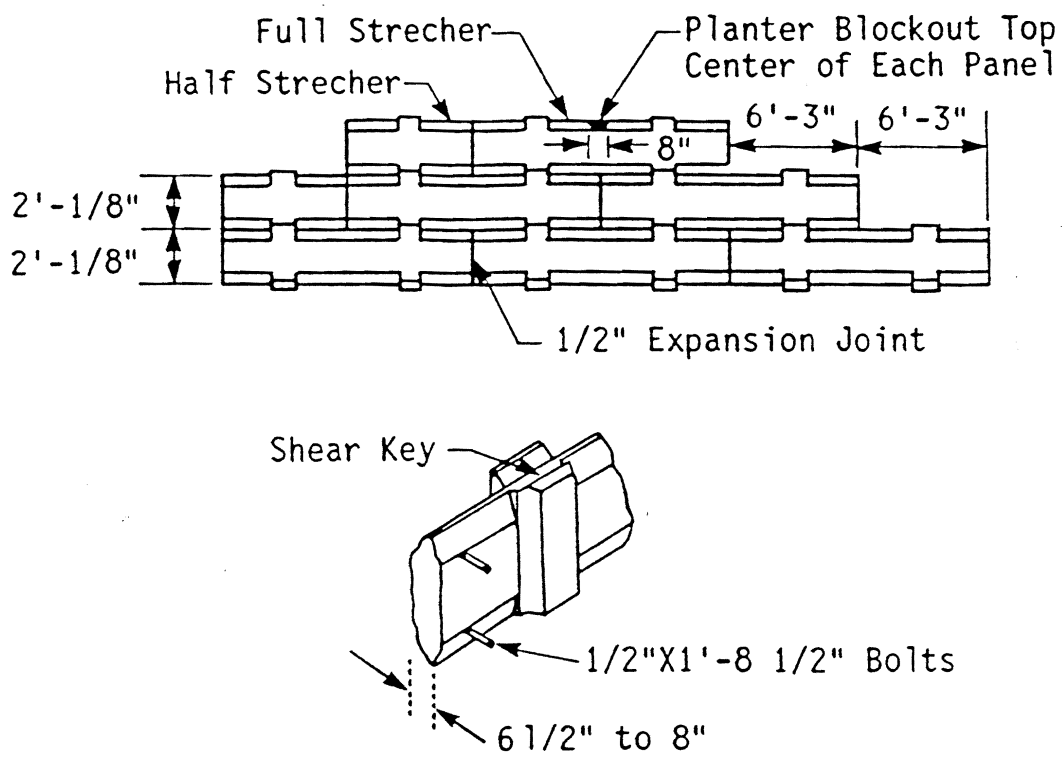
Figure 6.   Facing panels for mechanically stabilized
             embankment wall system.
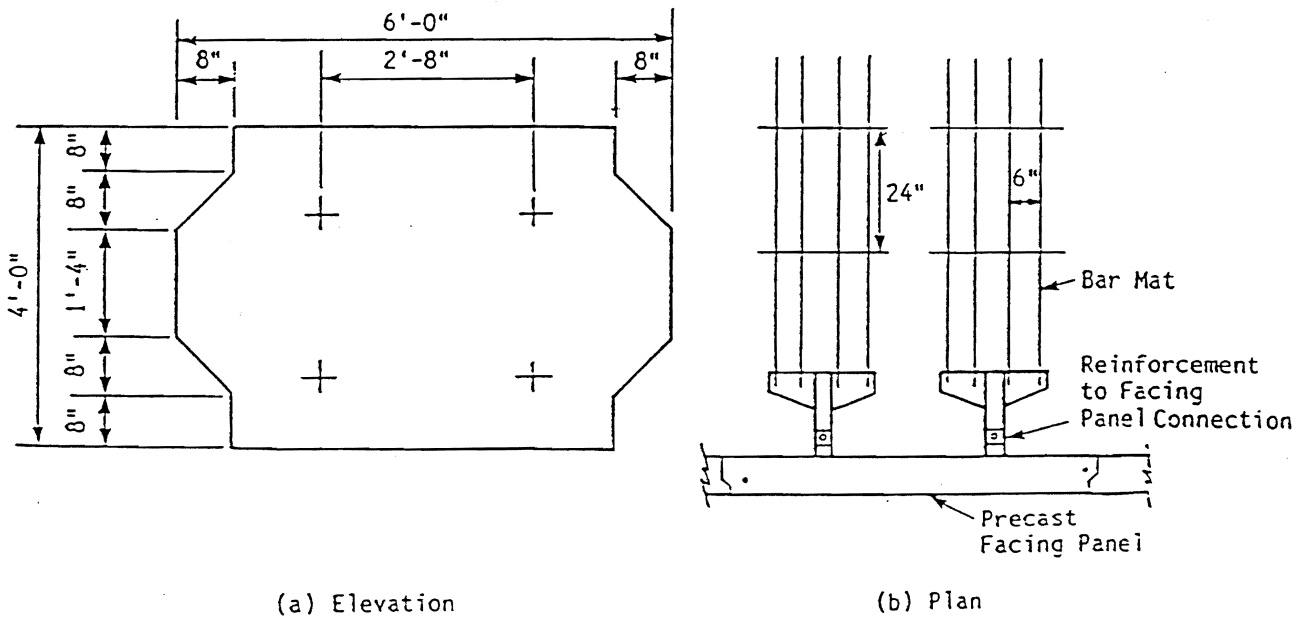
Figure 7. Georgia stablizied embankment facing panel
and reinforcement attachment.

The GASE system is also licensed under a Reinforced Earth Company patent.

f. "Websol" System

The "Websol" system was developed in 1977 by Soil Structures International Limited of the United Kingdom. The system, although superficially similar to other methods, has a number of important distinguishing features, the most important of which is that it uses a flexible synthetic corrosion resistant material.

The "Websol" system comprises a cladding of precast concrete facing units with stability being achieved through the interaction of the soil particles and the composite plastic frictional anchors and an anchor bar (figures 8 and 9).

The lateral pressures in the soil are contained by friction along the anchor ties and the bulkhead effect of the facing. The associated tension in the ties is anchored by friction and by the tail anchor bars in the zone remote from the face. The precast concrete facing units are 6.28 ft (2 m) wide by 5.25 ft (1.6 m) high and are normally 6.3 in (160 mm) thick. They are T-shaped in front elevation with a face area of 34.4 ft^2 (3.2 m^2). They are lightly reinforced with mesh.

The frictional anchors comprise a tendon made from high tenacity polyester fibers concentrated in ten separated bundles encased in a durable polyethylene sheath. The tendon material, which is called "Paraweb," was developed by Imperial Chemical Industries (ICI) and has been in use in a variety of adverse environments either in the flat form, or as a high strength rope under the name of "Parafil," for more than 20 years. The strength of the material is in the fibers whereas the sheath forms the size and shape of the anchor and provides protection to the polyester core yarns.

The frictional anchors are laid continuously in a zig zag pattern passing around the anchor bar at the rear of the structure (figure 8) and are connected to the panels by a simple loop and toggle bar arrangement. The continuity of the anchor elements in both plan directions helps to maintain the coherence of the anchored mass, particularly when subjected to differential settlement. The loop and toggle attachments are normally round reinforcing steel with their exposed parts coated in resilient plastic or a fusion bonded powder epoxy coating.

The system is certified for use in the United Kingdom on Government projects to have a service life of not less than 120 years.

Most on site fill materials may be used although fills with fines contents of more than 20 percent passing a No. 200 U.S. sieve (75 micron) sieve require particular care. There is no upper limit to the size of rock which may be used except that imposed by normal compaction requirements and by the depth between layers of frictional anchors. The resilient and flexible nature of the

PLAN VIEW

EUBIPLAST END SEALANT

PARAWEB STRIP (TOTAL OVERLAP. 6.6 ft.)

ALTERNATIVE POSITION OF CLAMP

6 in. MIN. OVERLAY TERRAM FABRIC

CLOSED CELL POLYETHYLENE FOAM FILLER

TERRAM FABRIC OVER ENTIRE LENGTH

ANCHOR BAR FOR TENSIONING (DIAMETER NOT LESS THAN 0.63 in.)

ATTACHMENT LOOP

ATTACHMENT BAR

STEEL PINS (DIAMETER NOT LESS THAN 0.63 in. AND LENGTH TO BE LESS THAN PARAWEB VERTICAL SPACING)

PRECAST CONCRETE FACING PANEL

EUBIPLAST END SEALANT

CLAMP

ALTERNATIVE POSITION OF CLAMP

6.6 ft.

15 ft.

TERRAM FABRIC 0.18 in. THICK

ELEVATION

ATTACHMENT LOOP

ATTACHMENT BAR

ANCHOR BARS

PRECAST PANELS

COMPACTED FILL

STEEL PINS

CONCRETE UPSTAND TO FOUNDATION (OPTIONAL)

CONCRETE STRIP FOUNDATION

PARAWEB STRIPS
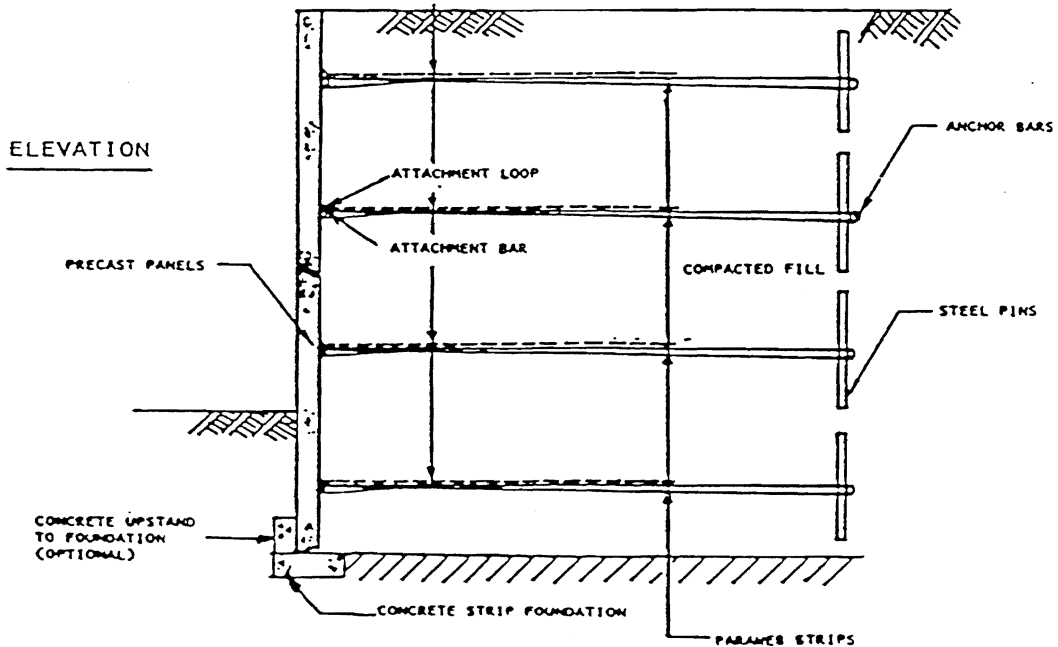
Figure 8.   The Websol system.

20

TYPICAL FACING UNIT
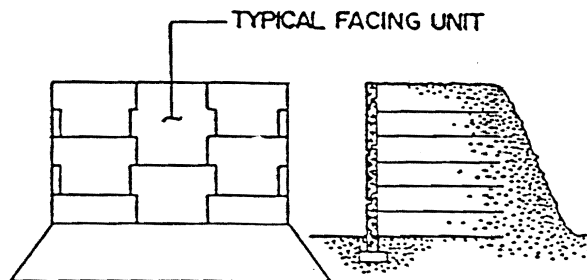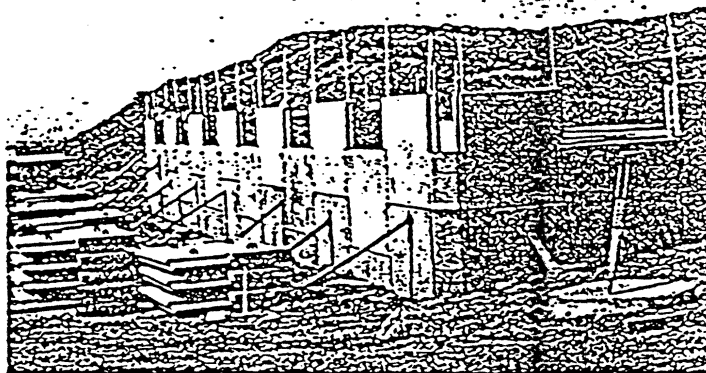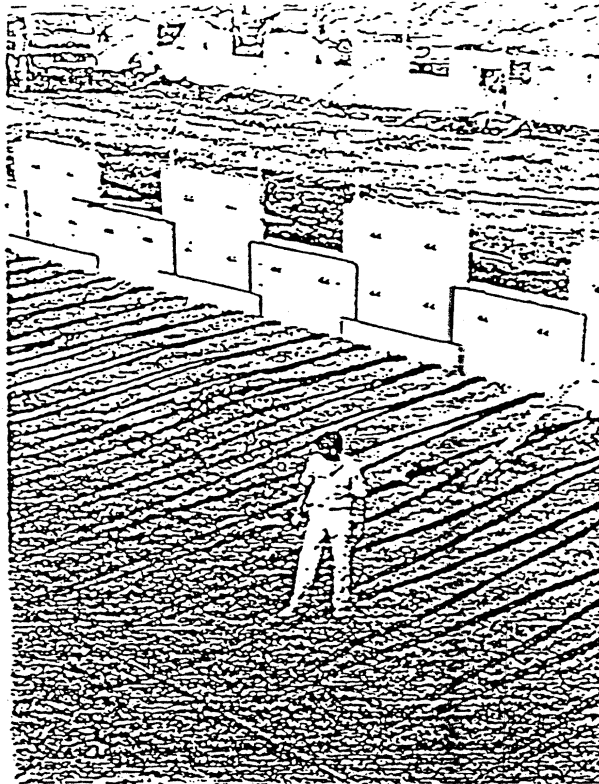
Figure 9.   Reinforcement and facing assembly for
the Websol system.

anchors permits them to follow the contours of most fills, however coarse or angular the particle are. In practice, fills which have been used to date range from fine desert sands to very coarse as blasted rock.

Several hundred Websol systems have been constructed to date. Patents on the system are owned by its developers, Soil Structures International Ltd., 58 Highgate High Street, London N6 5HX, England. The system was judged to infringe Vidal's U.K. patents nos. 1069361 and 1324686 in 1981 and cannot be used in countries where Vidal's patents are registered until these patents expire. Generally, this precludes use of the system in the United States until 1990.

g.   The York Method

This method was developed at the Department of Environment, United Kingdom in 1973, and so far its use has been limited to only two or three small government financed projects in that country. It uses the Vidal patent in every detail except it allows the inextensible reinforcing member a limited vertical movement during construction. It is really a connection method rather than a system as such. The York method has not been used for some years.

The York method most commonly uses a lightweight glass fiber reinforced cement facing unit weighing approximately 40 lb (14 kg). The units take the form of hexagon based pyramid, 9 in (225 mm) deep and 24 in (600 mm) across the flat. One pair of diametrically opposite flanges on each unit is drilled with large guide poles. These guide poles which serve as facing reinforcement are made up of short lengths of 1 3/8 in (35 mm) diameter PVC tube with spigot and socket connections (figure 10). In the finished wall, these pipes are reinforced with mild steel bars grouted in-situ to render the vertical pipe rigid.

The reinforcement is in the form of strips with drilled holes at one end which allows them to be threaded onto the vertical pole at the required vertical spacing. When any settlement occurs in the fill, the reinforcing strips slide on this vertical pole and alleviate any settlement induced stresses in the connection.

The facing units interlock with one another both vertically and horizontally. There is a compressible gasket between the facing units to accommodate irregularities in the units and to prevent leaking out of fill on to the face of the wall.

The reinforcing strips used with the facing panels consist of either galvanized mild steel, stainless steel or glass fiber reinforced plastic. However, the use of continuous lengths of Terrylene reinforced plastic strips (Paraweb) or unidirectional fabric reinforcement (Terram) can be accommodated easily.

22
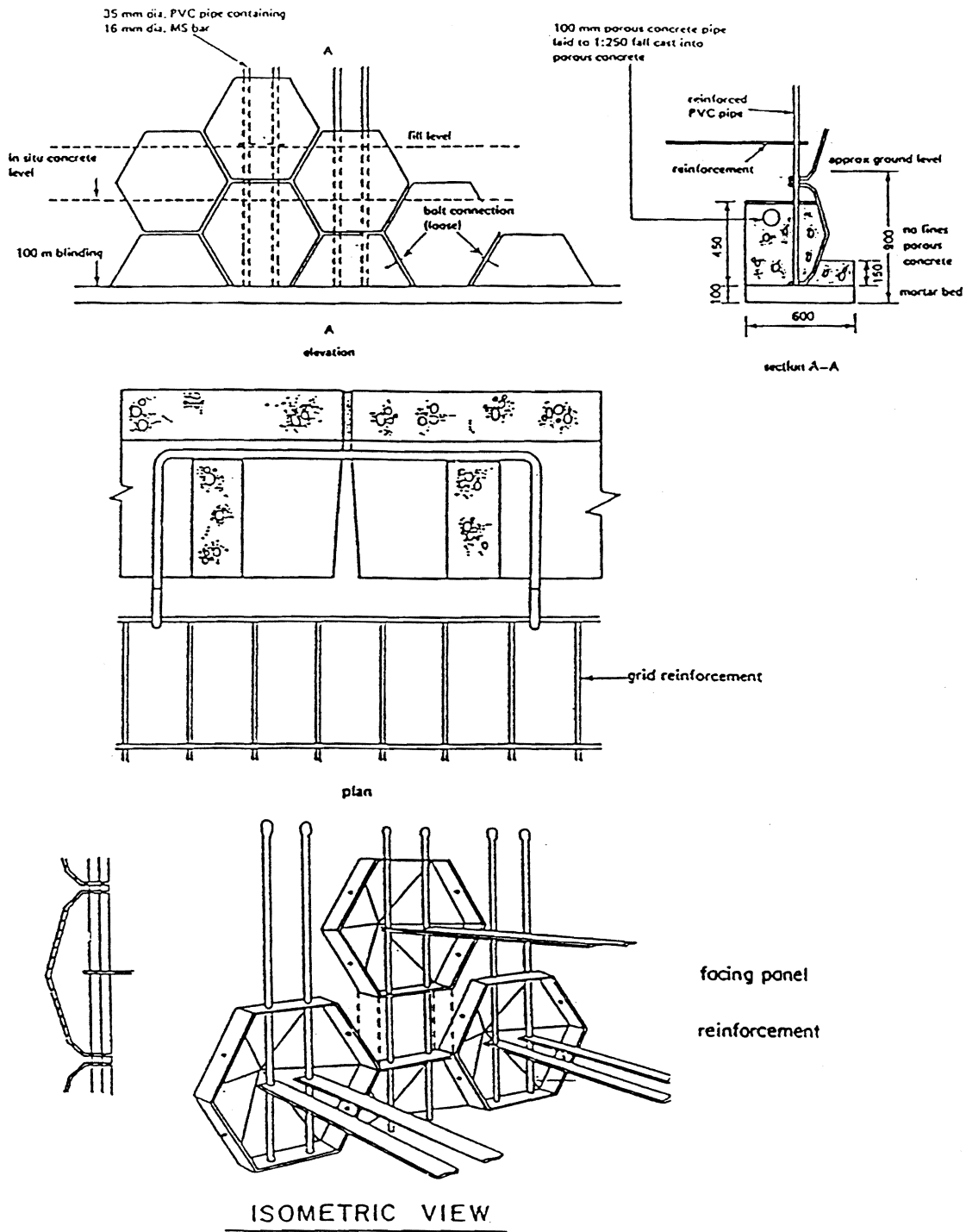
Figure 10. The York system.

h.   The Anda Augmented Soil System

The Anda system is a recent development of the principle of reinforced soil and utilizes an unique combination of "Fibretain" reinforcing elements and "Anda crib" type facing.

The facing consists of precast concrete header units 12 in (30 cm) high, spaced 47.2 in (1.2 m) apart. In between the headers are precast stretcher and infill panels which can have any desired exposed face finish. Each header unit has two cast in place steel straps with holes to receive a vertical pin which holds the reinforcing strap (see figure 11). The "Fibretain" reinforcing elements are a patented pultruded Fiberglas Reinforced Plastic developed by Pilkingtons Ltd. of England and manufactured from continuous 'E' glass voings, combined with "Dere kane" thermosetting resin. The straps are 1.6 in to 6.3 in (40 mm to 160 mm) wide and 5/64 in to 5/32 in (2 to 4 mm) thick and have ultimate strength of 14,400 to 72,000 lb (6,532 to 32,659 kg).

The Anda System is patented by the Anda Augmented Soils Ltd., Oaklands House, Solarton Road, Farnborough, Hants, GU147QL, England (UK patent no. 1,443,167).

i.   Tensar Geogrid System

This type of soil reinforcement utilizes a nonmetallic tensile resistant polymeric grid mat, produced and marketed under the trade name Tensar by Netlon, Ltd. This type of reinforcement was made available in 1980. It is marketed in North America by the Tensar Corporation of Atlanta, Georgia and by Contech Construction Products, Inc.

The Tensar geogrid is a high strength polymeric grid reinforcing mat made form high density polyethylene of polypropylene using a stretching process (figure 12) that imparts a high tensile strength to the polymer (in excess of 30,000 psi [2,100 kg/cm^2]). This results in reinforcements with strengths on the order 100 to 500 lb/in (87.5 kN/m based on ASTM D-4595. The geogrid system of reinforcement has the advantages of being high strength (close to mild steel), ductile, durable, resistant to corrosion, ease of handling (being relatively light), and ease of installation as no special tools or equipment are required. Some of the disadvantages are prone to degradation due to aging, vandalism, and fire, and creep under high stress.

Facing elements of different types can be used such as by looping the reinforcement at the face with a wrap around, by secondary grid reinforcement joined to the main reinforcement, or by attaching to structural elements, for example, gabions, concrete panels, etc. (see figure 12). The material is supplied in rolls 3.3 ft (1 m) wide. Connections may be made by using a rod or by stitching with synthetic cord. The reinforcing grid can be turned up at the face of the slope and turned into the embankment below the next reinforcing layer. A shotcrete layer
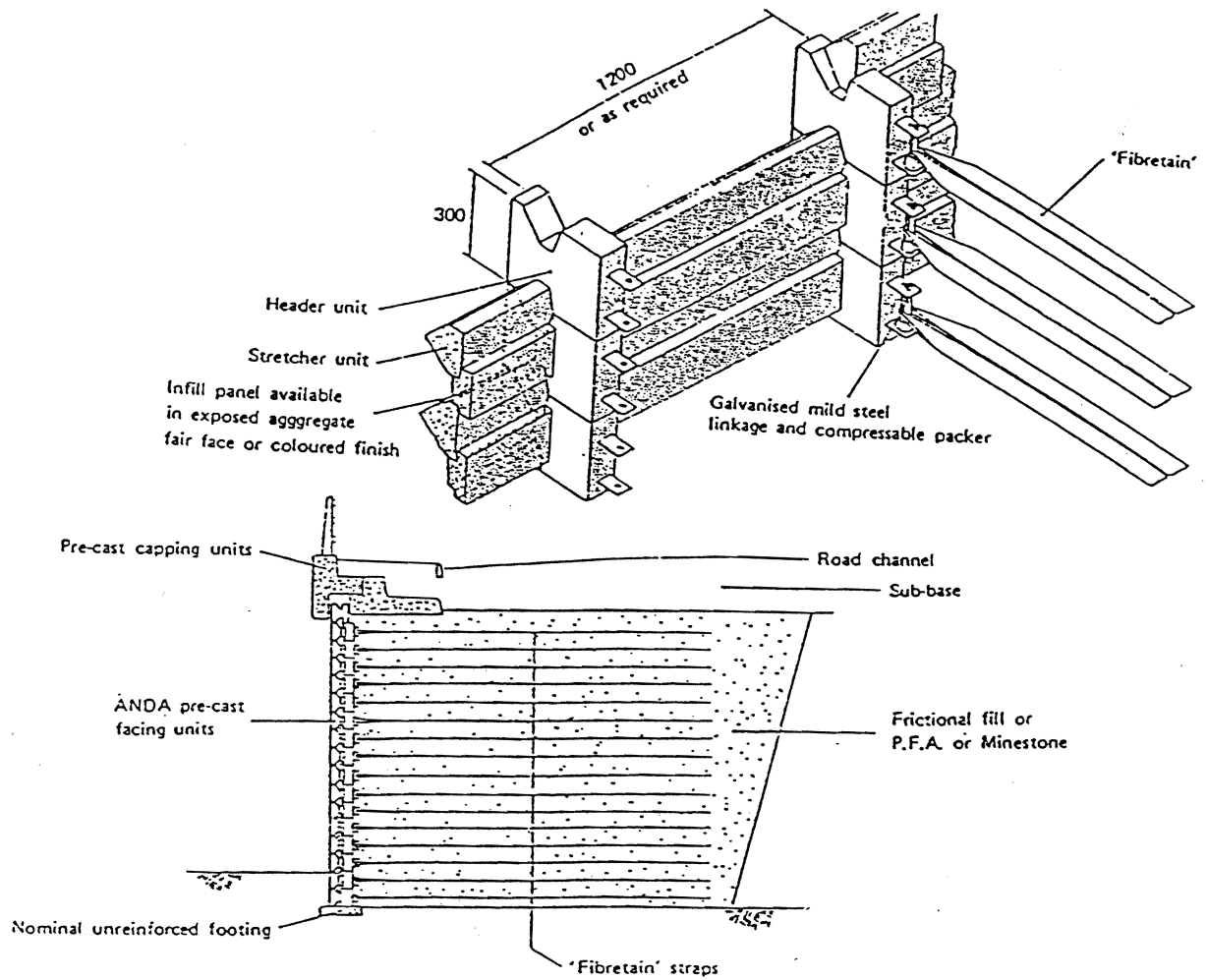
Figure 11. The Anda augmented soil system.

FACING ————— GEOGRID REINFORCEMENT

SCHEMATIC OF WRAP-AROUND FACING

Longitudinal rib

Uniaxially orientated grids (Figure 2) are
manufactured by stretching the punched sheet in
one direction under carefully controlled conditions.

Transverse bar

Biaxially orientated grids (Figure 3) are produced by
stretching uniaxially orientated grids, again under
carefully controlled conditions, in the direction
normal to the uniaxial orientation (4).

Longitudinal rib

Junction

Transverse rib

TENSAR GRID

Figure 12.   Tensar geogrid reinforced soil wall.

26

can be applied on the geogrid for a different type of facing.
Several precast concrete facing systems have also been developed
by the Tensar Corporation.

Several hundred walls and slopes have been constructed with this
system. There are no proprietary restrictions on the system
except that the reinforcing material is patented by Netlon, Ltd.
and is available only through the Tensar Corporation and Contech
in the United States.

j. Other Polymeric Geogrid Systems

Several other polymeric geogrid reinforcement systems have
recently been developed. These include the Tenax system; the
Miragrid system by Mirafi, Inc., and the Matrex system by
Reinforced Earth Company.

k. Geotextile Reinforced Systems

In this type of retaining wall, continuous sheets of geotextiles
are laid down alternately with horizontal layers of soil to form
a composite material. Facing elements are formed by wrapping the
geotextile reinforcement around the exposed soil at the face
(figure 13) and covering the exposed fabric with gunite, asphalt
emulsion or shotcrete, or with soil and vegetation for long term
protection from exposure to ultraviolet light and vandalism.
Alternatively, structural elements can be used on the wall facing
such as precast concrete panels, steel soldier piles and wood
lagging, masonry, gabions, or even cast in place concrete walls
(figure 14). Connection between the geotextile reinforcing sheet
and the structural wall elements can be provided by a number of
methods including casting the geotextile into the concrete
element, by friction, by nailing and overlapping or other bonding
methods. Composite construction uses plastic reinforcing strips
along with geotextiles.

The face of a retained wall may be vertical or sloping. Stress
transfer between the retained soil and the geotextile is by
friction.

A wide variety of geotextiles with a wide range of mechanical
properties and environmental resistances can be used, including
nonwoven, needle punched or heat bonded polyester and
polypropylene and woven polypropylene and polyester. A majority
of the geotextile fabrics used in earth reinforcement are made of
either polyester or polypropylene fibers.

Geotextile reinforced walls can be constructed at most sites even
with poor soil conditions and very steep slopes and in remote
areas, because of limited requirements for heavy construction
equipment. The materials required are relatively light and
easily transportable. Geotextiles also permit a great
flexibility in the length of fabric and in the vertical spacing
of the reinforcing fabric.

There are no proprietary restrictions associated with geotextile
reinforced walls.

Figure 13. Geotextile reinforced wall.

Vertical Geotextile Facing

Sloping Geotextile Facing

Sloping Gunite or Structural Facing

Vertical Precast Concrete Element Facing

Sloping Soil and Vegetation Facing

Geotextile Gabion

Vertical Cast In-place Concrete/Masonry Facing

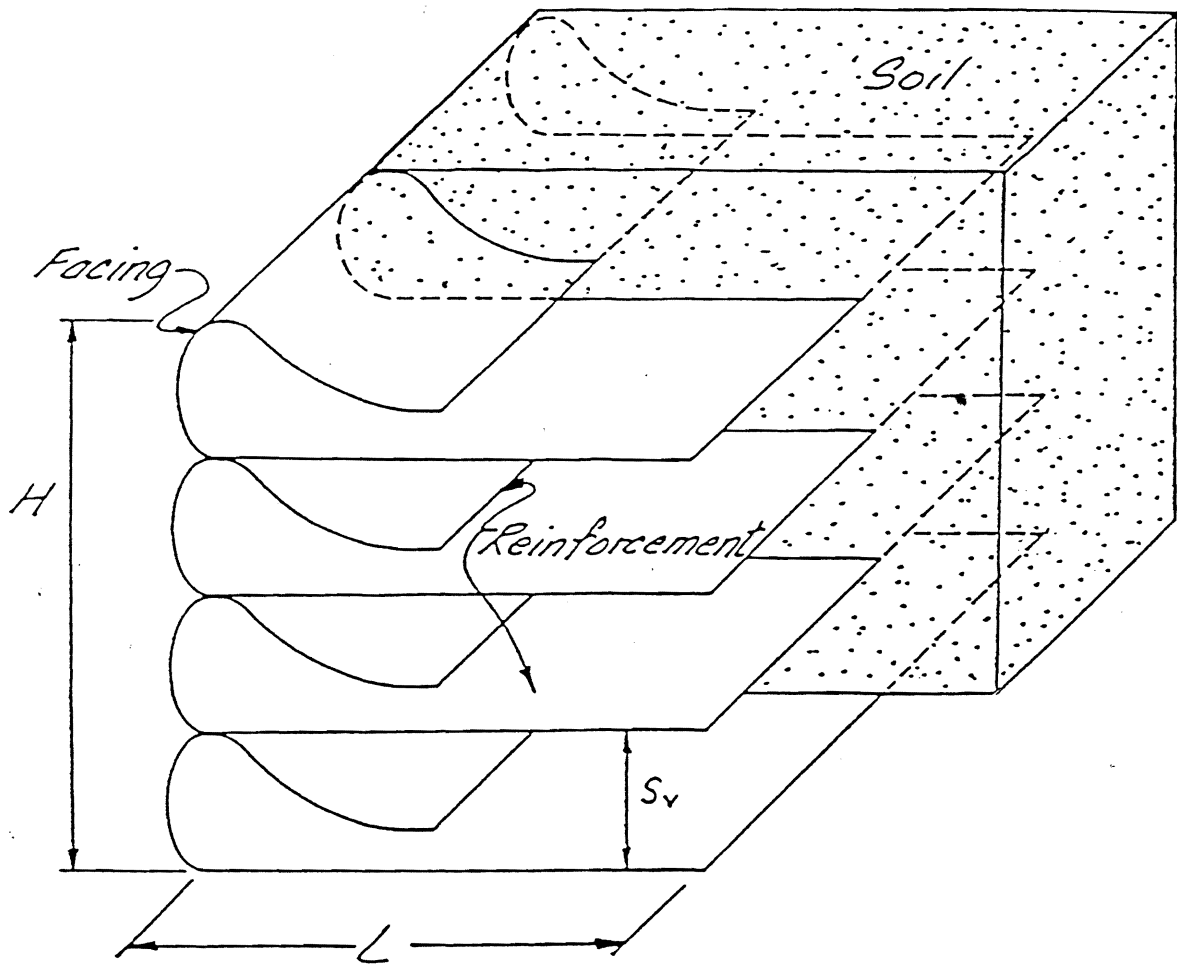Vertical Masonry Facing
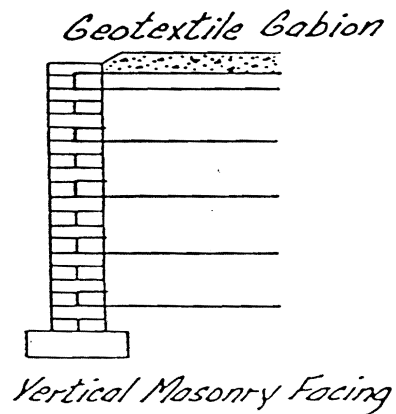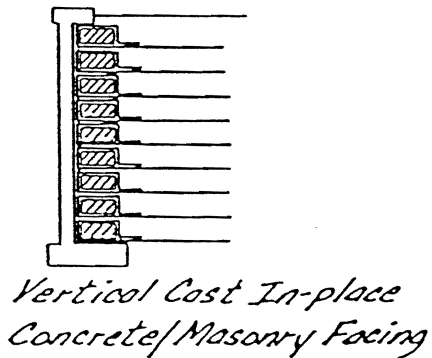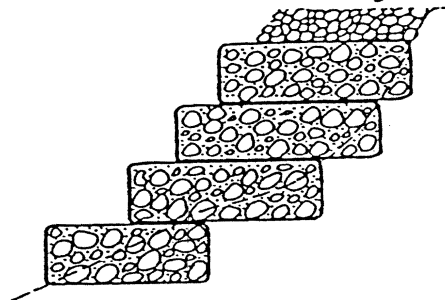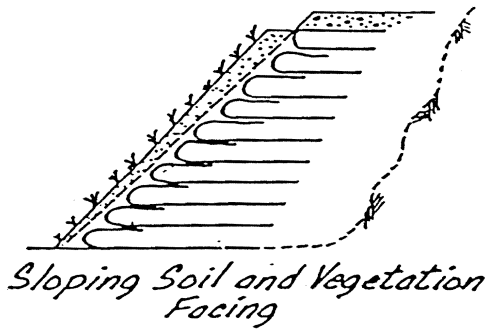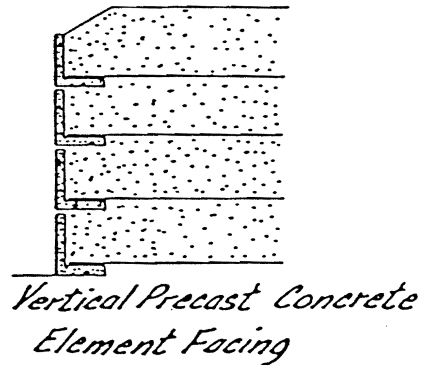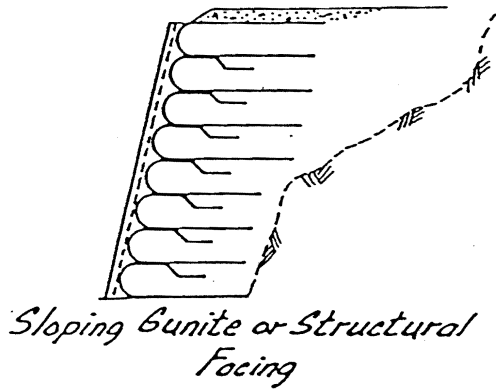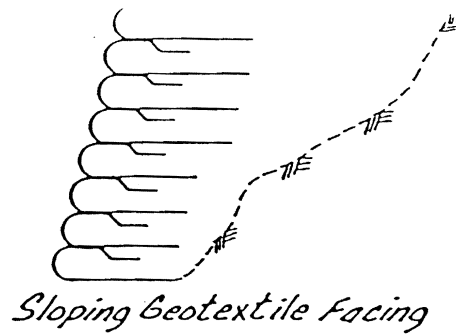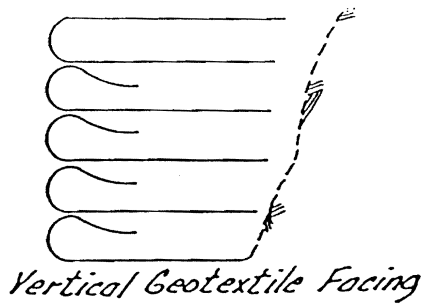
Figure 14. Types of geotextile reinforced walls.

1.   Gabion Reinforced Fill Wall System

These walls are made of large rectangular wire baskets, wired
together and filled with rock. Each basket or box gabion
consists of rectangular units fabricated from a double twist,
hexagonal mesh of soft annealed, heavily galvanized wire. The
gabions are divided into cells by fitting diaphragms which have
the function of reinforcing the structure and making assembly and
erection easier. They are flexible so they can undergo movements
without failing.

Once assembled and erected, the gabion structure acts as a
monolith rather than a system of separate cages placed side by
side. The structure remains flexible to absorb localized
settlements, deflections and stresses. It has permeable
structure and so no excess hydrostatic pressures act on it.

The gabion structures are designed as a reinforced soil structure
or as a nonreinforced gravity retaining structure. The
reinforced fill structure is designed similar to any other
mechanically stabilized extensible structure. Reinforcement
consists of double twisted wire mesh similar to that used in the
baskets or of a heavier gage, placed in between the baskets and
extending into the backfill. This reinforcing mesh may be of
uniform or of variable length in the various layers.

In the nonreinforced structure, the gabion walls are designed
similar to any gravity retaining structure. The wire mesh of the
baskets may be taken as an additional safety factor and is not
included in the design consideration. Various types of cross
sections can be considered, taking into account the soil
characteristics, the slope of the backfill, and any superimposed
loading. Front face of the wall can be vertical, stepped or
sloping (figure 15).

This type of wall was originally developed by the Maccaferri Co.
of Bologna, Italy, who have their USA head office and factory at
Maccaferri Gabions, Inc., Governor Lake Blvd., R.R. 2, Box 43A,
Williamsport, MD 21795. There is no patent on the system.

3.0 IN-SITU REINFORCED SYSTEMS

     a.   Soil Nailing

Soil nailing is a technique for strengthening an in-situ soil
rather than an earth fill as in the case of reinforced soil.
Soil nailing consists of three elements, the in-situ soil, the
reinforcement and a facing (figure 16a). However, facings are
not always used.

The reinforcement generally consists of steel bars, metal tubes,
or other metal elements which resist not only tensile stresses,
but also shear stresses and bending moments. The inclusions are
installed in the soil at relatively close spacings, one nail for
each 10 to 60 ft^2 (1 to 6 m^2). Nails may be prestressed to limit
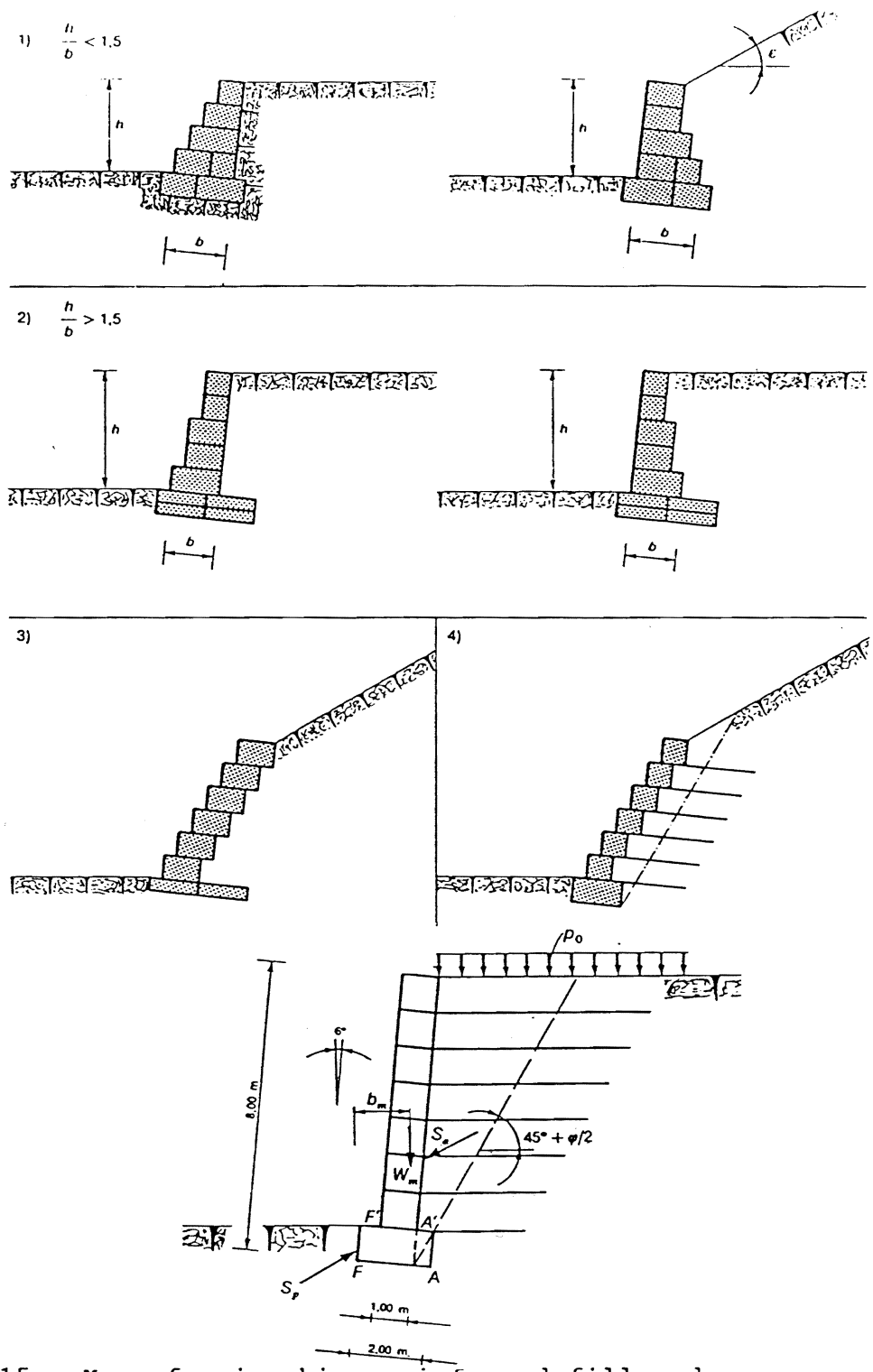
Figure 15. Maccaferri gabion reinforced fill and
gravity wall systems.

Original Grade — Facing
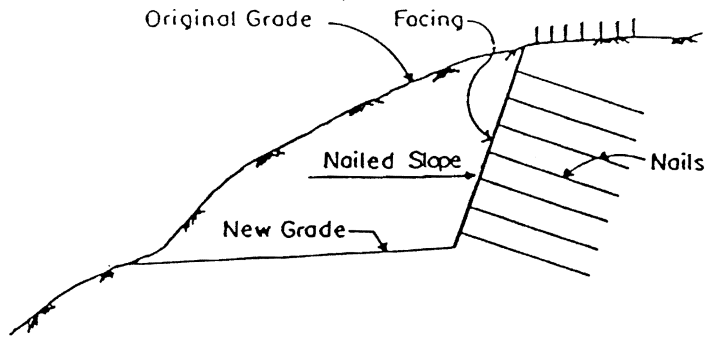
SOIL NAILING IN RETAINING STRUCTURE

(a)

Original Grade

Unstable Soil — Nails
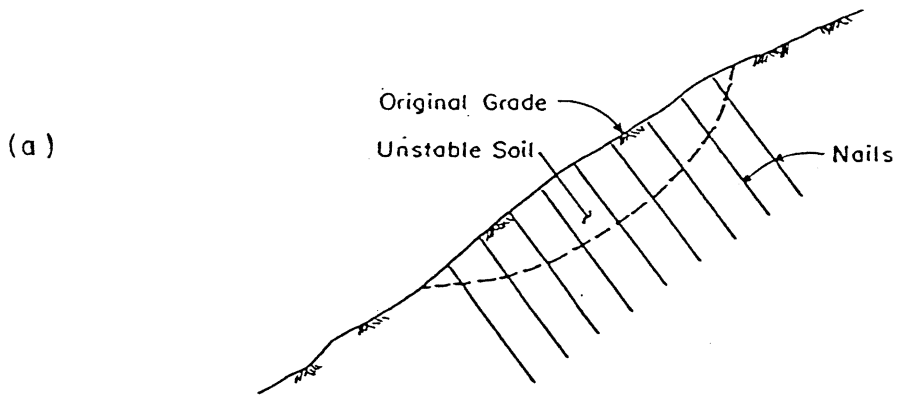
SOIL NAILING FOR SLOPE STABILIZATION

(b)

AREA TO BE EXCAVATED
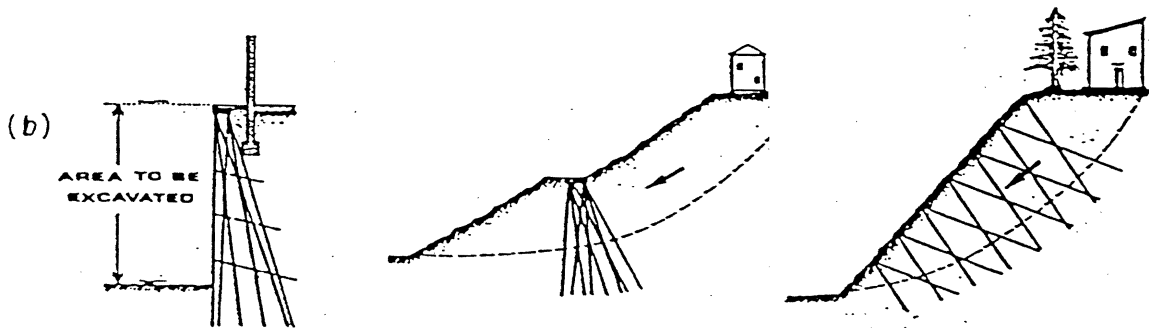
Figure 16. Uses of soil nailing and micropiles.

deflections. The inclusions are either placed in drilled boreholes and grouted along their total length or driven into the ground. The ground surface of the nailed soil usually is stabilized by a surface skin which may consist of a thin layer, 4 to 6 in (10 to 15 cm) thick, of shotcrete reinforced with wire mesh or by intermittent rigid elements which work like large washers on a bolt or by using prefabricated metal panels (which may later be covered by shotcrete).

There are no proprietary restrictions on the use of soil nailing. However, some systems of facing and reinforcements (nails) are patented (e.g. "TBHA" and "INTRAPAC" mails are patented by Solrenfor and Intrafor-Cofor companies, respectively).

b. Micropiles or Reticulated Root Piles (R.R.P.)

A similar method to soil nailing is by micropiles which are also called reticulated root piles. Micropiles and root piles have been used extensively during the past 20 years for underpinning and reinforcement of foundation soils. The use of this technique for slope stabilization and in retaining systems is a relatively new application (figure 16b). Most of these projects were executed in the least ten years or so.

The root piles are cast in place reinforced concrete piles with diameters ranging from 3 to 12 in (7.5 to 30 cm). In the smaller diameter range, these piles are provided with a central reinforcing rod or steel pipe, while those with larger diameters may be provided with a reinforcing bar cage bound with spiral reinforcement.

"Micropiles" consist of long and very strong (about 50 to 100 kips strength in tension) inclusions which are grouted in a predrilled borehole at a wide spacing of about one bar per 30 to 60 ft^2 (3 to 6 m^2). "Hurpinoise" is a term used to refer to nailing with shorter, less resistant bars (10 to 35 kips in tension) that are driven into the soil at a close spacing (approximately one bar per 5 ft^2 (0.46 m^2).

The piles are arranged according to a three dimensional pattern in order to form some sort of network in which the soil is encompassed. Therefore, whereas in the "soil nailing" the nails behave as independent resisting elements, in a Reticulated Root Pile structure the mutual action among the piles is essential and it must be encouraged. Therefore, the design of root piles has a completely different approach from soil nailing. The most important design element in a Reticulated Root Pile structure is the appropriate density of the piles.

Generally, there is no facing for the R.R.P., because the majority of these structures are intended to be buried in the subsoil, to behave like buried retaining wall, not to be exposed, or to be only partially exposed. This is the case of landslide prevention, protection of buildings in presence of excavations of tunnels for subways, etc.

One difference between micropiles or root piles and soil nailing is that the reinforcing bar(s) in the micropiles and root piles are grouted under pressure. The grout significantly increases the adherence of the bar to the in-situ silo, and it enables the bar to be installed at any orientation. Another difference between this system and soil nailing is that the behavior of micropiles or root piles is significantly influenced by a soil pile interaction due to three dimensional arrangement of the pile group.

The "Root Piles," (generally used for underpinning) and the "Reticulated Root Piles," were invested in the early fifties by F. Lizzi and patented by the Italian firm, Fondedile of Naples. The same firm introduced and installed the system all over the world. Although the original patents expired and therefore there are no more proprietary restrictions (except for the trade marks in the names of "Root Pile" and "Reticulated Root Piles") it must be stresses that the design of a Reticulated Root Pile structure requires specific experience.

c.   Composite In-situ Systems

Composite systems utilize combinations of reinforced soil and other types of retaining systems (gravity, cantilever or anchor). Similar combinations with in-situ reinforced systems can be utilized, depending on the existing and proposed situations.

4.0   MULTIANCHORED SYSTEMS

a.   American Geo-Tech System

This systems of retaining wall has been developed by American Geo-Tech, Inc. of Baltimore, Maryland. The retaining wall consists of precast reinforced concrete face panels, precast reinforced concrete deadman and steel tendons connecting them (figure 17). The system relies on passive pressures on the deadman panels for stability. Internal stability does not rely on friction between the reinforcement and the soil, but requires only adequacy of the face panels and the deadman to resist lateral pressures and the tendons to resist the generated loads. Standard face panels are 8 ft (2.44 m) wide and 5 ft 4 in (1.63 m) high. Up to a lateral pressure of 1500 psf (71.9 kPa), each panel has 8 tendons and for pressures of 1500 to 3000 psf (71.9 to 144 kPa) each panel requires 16 tendons. A transition row of panels having 12 tendons is also provided. The tendons are epoxy coated (8 mil thickness), 0.75 in (19 mm) diameter ASTM A36 steel, plain rods with ultimate yield capacity of 26.5 kips (118 kN) and ends of the tendons are threaded for connections to the face panels and the deadman.

American Geo-Tech, Inc., P.O. Box 9696, Baltimore, Maryland, 21237 has applied for a patent for this type of retaining wall. To date, this system has had very limited use.

Alignment Bars

Deadman

Tendons

Eight Inch Lifts
Of Soil Fill

Facing Panels

Leveling Footing

STANDARD 8" LIFT LAYOUT

LATERAL EARTH PRESSURE LESS THAN 1500 psf

LATERAL EARTH PRESSURE GREATER THAN 1500 psf

(16 tendons/panel)

(12 tendons/panel)

(16 tendons/panel)

16 tendons per panel.

16"
24"
16"
6"
6"

TENDON LOCATION
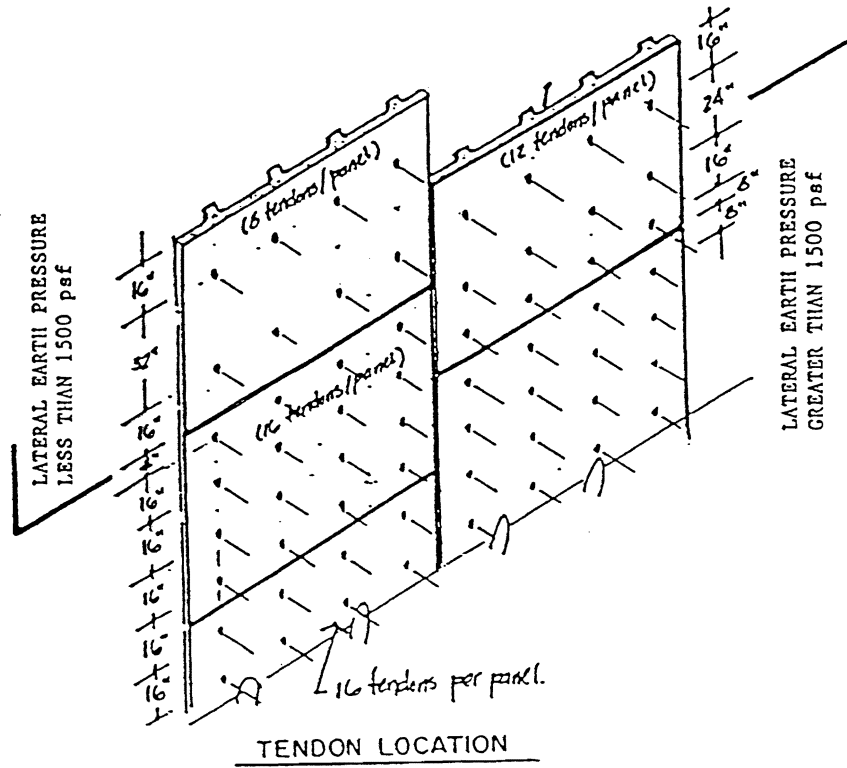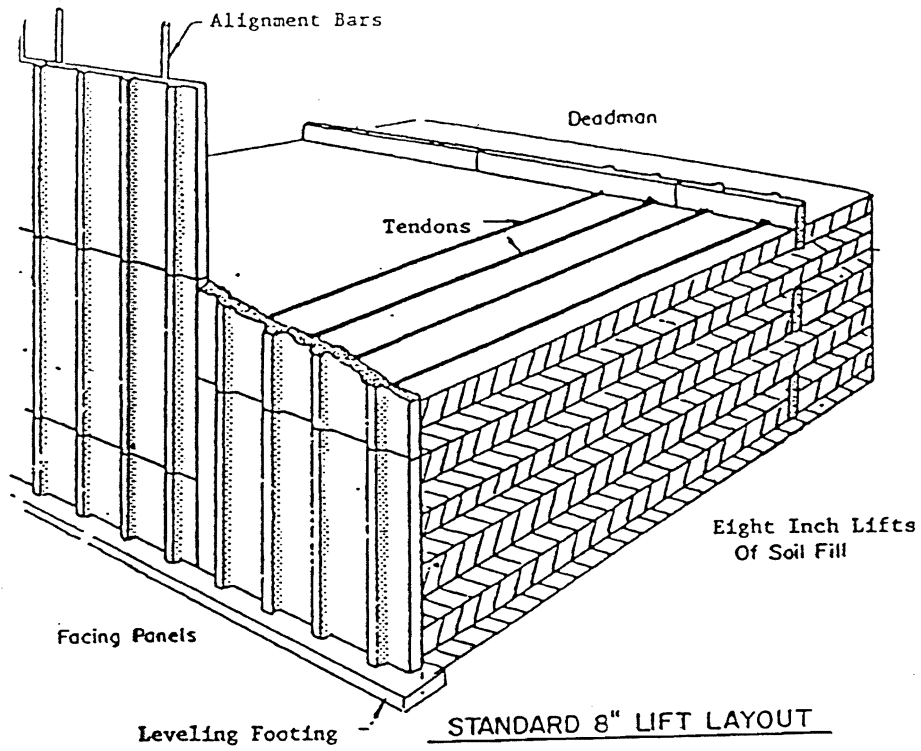
Figure 17.   American Geo-Tech system.

35

b.   Tension Retaining Earth System (TRES)

This is another method of retaining wall, developed by Columbia
Engineering Company of Silver Springs, Maryland. TRES uses
precast segmentally constructed face panels anchored by tendons
to earth anchors (figure 18). Wall facing is made of hexagonal
interlocking precast concrete panels in any desired size, from
man liftable to large rapid erection size. Tendons consist of
standard mild steel reinforcing bars, galvanized or epoxy coated
for corrosion protection. Most walls require only rocks or
concrete rubble for deadman anchors. Precast concrete anchors
are also available. Each face panel is anchored at four points
using tendons having attached anchor plates. The tendons have
loops formed (for deadman) and welded plates at each end for
connection to the face panel.

Patent on the TRES system is held by its developer, Walls
Systems, Inc., P.O. Box 2543, Columbia, Maryland 21045. Only a
few structures have been constructed with this system.

c.   Anchored Earth

The Anchored Earth retention system was developed and patented by
the Transport and Road Research Laboratory (TRRL) of Crowthorne,
England. This type of retaining wall is still in an
experimental stage and has not been used on any project in the
United States.

This system has precast concrete panels, rectangular in shape,
with adjacent panels having overlapping edges. The panels are
typically 47 in (1.2 m) wide, 6 in (15 cm) thick and of varying
heights. The reinforcement is by mild steel bars of 0.6 to 0.8
in (16 to 20 mm) diameter having a screw threaded portion at one
end. The other end of the anchor is formed by bending the bar in
the form of a Z or a triangular end in which the loop around is
welded to the main bar (figure 19). For anchorage of the
reinforcement to the panel, the rods extend through the facing
panels in slots and are secured by nuts. The reinforcing rod
extends through the overlapping portion of the two adjoining
panels. The protruding rods and the nuts can be housed in a
recess cast in the facing panels and then capped to provide a
flush appearance.

Anchored Earth is designed on the basis that passive resistance
is developed only at the deformed ends of the reinforcing
members. It is likely to be more efficient in cohesive soils
than the other systems which rely predominately on friction. The
pullout resistance is not sensitive to the surface
characteristics of the anchors because of the relatively large
area available for passive resistance at the deformed end.

The Anchored Earth system is patented in the United States and
elsewhere by the Transport and Road Research Laboratory,
Crowthorne, England.

CONCRETE CAP

BACK ANCHOR

TENDON

FACE PANEL

LEVELING
FOOTING

Optional
Capping

Rock Anchors

TENDONS

Face

Sand Drainage
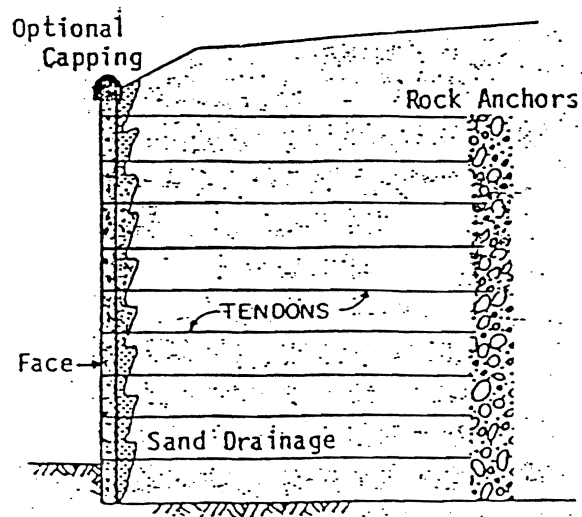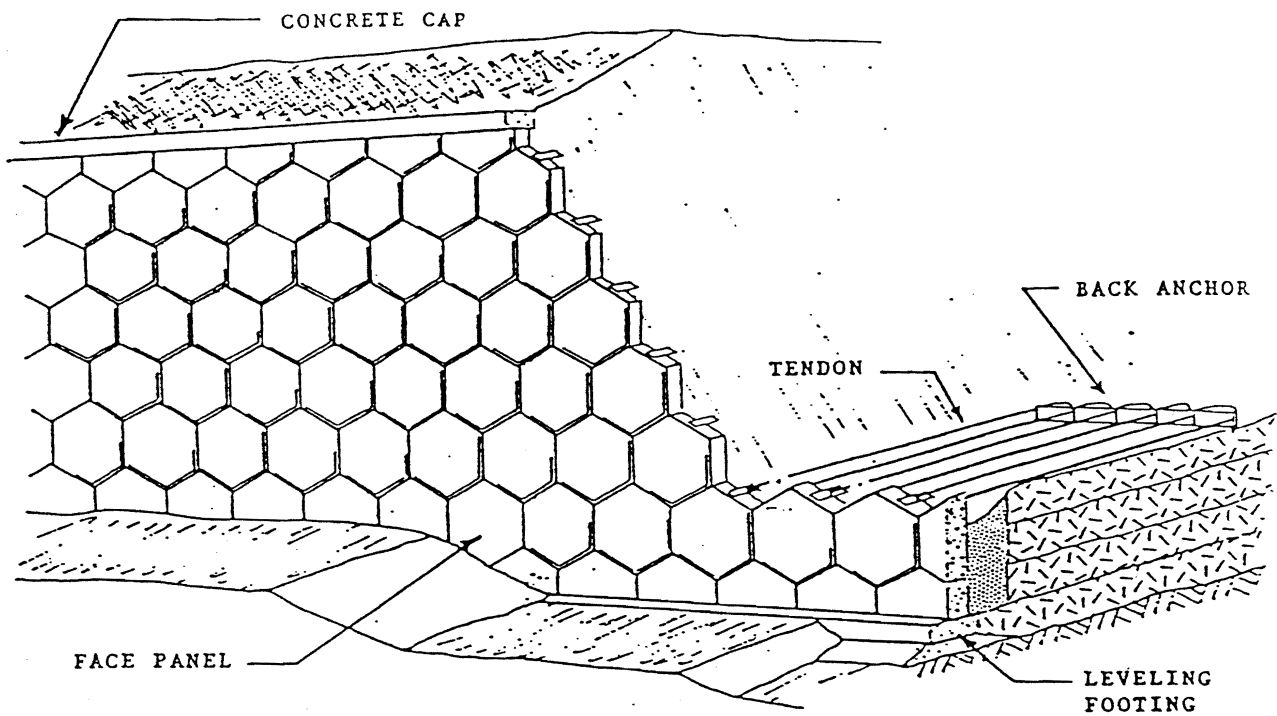
Figure 18.   Tension Retaining Earth System.

FACE PANEL

ANCHOR ROD

TRRL anchored earth system

1.3 ft.

6.9 ft

1.3 ft

6.9 ft

ELEVATION

overlapping facing units

thick washer

anchor bar

nut

compressible filling

compressible cap

PLAN
FACING UNIT

ANCHOR FACING CONNECTION
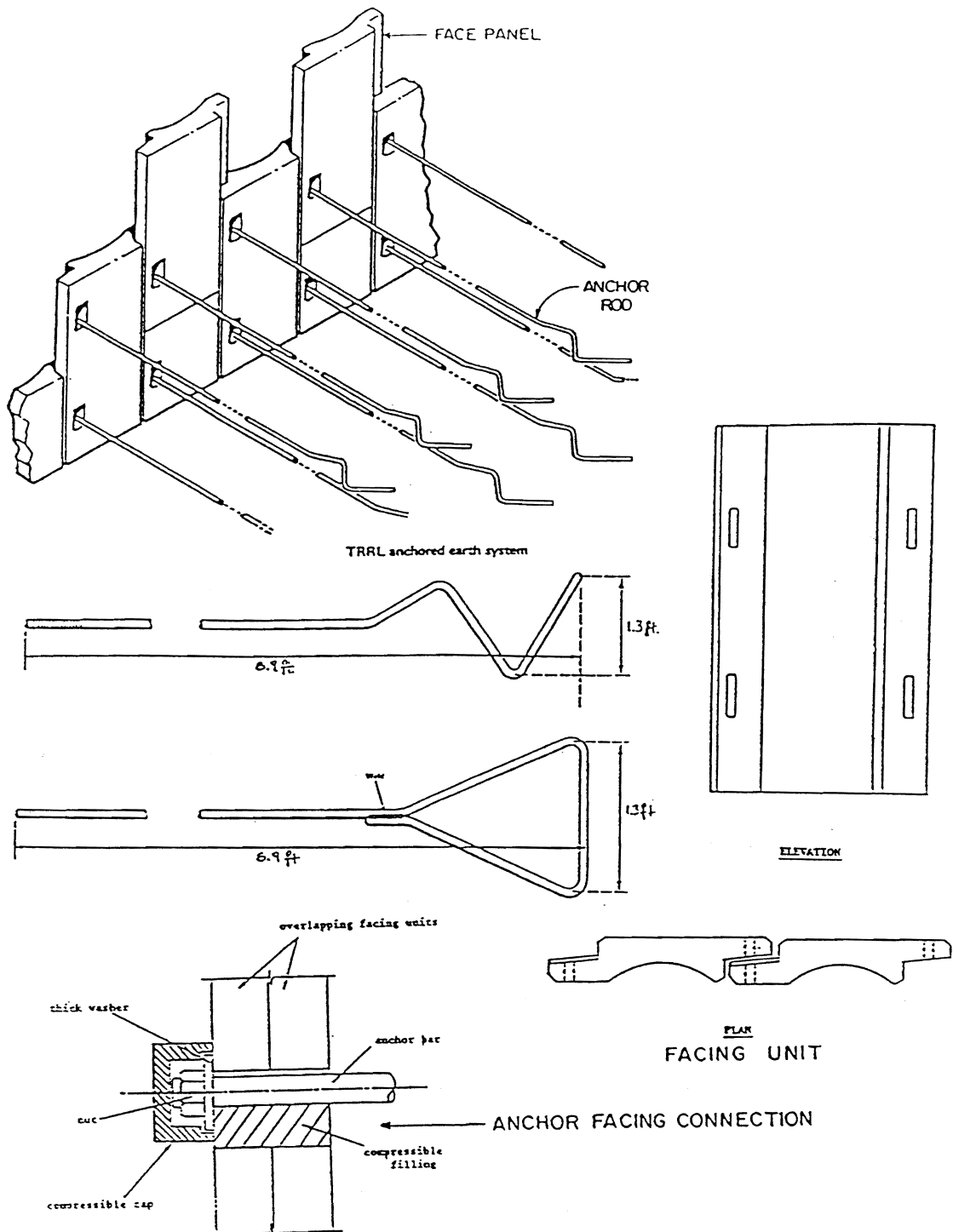
Figure 19.   TRRL anchored earth system.

38

precast concrete
facing units
(1.5 m x 0.8 m)

ties with anchors

selected stone fill

ordinary fill

1
2
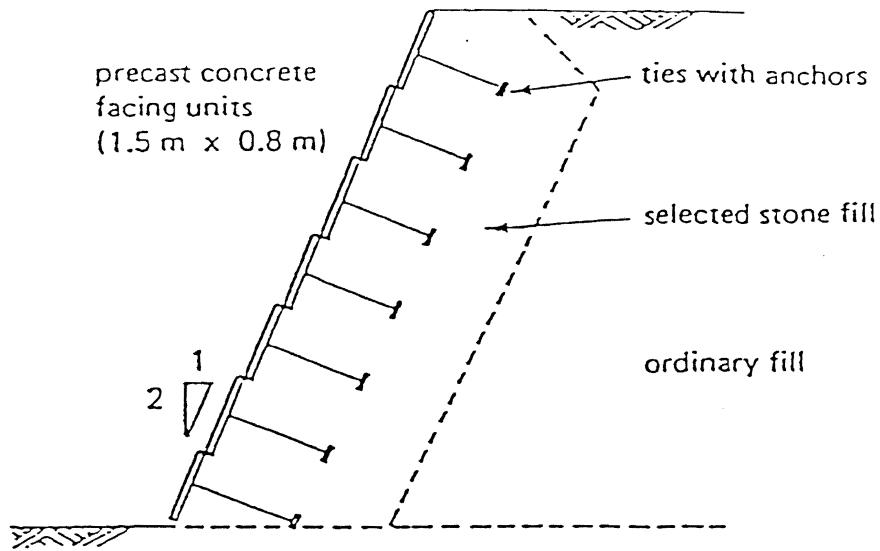
Figure 20. Ladder wall-sloped face.

Steel Rods Encased
in Concrete

H

Face Wall

Deadman (Beams of
Reinforced Concrete)
Typ.
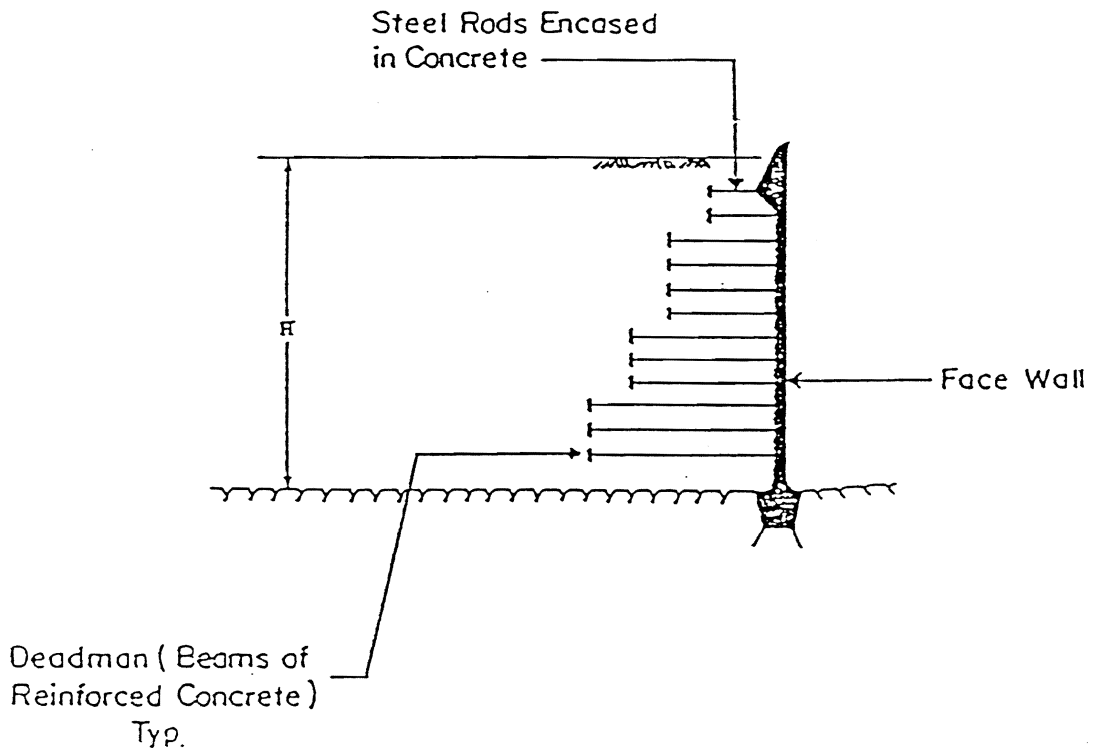
Figure 21. Ladder wall with vertical face.

39

d. Ladder Wall

The "Ladder Wall" (Mur Echelle) system invented by Coyne in
France in 1926 consists of a multitied back system associated
with thin facing made either of concrete panels or of a
continuous wall (figure 20). The ties withstand tensile forces
which are constant along the sides. The soil reinforcement
interaction is essentially realized by the passive lateral thrust
on the anchors.

5.0 ALTERNATIVE SYSTEMS

a. Gravity Walls

Traditional Gravity Walls: These walls are well known and need
no special description in this manual.

Crib Walls and Peller Walls: Crib type retaining walls are built
of interlocking prefabricated reinforced concrete units, which
are essentially stretchers at front and back and headers
connecting them, similar to "crib lock" system described below.
The spaces between these units are filled with a free draining
soil. Crib walls permit some economy of concrete and can be
erected quickly. They permit excellent drainage of the backfill.
With a sloping front and back faces, lateral pressures acting on
it are less than those for a vertical retaining wall.

Crib Lock:

This system was invented in New Zealand and has been used in
California since 1977. The retaining wall is comprised of
precast reinforced concrete members which interlock to form
skeletal braces. The various elements for front and back
(stretchers) and the headers connecting them are put together
like Lincoln logs. The boxes formed thus are filled with a free
draining material and a gravity retaining wall is created (figure
22). The system is particularly useful in remote and mountain
areas where heavy equipment cannot easily be used. A novel feature of
 this wall is the small dimensions of the elements.

Bin Walls: Bin Wall is a gravity retaining wall in which
tenuously connected steel bins are filled with earth. The earth
mass acts as the gravity wall with the steel members serving to
hold the earth mass intact. Bin walls thus utilize the cellular
or crib wall concept but are not merely steel crib walls. Bin
walls are constructed of lightweight, deep corrugated steel sides
with bolted corners. Deflection is thus available in the sides
of the bins, permitting some stress relief from soil pressures
while the corners are positive connections able to distribute
shear forces. Conventional crib walls with articulated corners
and rigid sides do not have these characteristics.

SINGLE DEPTH WALL (TYPICAL)
NO SCALE

DOUBLE DEPTH WALL
NO SCALE

TREBLE DEPTH WALL
NO SCALE

MULTIPLE DEPTH WALL (TYPICAL)
NO SCALE

NOTE: FALSE HEADERS ARE NOT USED IN THE INTERIOR SECTIONS OF MULTIPLE DEPTH WALLS.

WALL ELEVATION (TYPICAL)
NO SCALE
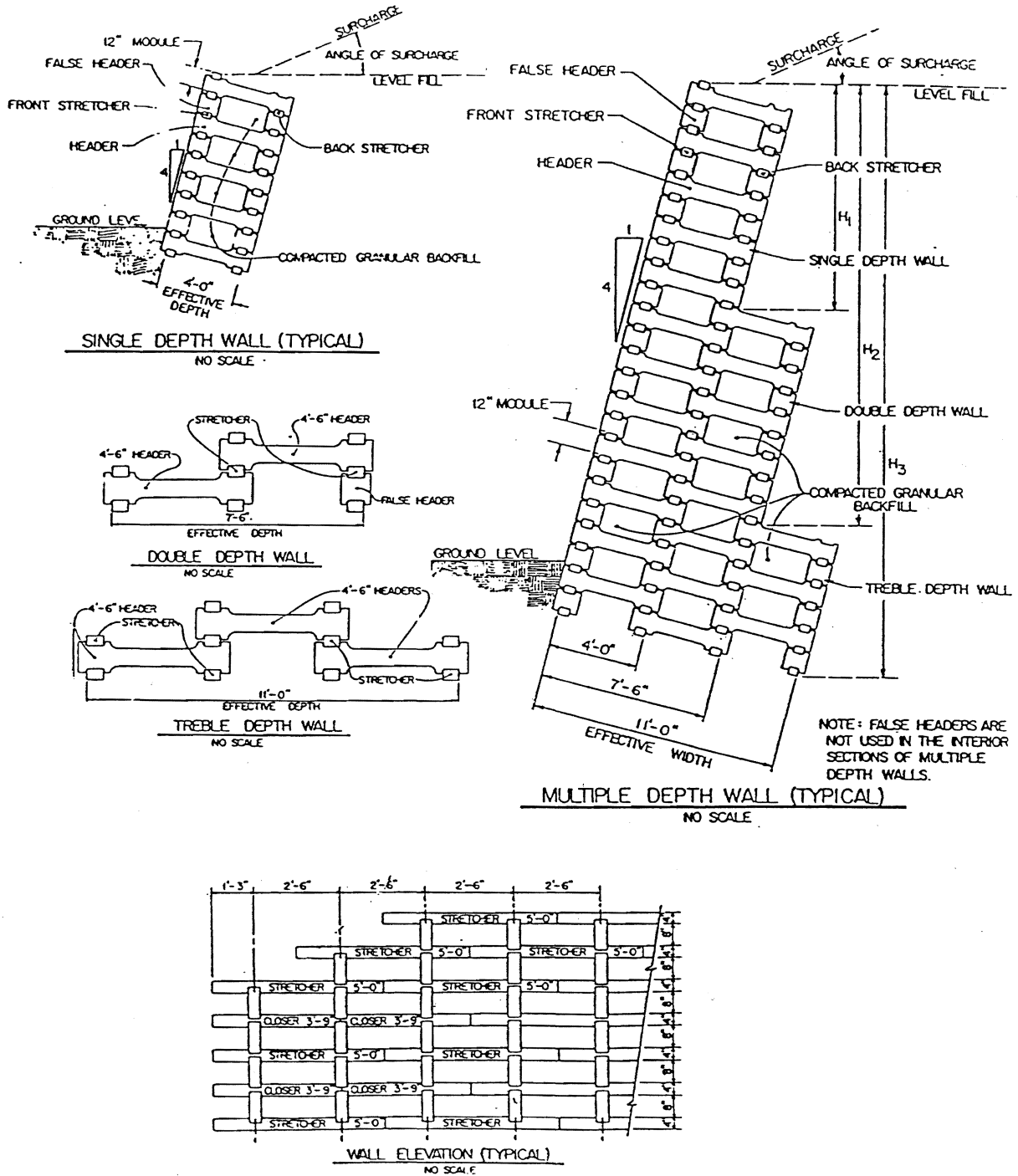
Figure 22.   Crib lock retaining wall.

41

Doublewal:

"Doublewal" is a gravity retaining wall system which consists of large precast, interlocking, reinforced concrete modules that are placed like building blocks (without the use of fasteners) and then backfilled with select material to form a gravity retaining wall (figure 23). Each module consists of two face panels held rigid and apart by connecting beams. Wall segments are available in different sizes and like other precast systems, can be reused. The wall can be built quickly. The system is patented by the Doublewal Corporation, 59 East Main Street, Plainville, Connecticut 06062.

Evergreen: The Evergreen wall is composed of precast elements stacked on top of each other.

This precast concrete wall system has open spaces on its face into which are planted shrubs, vines, etc. (figure 24). It has better acoustic characteristics, antigraffiti surface, and good aesthetic appearance. This system was developed in Switzerland and is patented. The licensee in the United States was Evergreen Systems, Inc., P.O. Box 345, Kings Park, New York 11754.

Stresswall: The Stress wall system was developed by Stresswall International Inc., P.O. Box 10838, Denver, Colorado in collaboration with International Engineering Company, Inc. Patent on the system is pending.

This system has L shaped precast concrete elements called counterfort or tieback units stretching into the backfill form the wall face and hollow core wall panels completing the wall space between the counterforts (figure 26). The elements are assembled in vertical tiers. It is claimed by the patentee that the key mechanism for stability is soil arching between the counterforts. A counterfort unit is held from moving down or out from the wall by the soil arching from neighboring counterforts. Thus, the counterforts have far less depth into the backfill than if it were purely a gravity system.

b.   Cantilever Walls

In certain favorable soil and rock conditions, cantilever walls can be utilized for moderate heights of retained earth. The cantilever wall may consist of reinforced concrete with an extended footing, steel sheet piles or sheet H piles with treated wood lagging or precast concrete planks, or a row of large cylindrical pipe piles bearing on rock and held with vertical anchors installed eccentrically to resist the moments from earth pressures. In certain situations, reinforced concrete slurry walls or precast concrete walls installed by the slurry method can also be utilized to serve as cantilever retaining walls.

Figure 23. "Doublewal" retaining wall.

43
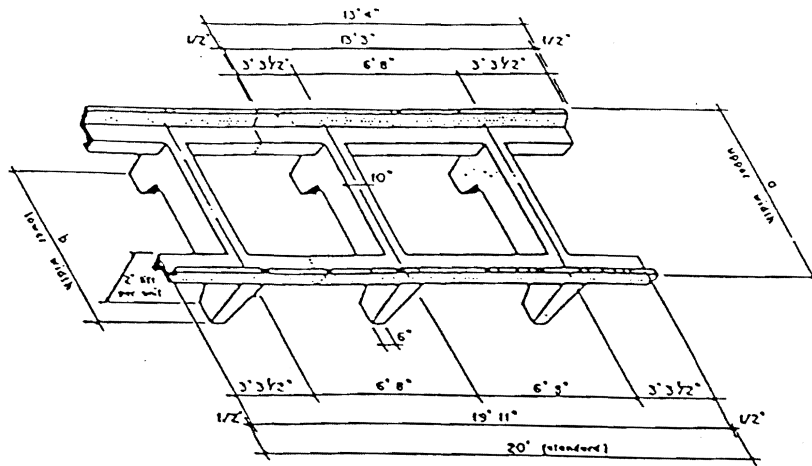
Figure 24. Typical element of Evergreen retaining wall.
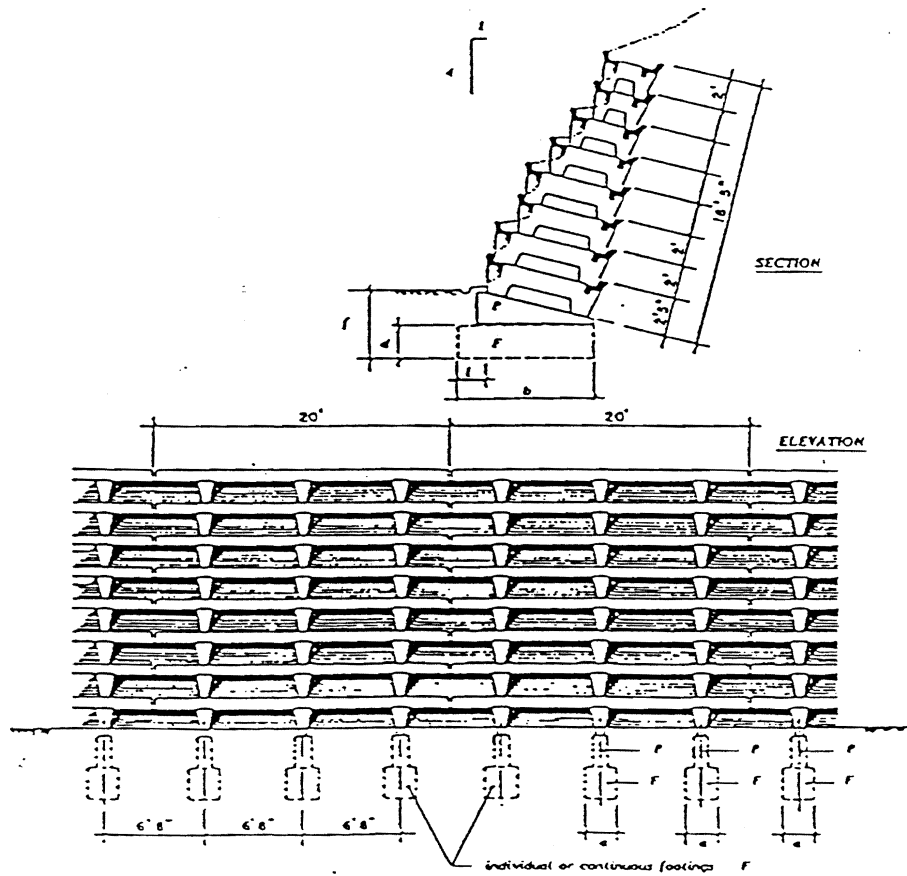
Figure 25. "Evergreen" retaining wall - front view.

44

TYPICAL SECTION $\left(\dfrac{A}{-}\right)$

SCALE: $\frac{1}{2}"=1'-0"$

TYPICAL WALL SECTION

STRESSWALL ASSY.
INTERIOR VIEW
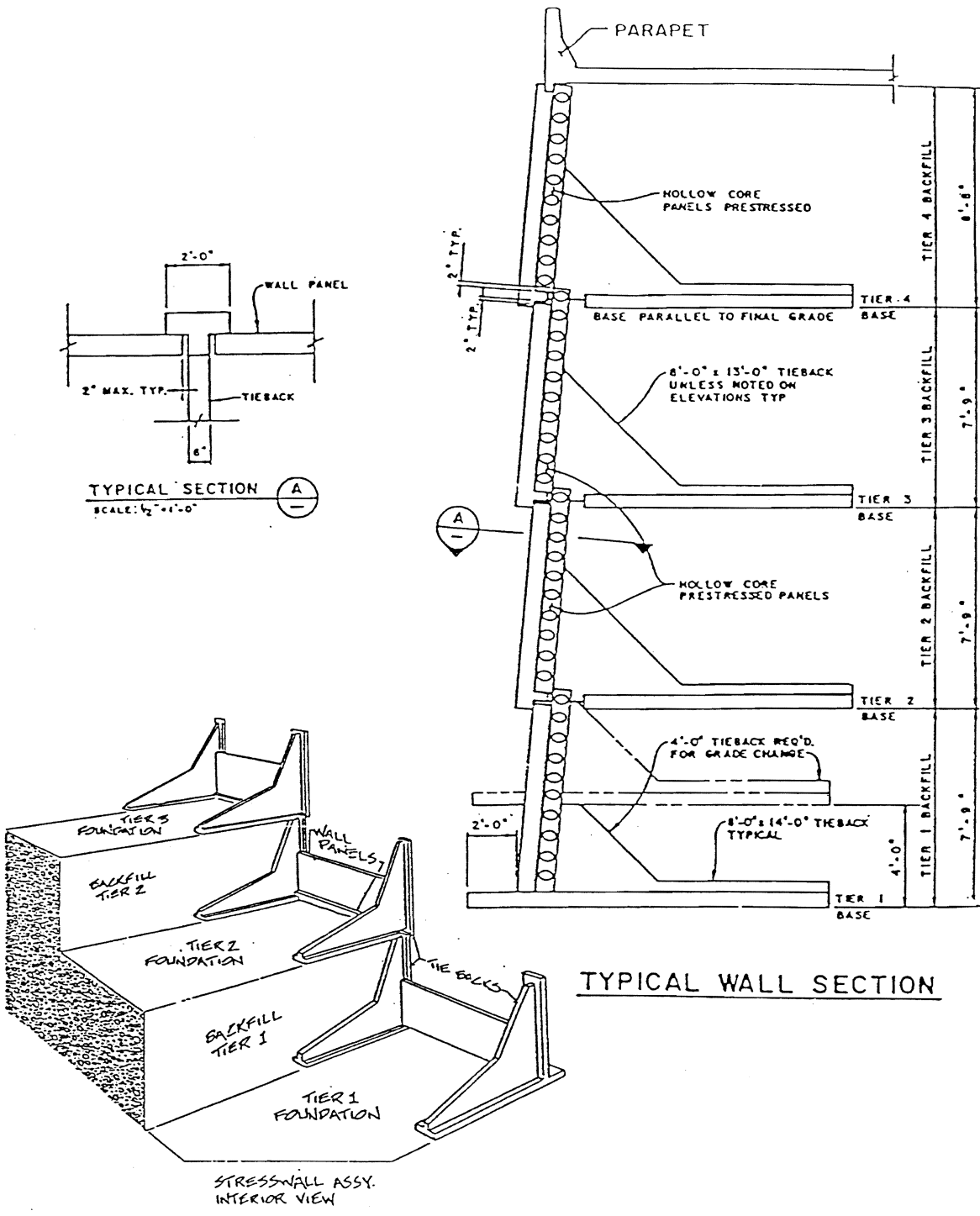
Figure 26.   Stesswall details.
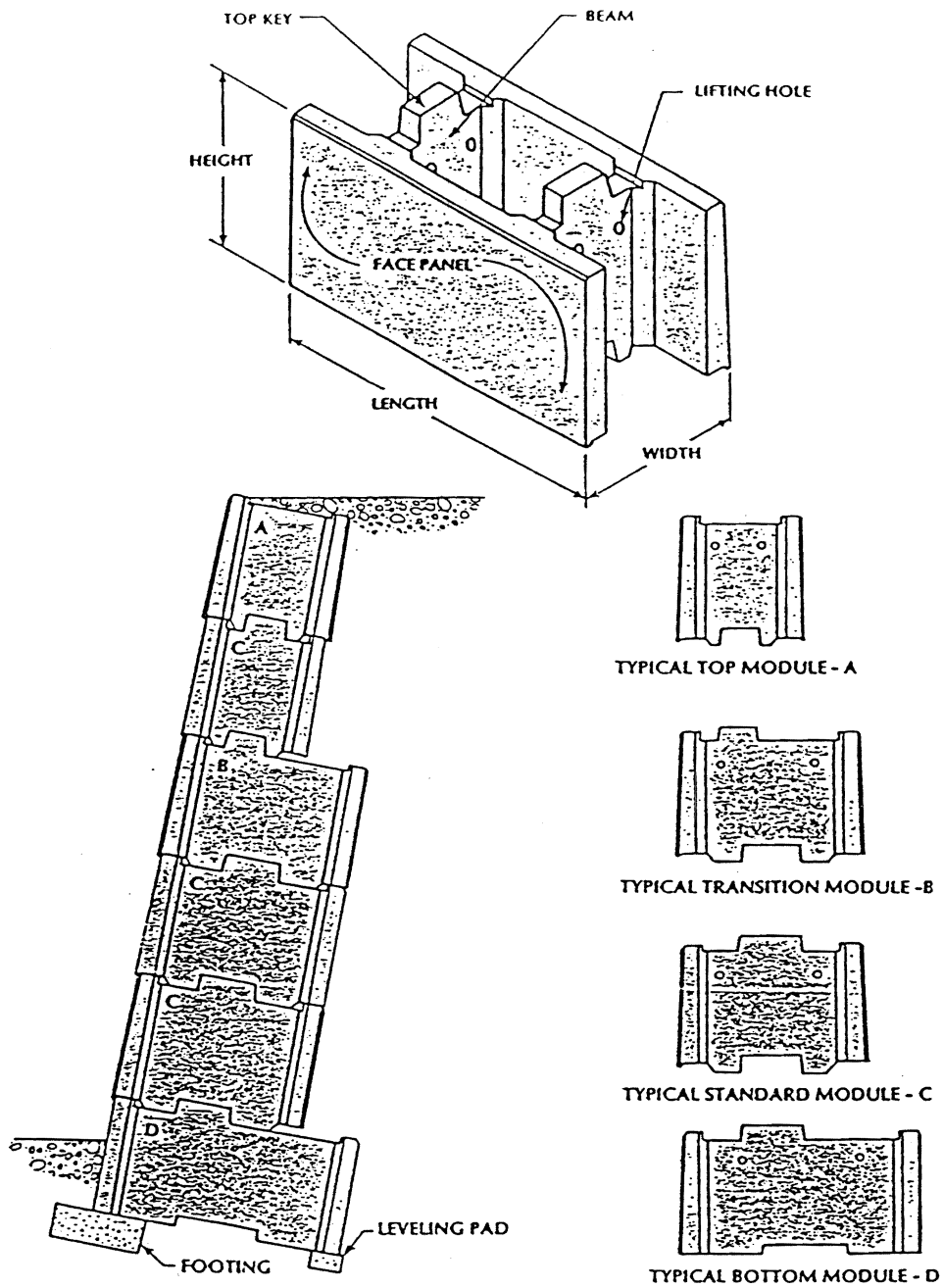
45

c. Grouted Anchor Walls

In this case a vertical or sloping retaining wall is supported by anchors situated deep into or behind the backfill, beyond the likely failure plane (figure 27). These systems are very useful when it is not feasible to excavate behind a proposed wall. In many cases the anchored wall system is the retaining wall. The wall consists of sheetpiles or a slurry wall installed before the start of excavation, or soldier piles installed before the start of excavation and lagging installed as the excavation proceeds. The excavation is done in stages 5 to 10 ft (1.8 to 3 m) depths (the stages can be larger depending on the vertical spacing of anchors) to a level about 1 to 2 ft (30 to 61 cm) below the design location of the anchors. Before proceeding further with the excavation, a row of anchors is installed into the earth behind the wall. Thus, the wall is held in its original plane.

Excavation is then extended to the next anchor level and the anchors installed at that level and so on until the final grade is reached. A cast in place or precast concrete retaining wall is constructed on the face of the retained earth. The anchors can be designed for permanent support of the retaining wall.

The application and design of anchors is described in a Federal Highway Administration report entitled "Permanent Ground Anchors, Report No. FHWA-DP-68-1", dated March, 1984.

d. Deadman Anchored Walls

In this design, deadman anchors (e.g. solid masses such as concrete, rock, or plate elements such as sheet piles, etc.) are placed in the embankment behind the wall (figure 28). Deadmen are connected to the wall by reinforcing steel bars which are protected against corrosion by galvanizing, epoxy coating or by wrapping with tar impregnated cloth or paper. The wall may consist of sheet piles of soldier pile and wood lagging or precast concrete.

e. Composite System

In addition to the different proprietary systems described above, it is possible to combine two systems for certain prevailing conditions. For example, a composite system may consist of a gravity system of retaining wall at the base with a reinforced soil system at the upper part. The lower gravity system could be anchored into the rock base (if one exists) or a permanent grouted anchor system can be utilized in the lower gravity system. The upper system may consist of reinforced soil using one of the proprietary systems described above to reduce the overall cost of the system.

It is necessary to evaluate the stability and performance of such composite systems carefully because of possible differential lateral displacement at the junction between the two systems.
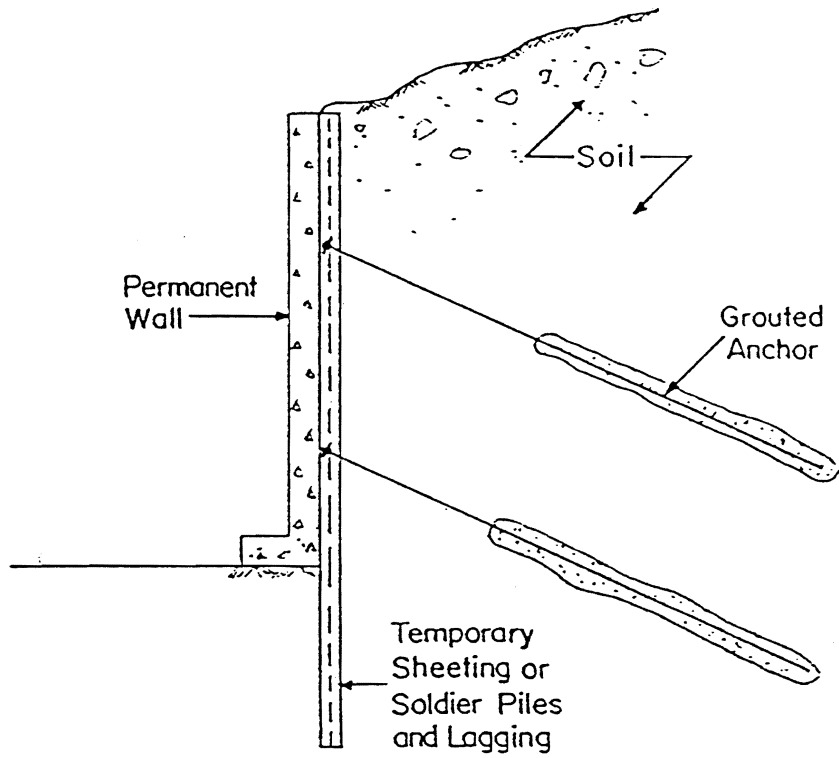
Figure 27. Grouted anchor wall.
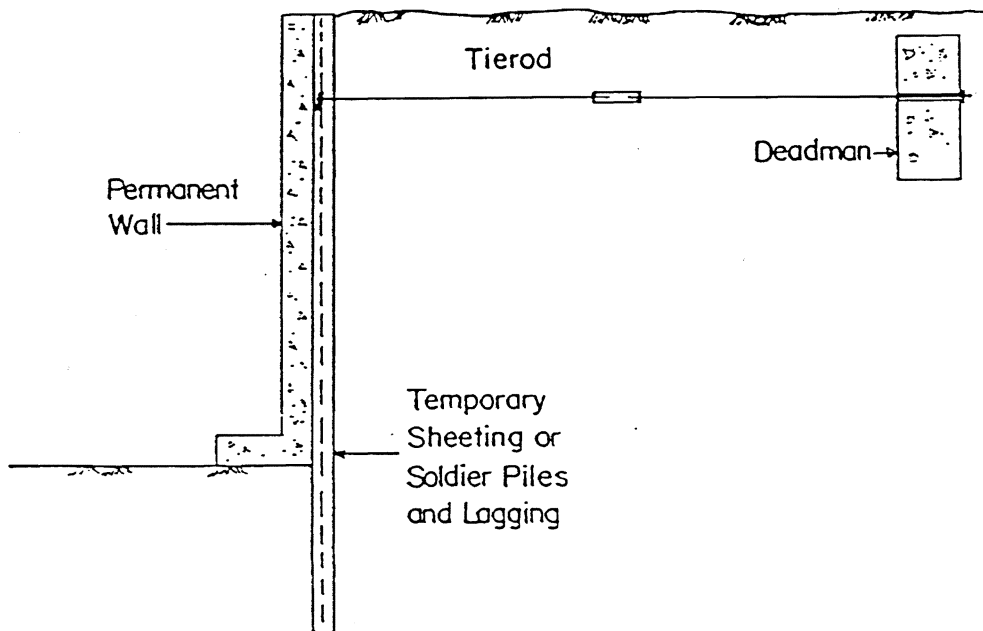
Figure 28. Deadman anchored wall.

A combination of any two systems can be considered provided there compatibility can be assured and the overall system can be designed to perform satisfactorily.

CHAPTER 2

PULLOUT RESISTANCE EVALUATION

1.0 <u>INTRODUCTION</u>

This section provides supporting information for the evaluation of pullout resistance using empirical relations and pullout test results. In addition, information on using the pullout data to evaluate the deformation response is reviewed. Also, evaluation of long term soil and reinforcement creep considerations are discussed.

As indicated in chapter 2 of volume I, the pullout resistance per unit width P_r for any reinforcement system can be estimated using the following general equation:

$$P_r = F^* \cdot \alpha \cdot \sigma'_v \cdot L_e \cdot C$$

where $L_e \cdot C$ = the total surface area per unit width of the reinforcement in the resistivity zone behind the failure surface

L_e = the embedment or adherence length in the resisting zone behind the failure surface

C = the reinforcement effective unit perimeter; e.g., C=2 for strips, girds, mesh and sheets; C=π for nails, in which b = width of strip, grid, or sheet, d = diameter of nail

F^* = the pullout resistance (or friction bearing interaction) factor

α = a scale effect correction factor

σ'_v = the effective vertical stress at the soil reinforcement interfaces.

This equation varies from the conventional equation in that it has been normalized with respect to width to allow for a more general evaluation of any reinforcement geometry. The actual resistance available for any specific type of reinforcement can then be obtained by multiplying P_r by the coverage ratio R or the gross width of the reinforcement b divided by the center to center horizontal spacing between the reinforcements s_h. In addition, to account for nonlinearity of stress distribution along the length of the reinforcement, especially for extensible reinforcements, the scale effect correction factor α has been added to the equation.

The pullout resistance factor F* can most accurately be obtained from pullout tests performed in the specific backfill to be used on the project. Alternatively F* can be derived from empirical or theoretical relationships developed for each soil reinforcement interaction mechanism.

The following subsections provide the necessary information to determine F* and α for the different types of reinforcement.

2.0 ESTIMATE OF FRICTIONAL PULLOUT RESISTANCE

As indicated in equation 1, the pullout resistance of the reinforcement will be dependent on: the pullout resistance factor $F*$; the scale effect correction factor α to account for nonuniform load transfer along the length of the reinforcement; the effective unit perimeter C to account for the effective cross sectional pullout surface for the specific type of reinforcement; and, the design conditions of length and overburden pressure. This section provides guidance for evaluating the coefficients $F*$, C, and α for the various reinforcement types.

a. Inextensible Linear Strip Reinforcements

For inextensible linear strip reinforcement:

$$F* = \mu*, \quad C = 2, \quad \alpha = 1$$

$\mu*$ is an apparent friction coefficient obtained from pullout tests.

The apparent friction coefficient $\mu*$ is mainly dependent upon the surface characteristics of the reinforcements (e.g. rib effect) soil properties (specifically, internal friction angle and dilatancy) and the overburden confinement stress which restrains the tendency of the soil to dilate. Figure 29 shows typical results of pullout tests on smooth and ribbed metallic strips used in Reinforced Earth structures.[63] Figure 30 shows the recommended design μ values.

For ribbed linear strips the maximum apparent friction coefficient at the top of the wall can be estimated from the following relationships:

$$\mu_o* = 1.2 + \log C_u$$

> where: $C_u = D_{60}/D_{10}$ is the uniformity coefficient of the reinforced backfill (D_{60} and D_{10} are the grain diameters at which 60 percent and 10 percent of the soil sample weight is finer). If C_u is not known, assume $\mu_o* = 1.5$ for well graded fill. If a very uniform fill is to be used, assume $\mu_o* = 1$. The design μ value decreases linearly to tan ϕ at a depth of 20 feet (where ϕ is the internal friction angle of the soil).

For smooth strips

$$\mu* = \tan \simeq 0.4$$

> where: ρ is the soil strip friction angle that can be measured by a direct shear test.
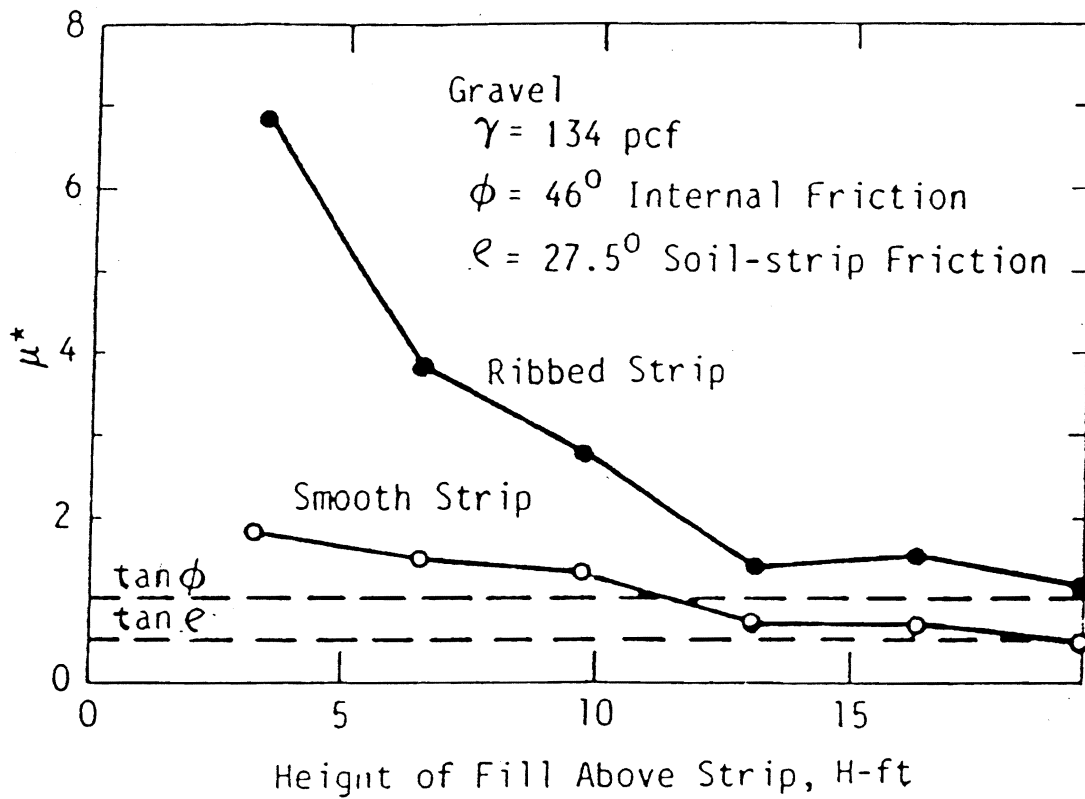
Figure 29. Influence of reinforcement type and overburden stress
on apparent friction coefficient.
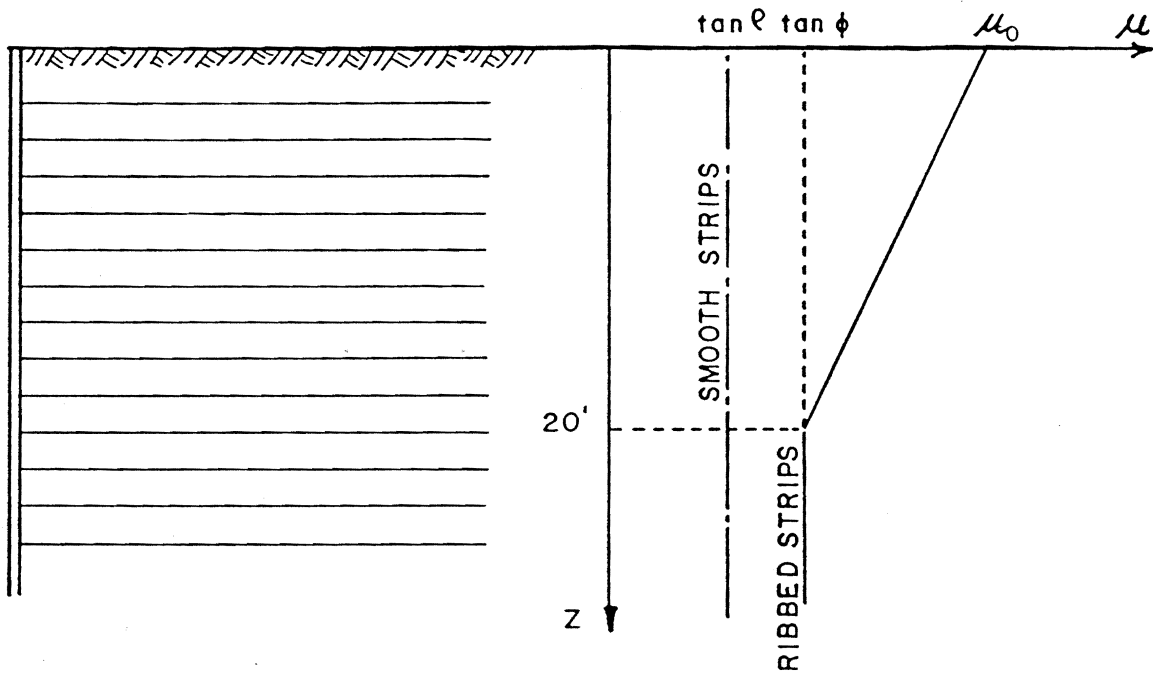
Figure 30. Reinforced earth design $\mu*$ values for smooth and ribbed strips.

<u>Rod Reinforcements</u> (e.g., rods, bars, wires)

$$F* = K \cdot \mu*; \quad \mu* = \tan \rho = 0.4; \quad \alpha = 1$$
$$C = \pi$$

$$K = \frac{\sigma_n'}{\sigma_v'} = \frac{1 + K_o}{2}; \quad K_o = 1 - \sin \phi' \quad\quad (3)$$

where: σ_n' is the average effective normal stress acting on the circumference of the reinforcement

K_o is at the rest earth pressure coefficient

ϕ' is the internal friction angle of the backfill material

K_o value of 0.44 is commonly assumed yielding $K = 0.72$.

b.   <u>Extensible Geotextile Sheet Reinforcements</u>

$$F* = \tan \rho_{peak}; \quad C = 2 \quad \alpha = 1$$

α = should be determined from pullout tests on instrumented geotextile specimens as explained later in this section.

The peak soil fabric friction angle ρ_{peak} can be obtained from direct shear tests carried out in accordance withe the proposed ASTM test method (modified ASTM 3080 using a large 12 in x 12 in (300 mm x 300 mm) direct shear box with the geotextile clamped at the shear interface (FHWA Geotextile Engineering Manual, Appendix B).[25]   The interface shear stress shear displacement curve obtained from the direct shear test will exhibit strain softening which as shown in figure 31 will result in a residual direct shear interface friction angle ρ_{res}.

The scale effect correction factor α indicates the nonlinearity of the P_r – L relationship which is primarily dependent upon the extensibility of the reinforcement. Due to the extensibility of the application of a pullout force on the reinforcement results in a nonuniform shear displacement distribution (figure 32). The interface shear stress is therefore not uniformly mobilized along the total length of the reinforcement. The average shear stress τ_{av} mobilized at the peak pullout load depends upon the reinforcement elongation during pullout which in turn depends upon the extensibility of the reinforcement materials and the reinforcement length. The scale effect correlation factor α can be defined as:

$$\alpha = \frac{\tau_{av}}{\tau_p} = \frac{\tan \rho_m}{\tan \rho_{peak}} \quad\quad (4)$$
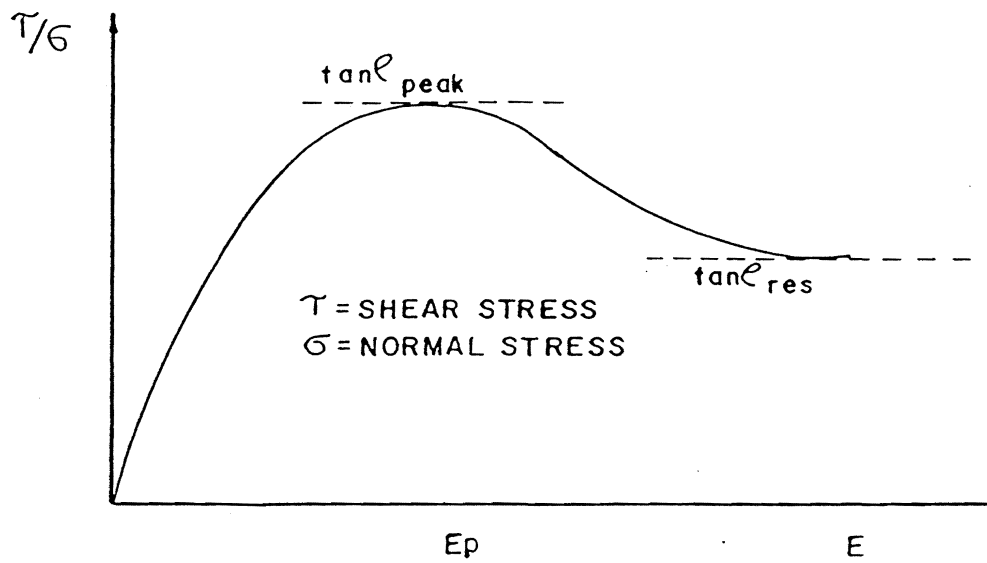
E_p is typically 2 to 5 percent

Figure 31. Stress shear displacement curve from
direct shear test.
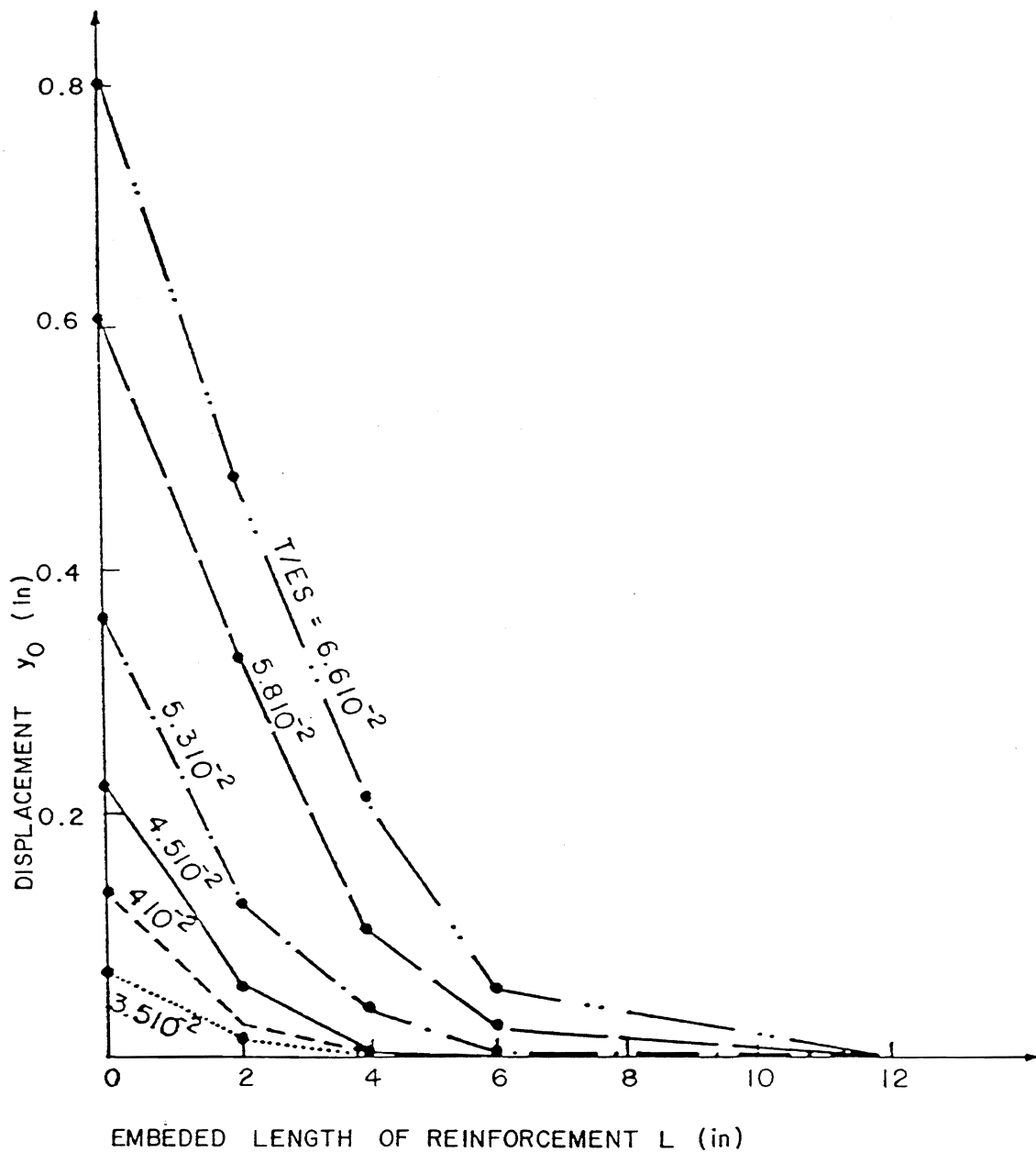
Figure 32. Variation of displacements along a woven polyester strip during a pullout test.

where: τ_{av} and τ_p are, respectively, the average and ultimate interface lateral shear stresses mobilized along the reinforcement.

ρ_m and ρ_{peak} are, respectively, the average and peak interface friction angle mobilized along the reinforcement.

The correction factor α depends therefore primarily upon the strain softening of the compacted granular backfill material, the extensibility and the length of the reinforcement.

Determination of α: Experimental Approach – Pullout Tests

1. Conduct displacement rate controlled pullout tests using proposed ASTM procedures (see Geotextile Engineering Manual, Appendix B) on specimens with different embedment lengths under a specified normal stress.[25]

2. Establish the normalized pullout load ($P_r/R.\sigma_v$) versus length (L) curve as illustrated in figure 33a. (R is the coverage ratio used to equate the force per unit width of discrete reinforcement to the force per unit width across the entire structure. R is equal to the gross width of the reinforcement b divided by the center to center horizontal spacing s_h between strips, sheets or grids).

3. The P_r pullout load is the force applied to the confined portion of the geotextile sample.

4. The initial tangent at the origin of the ($P_r/(R.\sigma_v$) versus L) curve corresponds to the peak interface friction angle ρ_{peak}. The ρ_{peak} angle derived from pullout tests using this procedure can be different from that obtained from the direct shear tests due to differences in the testing procedure, sample preparation and restricted relative soil-to-geotextile movement. The pullout test provides a more appropriate ρ_{peak} value for the estimate of the pullout capacity.

5. Establish the α-L curve as illustrated in figure 33b. α value for a specific L value is defined by the ratio of the secant tangent tan ρ_m for this L to the initial tangent than ρ_{peak}.

Experimental Procedure to Determine α with Instrumented Geotextile Reinforcements

1. Conduct displacement rate controlled pullout tests on instrumented reinforcements under a specified normal stress.

2. Establish the normalized pullout load mobilized length [$P_r/R.\sigma_v$) - L_m] curve. A section of the reinforcement is considered to be mobilized when the wire extensometer indicates movement at its end. The corresponding pullout force is plotted versus the length of the section.

Figure 33.   Experimental procedure to determine α
for geotextile sheets.

Analytical/Numerical Procedure to Determine α

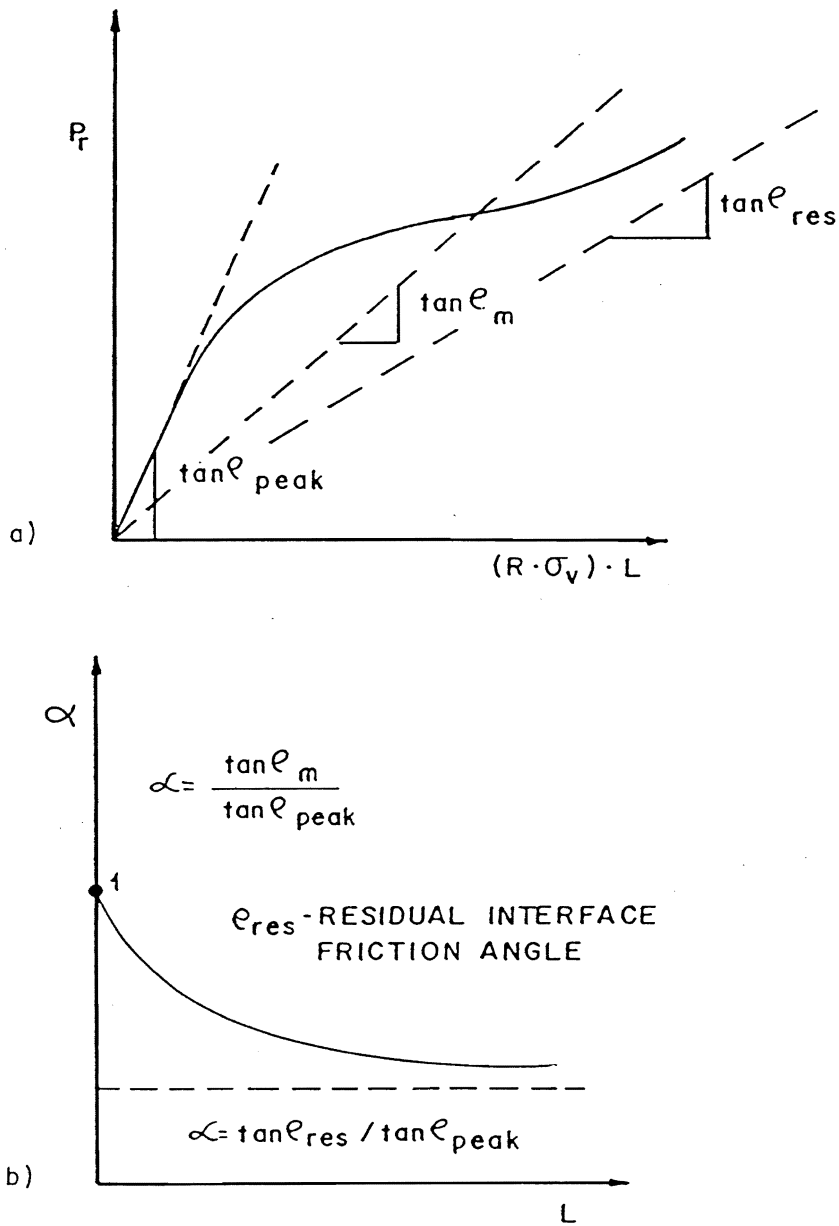Modeling the load transfer mechanism in a pullout test on extensible inclusions, requires appropriate constitutive equations for the soils and the inclusions as well as a rational interaction for the low, relating the shear stress mobilized at any point of the interface to the soil reinforcement shear displacement. This interaction low can be obtained from direct shear tests with soil geotextile interface following the proposed ASTM testing method (modified ASTM 3080).[64] The load transfer model should allow for an estimate of the shear stress distribution along the reinforcement and of the front edge displacement caused by the applied pullout force. The "t-z" method which is commonly used in the design of friction piles can be combined with the nonlinear displacement shear stress relationship obtained from direct shear tests to derive a rational load transfer model.

The load transfer model should be "calibrated" by numerical simulations of pullout tests conducted on the geotextile reinforcement specimens and will then provide an appropriate engineering tool to predict the pullout capacity as a function of the reinforcement length. The use of such a model allows to parametrically evaluate the effect of material properties and interface shear behavior (i.e., strains softening) on the pullout capacity. Figure 34 illustrates the use of such a model for the evaluation of the average limit shear stress at the peak pullout load for different reinforcement lengths and stiffnesses.

3.0   ESTIMATE OF PASSIVE PULLOUT RESISTANCE

In anchored systems that rely on multideadman elements or in reinforced soil systems that use resisting elements oriented transverse to the pullout force direction (e.g., bar mats, wire meshes or geogrids) the pullout resistance is derived entirely or partially from the passive soil pressure on the transverse elements (or deadman).

The maximum passive pullout resistance on deadman or grid transverse elements can be estimated from bearing capacity formula for deeply embedded strip footings (i.e., embedment depth − Z significantly greater than the thickness − t of the bearing number). A generic equation for the pullout passive capacity per unit width of reinforcement can be derived:

$$P_r = [c.t.F_c + \gamma' Z.t.F_q + \gamma' Z t^2 F_\gamma] . f_b . N \qquad (5)$$

where: P_r = the pullout resistance per unit width of reinforcement.

c' is the effective soil cohesion, γ' is the effective unit weight of the soil

59
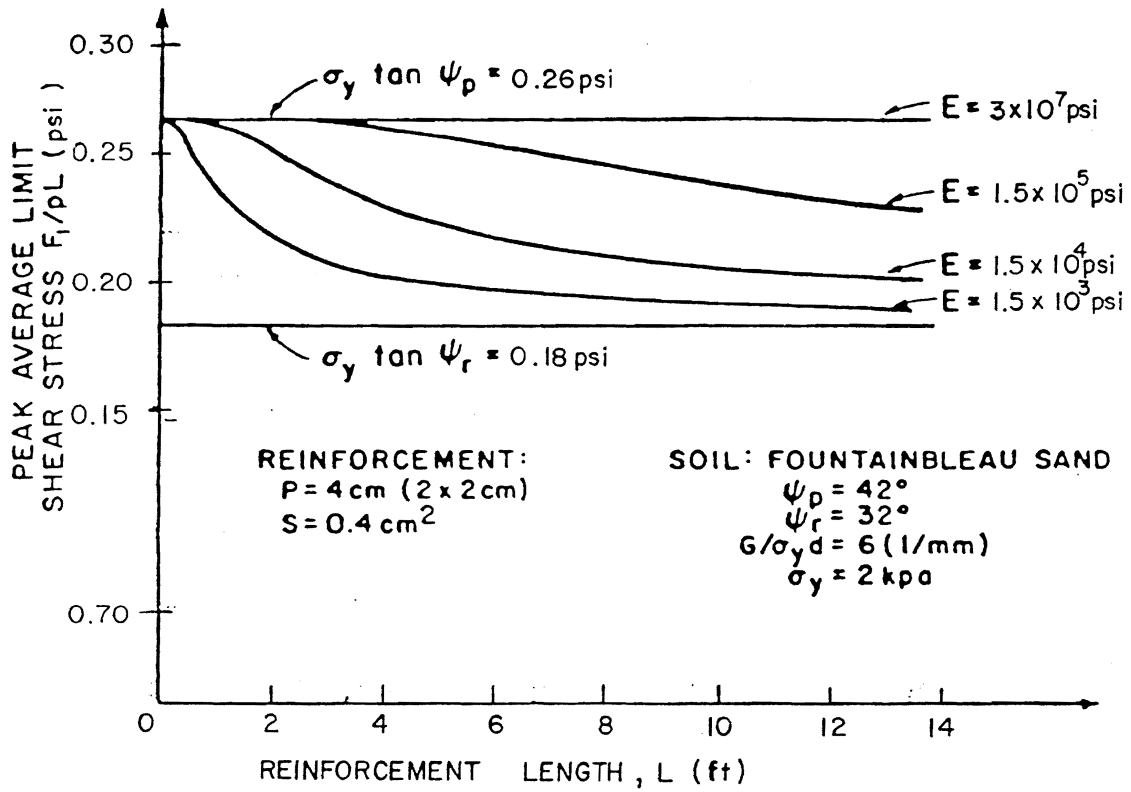
Figure 34. Numerical procedure simulating pullout tests to
establish α-L curve for specific soil
type and reinforcement properties.

f_b is the fraction of the transverse member on which bearing can be fully developed

N number of transverse bearing members

F_c, F_q and F_γ are, respectively cohesion, surcharge (or embedment) and friction bearing capacity factors.

As soil cohesion c' of the backfill material is usually very small the cohesion bearing term can be neglected. In addition, for the deeply embedded transverse members (i.e., t << z) the frictional bearing term can also be neglected as it too is relatively small at that depth. Hence, eq 5 becomes:

$$P_r = F_q \cdot \gamma'z \cdot f_b \cdot t \cdot N \tag{6}$$

Substituting: $N = L_e/S_x$; where S_x is the longitudinal spacing between transverse elements and L equals the length of the reinforcement.

$C = 2$; $\sigma_v' = \gamma'z$; and,

$$\alpha_\beta = \frac{f_b}{2} \cdot \frac{t}{S_x}$$

where α_β is a structural geometry factor for pullout resistance.

Eq. 5 becomes:

$$P_r = F_q \cdot \alpha_\beta \cdot \sigma_v' \cdot L_e \cdot C \tag{7}$$

Note that eq. 7 extends the pullout equation to account for the effect of the structural geometry of the reinforcement on the passive pullout resistance per unit width of reinforce. Introducing the scale effect correction factor α into eq. 8 yields the generic equation for passive pullout resistance:

$$P_r = F^* \cdot \alpha \cdot \sigma_v' \cdot L_e \cdot C \tag{8}$$

with $F^* = F_q \cdot \alpha_\beta$

The maximum passive pullout resistance is obtained as the grid and the soil contained within the grid act as a rough sheet of thickness t being pulled through the soil. For this case the optimal structural geometry is:

$$\frac{S_{opt}}{t} = F_q \frac{f_b}{2 \tan \phi} \tag{9}$$

61
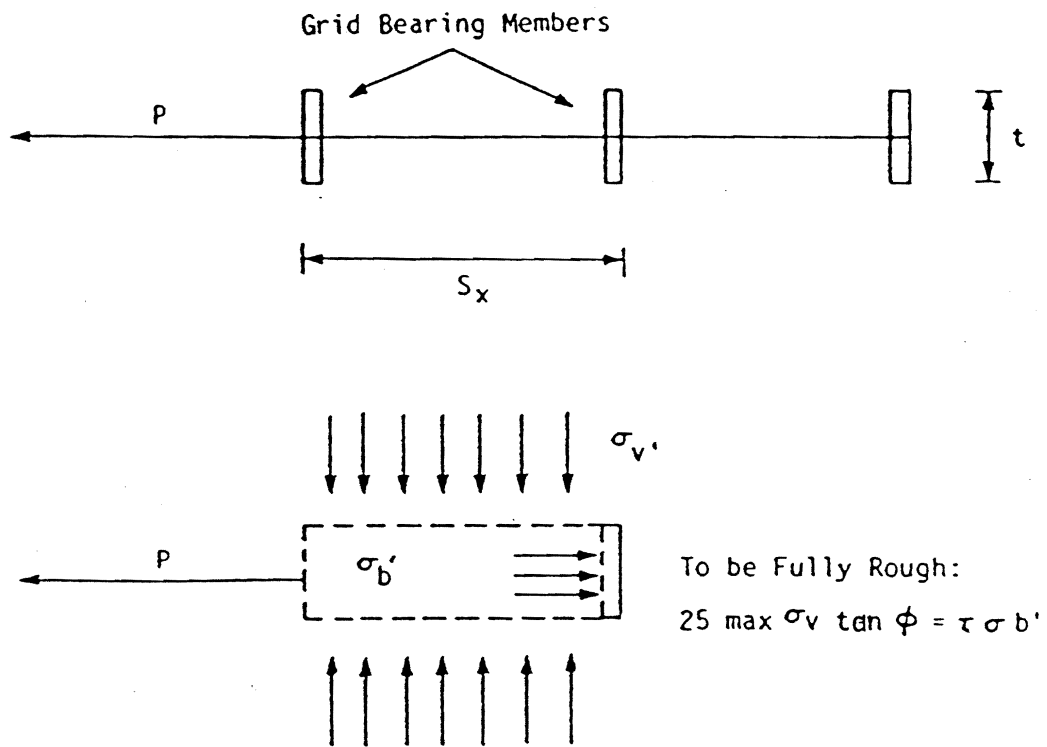
Figure 35. Definition of bearing stresses on
transverse elements.

There would be no increase in the passive pullout resistance for S/t values smaller than those calculated from eq. 9. Greater S/t values will result in a system that does not fully mobilize the maximum passive resistance within the area of reinforcement.

a. Determination of α_β

For anchored systems

$$f_b = 1; \quad S_x = L; \quad \alpha_\beta = \frac{1}{2} \cdot \frac{t}{L}$$

For bar mats and wire mesh systems, the transverse and longitudinal members are in different horizontal planes; hence:

$$f_b = 1; \quad \alpha_\beta = \frac{1}{2} \cdot \frac{t}{S_x}$$

For geogrid systems, all members are in the same horizontal place; hence:

$$f_b = 0.6 \text{ to } 1; \quad \alpha_\beta = \frac{f_b}{2} \cdot \frac{t}{S_x}$$

b. Determination of F_q

The bearing capacity factor F_q, defined as the ratio of the effective bearing resistance σ_b', developed on the transverse elements to the effective vertical stress σ_v', (i.e., $F_q = \sigma_b'/\sigma_v'$, see figure 35) is primarily dependent upon soil strength characteristics and dilatancy properties. The effect of reinforcement roughness and initial stress state in the soil on the bearing capacity of these deeply embedded members can be neglected.

F_q values obtained as a function of soil friction angle using several analysis procedures are shown in figure 36. Rowe and Davis's curves are derived from finite element analysis of horizontally loaded vertical surfaces considering respectively (1) soil dilation, and (2) constant volume (no dilatancy).[65] The upper and lower bounds are derived from Prandtl's bearing capacity solutions for the two failure mechanisms, frictional and bearing, illustrated in figure 35.[34]

The upper bound is given by:

$$F_q = \tan^2 \left(\frac{\pi}{4} + \frac{\phi}{2} \right) \exp [\pi \cdot \tan\phi] \qquad (10)$$

The lower bound is given by:

$$F_q = \tan^2 \left(\frac{\pi}{4} + \frac{\phi}{2} \right) \exp \left[\frac{\pi}{2} \cdot \tan \phi \right] \tag{11}$$

The results of several pullout tests (and large direct shear tests reported in figure 36 show that Rowe and Davis's curves define reasonably well the range of experimental values.[25]

F_q design values have been specified for different reinforcement systems and are summarized in the NCHRP report No. 290 as follows:[2]

Bar mats: Pullout test results on VSL bar mats and bearing capacity factor design values (F_q) are shown in figure 37.[66] In spite of the spread and variability in the test results obtained in different types of soils, the F_q values obtained for the range of backfill materials commonly used are within the predicted range of F_q values indicated in figure 36. Most of the experimental values approach the upper bound defined by eq. 10 or by Rowe and Davis's solution.

Welded Wire Meshes: For commonly used backfill materials (i.e., pea gravel, silty sand, clean sand) pullout tests yielded:[67]

$$F_q = 36.5 \text{ to } 38$$

These values approach the upper bound solution defined by eq. 10.

The pullout test results are reported in figure 38 as passive pullout resistance component versus the overburden pressure. Linear regression of the test results yielded a "cohesion intercept" term F_c for the noncohesive soils (i.e., for clean sand F_c = 633 lb/ft, for pea gravel (F_c = 712 lb/ft) that has been incorporated in empirical correlations developed for design purpose.[2, 67] Because of the uncertainties inherent to these correlations a more conservative approach is retained in this manual neglecting the F_c values in noncohesive soils.

Geogrids: Recommended F_q design values for the estimate of the passive pullout resistance of geogrids are indicated by the dashed line in figure 36.[34]

Anchored Systems (Anchored Earth, Geo-Tech Systems, Tension Retaining Earth System: F_q values for both triangular and "z type" anchors can be calculated from the equation developed by Murray:[68]

For individual triangular anchor ($\Omega = 70°$)

$$F_q = \tan^2 \left(\frac{\pi}{4} + \frac{\phi}{2} \right. \frac{\exp \left[2(\pi - \Omega) \cdot \tan \phi' \right]}{\cos \Omega} \tag{12}$$

where: Ω is the angle defining the bearing wedge ($\simeq 70°$)

64

Figure 36. Theoretical relationship and experimental results bearing stress versus soil friction angle.
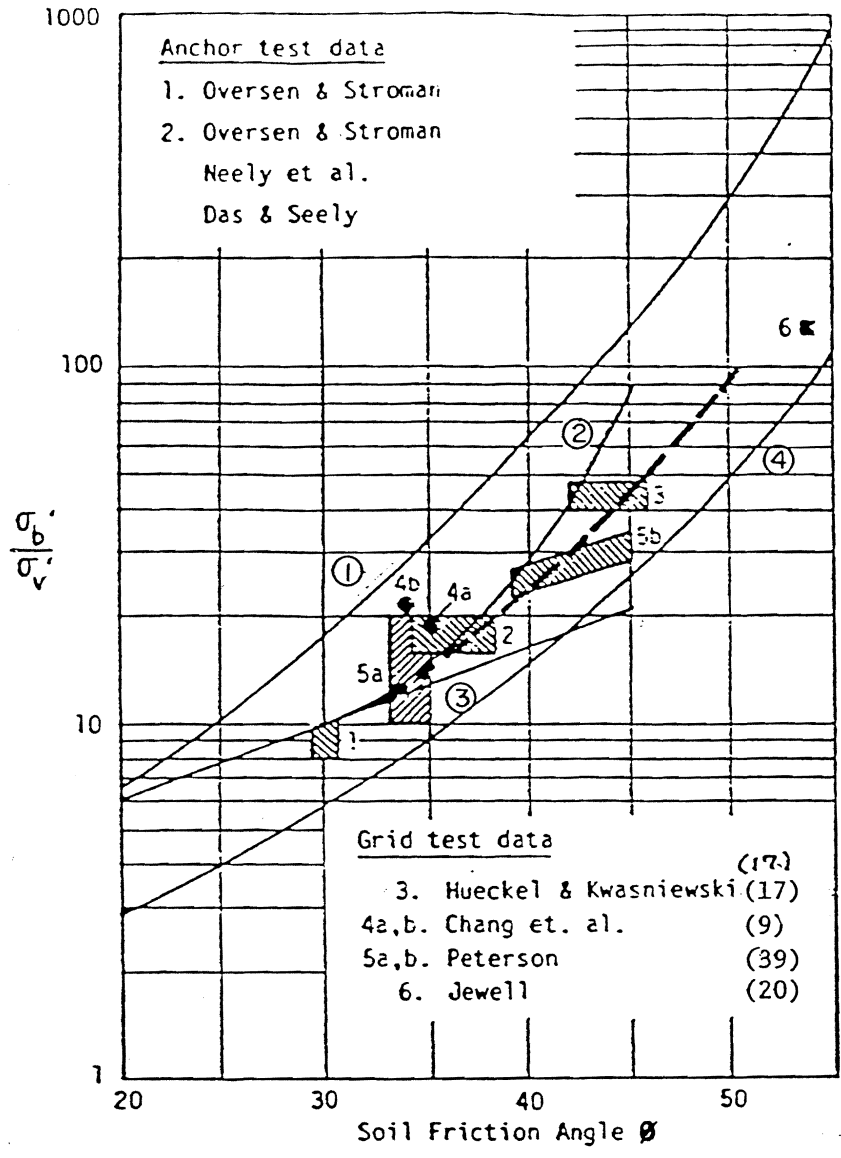
(1) Prandtl (Adapted by Jewell et al.)[34]
(2) Rowe and Davis[65] – Dilation
(3) Rowe and Davis[65] – No Dilation
(4) Jewell et al.[25] – Punching Failure

Figure 37. Pullout test results – VSL bar mats and bearing
            capacity factor design values.

For closely spaced anchors

$$F_q = \tan^2 \left(\frac{\pi}{4} + \frac{\phi}{2} \quad \frac{\exp [2 \frac{3\pi}{\cos \Omega} - \Omega) \tan \phi']}{} \right) \tag{13}$$

Figure 39 shows a comparison between field pullout tests and eq. 12. F_q values for the passive pullout resistance of deadmen can be estimated using eq. 11.

c.   Determination of the scale effect correction factor α

At present, there exists no theoretical formula to account for the scale effect in the estimate of passive pullout resistance. The following are preliminary guidelines but further research on the load transfer along reinforcements that rely on passive earth resistance is required to provide the necessary data basis for more reliable methodologies:

.   Anchor deadman   : $\alpha = 1.$
.   Inextensible metallic grids : $\alpha = 1.$
.   Geosynthetic geogrids   : $\alpha < 1.$

For geogrids the α value should be obtained from pullout tests on instrumented samples following the testing and interpretation procedures outlined in section 2.b. In the absence of pullout test data use $\alpha = 0.6$ for geosynthetics.

4.0   ESTIMATE OF THE PULLOUT CAPACITY OF COMPOSITE REINFORCEMENTS COMBINING FRICTIONAL AND PASSIVE SOIL RESISTANCES

Several composite soil reinforcement systems (e.g., bar mats, wire meshes, geogrids) mobilize their pullout capacity through combination of interface sliding friction and passive soil resistance on the transverse elements. The relative proportions of the pullout capacity mobilized through each mechanism depends primarily upon the ratio of grid aperture size to soil particle size. The relative soil to reinforcement displacement required to fully mobilize these two interaction mechanisms is significantly different (see table 7, volume I) and therefore their relative contribution to the pullout capacity depends upon the displacement. The ultimate pullout capacity of these composite soil reinforcement systems is estimated per unit width of reinforcement by superposing the interface sliding frictional resistance P_f onto the passive pullout resistance per unit width of reinforcement P_p.

$$P_r = P_f + P_p \tag{14}$$

where: $P_f = \mu^* . \alpha . \alpha_f . K . \sigma_v' . L_e . C$

$\alpha = A_s / A_R$ is the fraction of the reinforcement surface area that resists direct shear with soil.

67
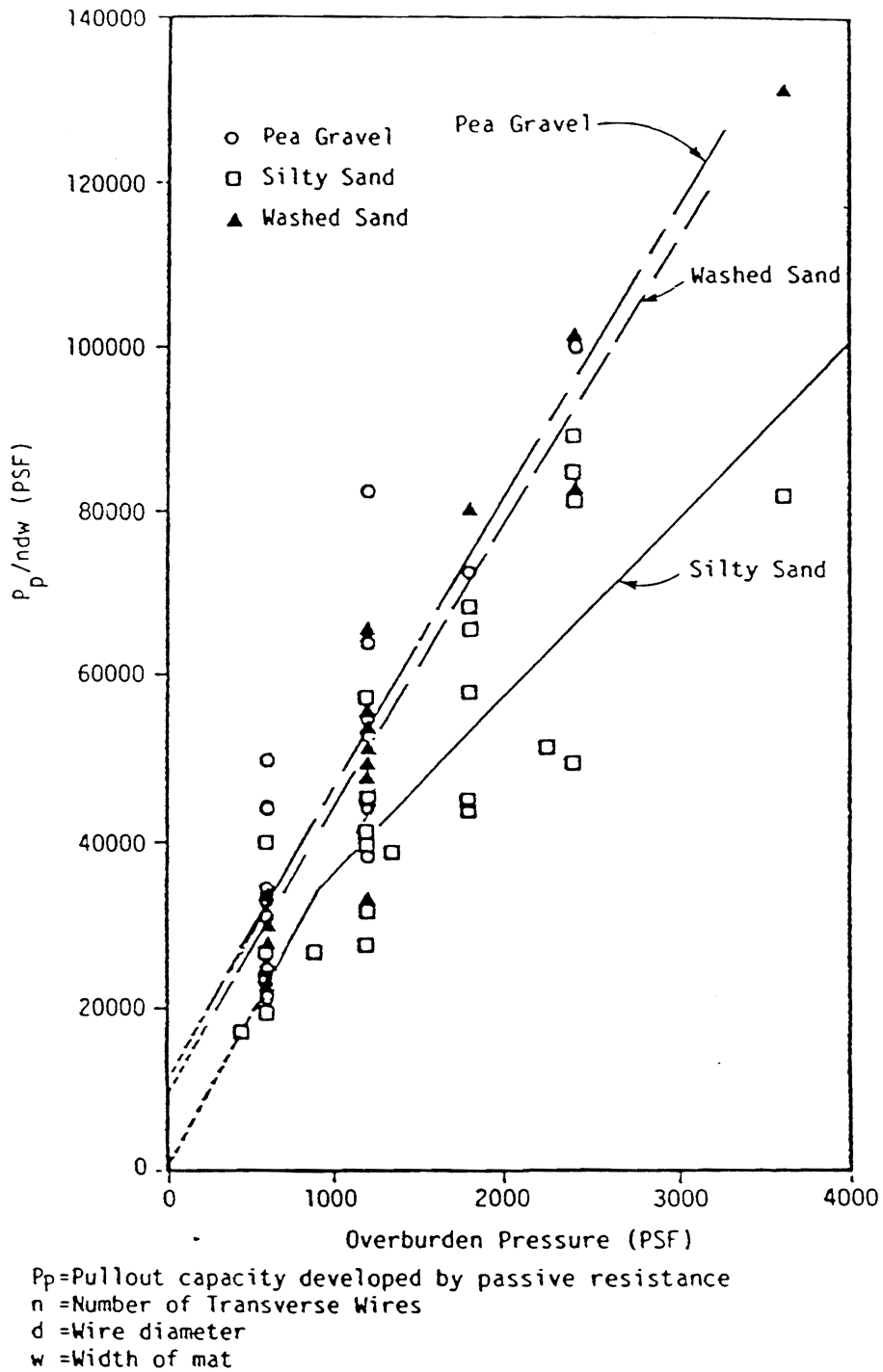
Figure 38. Pullout test results – welded wire meshes.

P_p =Pullout capacity developed by passive resistance
n =Number of Transverse Wires
d =Wire diameter
w =Width of mat

68
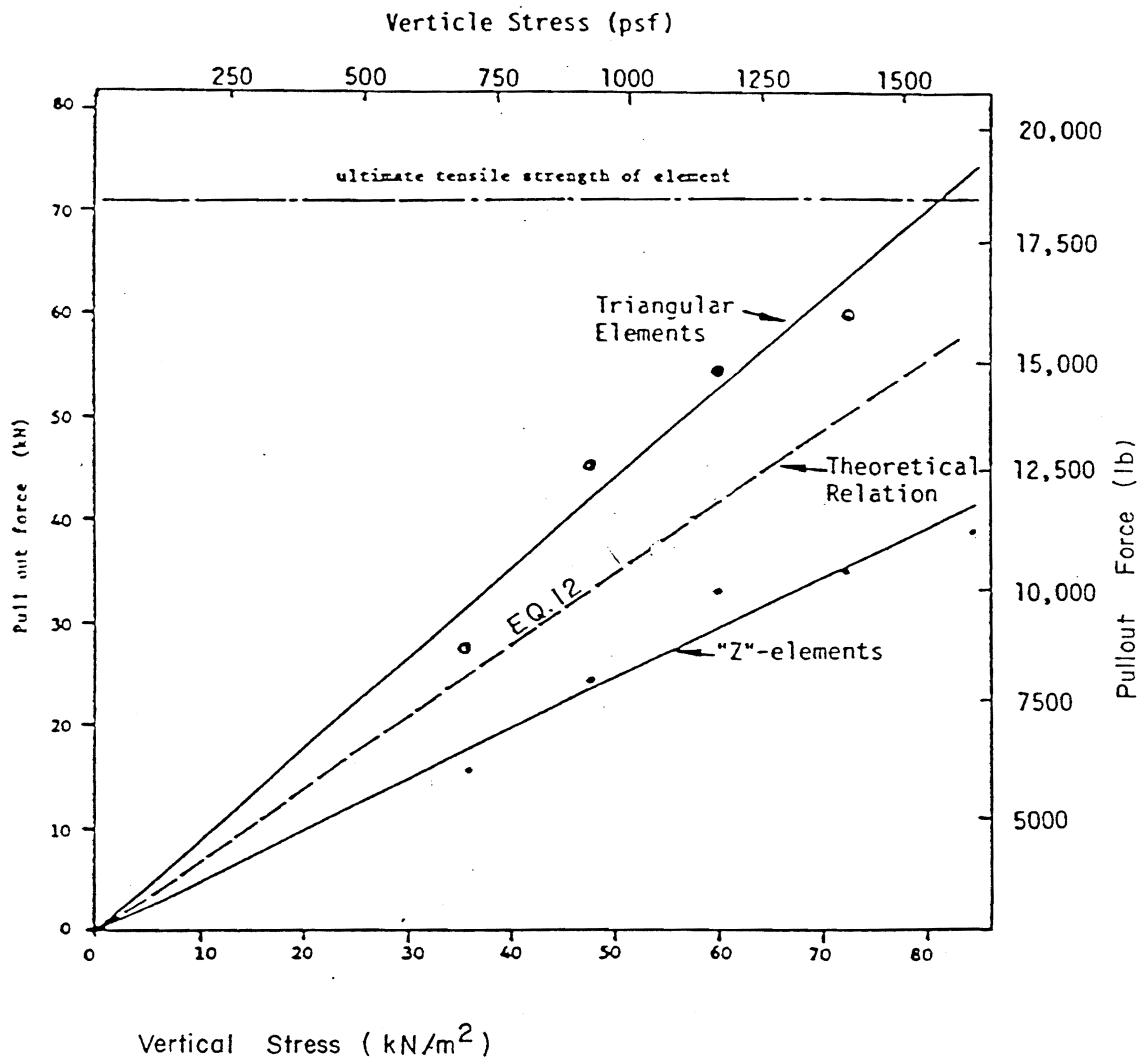
Figure 39. Relation between pullout force and vertical stress.

where: A_s is the surface area of the elements of the reinforcement and A_R is the gross area of the reinforcement.

$$P_p = F_q . \alpha . \alpha_\beta . \sigma_v' . L_e . C$$

Hence:

$$Pr = (F_q . \alpha_\beta + K_\mu* . \alpha_f) . \alpha . \sigma_v' . L_e . C \qquad (15)$$

Note that eq. 15 extends the pullout equation to account for the effect of the structural geometry on the pullout capacity of composite reinforcement with:

$$F* = F_q . \alpha_\beta + K\mu* . \alpha_f \qquad (16)$$

The maximum pullout resistance of a planar composite reinforcement is obtained fro the optimal structural geometry ($S_x = S_{opt}$) defined by eq. 9.

For $S_x \leq S_{opt}$: $F* = \tan \phi$; $\alpha_f = 1$; $K = 1$; $\alpha_\beta = 0$.

a.   Determination of F* for composite reinforcements

Welded wire mesh and bar mat systems

$$\alpha_f = \frac{\pi}{2} . \frac{D}{S_y}$$

where: S_y is the lateral spacing between longitudinal elements.

D is the diameter of the longitudinal elements.

$$\mu* = \tan \delta' \quad K = 0.75; \quad \alpha_\beta = \frac{1}{2} . \frac{t}{S_x}; \quad F_q = 37;$$

$$F = 18.5 \frac{D}{S_x} + 0.475 \frac{D}{S_y}$$

Welded wire meshes frequently used:

W1.7   0.148 in diameter D, 6 in x 6 in or 6 in x 9 in
W2.5   0.178 in diameter D, 6 in x 6 in or 6 in x 9 in
W3.4   0.207 in diameter D, 6 in x 6 in or 6 in x 9 in

Bar mats frequently used:

W11   0.375 in diameter D, 6 in x 24 in
W20   0.5 in diameter D,   6 in x 24 in

70

Geogrids

The pullout resistance and direct sliding resistance of geogrids depend upon the Grid Aperture/Average Grain Size (D_{50}) ratio. Eq. 16 provides a reasonably conservative design value for Grid Aperture/Grain Size ratio > 3.[69] Hence:

For $S_x < S_{opt}$ (Eq. 8)

$$F* = \tan \phi; \quad \alpha_f = 1; \quad \alpha_\beta = 0; \quad K = 1$$

For $S_x > S_{opt}$

$\mu* = \tan \delta$; where δ is the interface soil plastic friction angle

$\alpha_f = \alpha_s$; where α_s is the fraction of solid surface area in the grid

$$\alpha_\beta = \frac{f_b}{2} \cdot \frac{t}{S_x}; \quad f_b = (1 - \frac{r}{S_y})$$

where: r is the width of the longitudinal element in the grid

$$F^* = F_q \cdot \alpha_\beta + \tan \delta \cdot \alpha_s$$

For large soil particles that cannot penetrate the grid aperture (Grid aperture/Grain Size ratio < 1):

$$F^* = \mu^* = \tan \delta; \quad \alpha_f = 1; \quad \alpha_\beta = 0$$

71
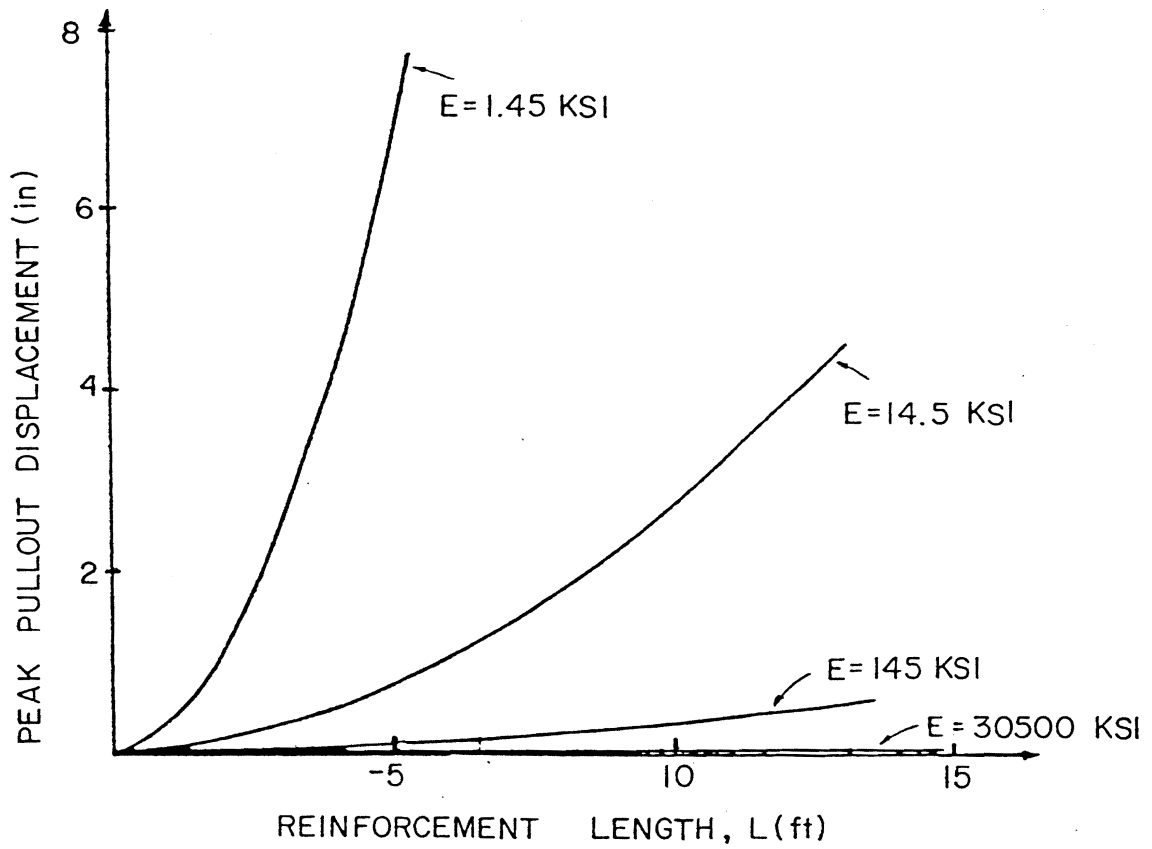
Figure 40. Peak pullout displacement for geosynthetic
reinforcements vs. reinforcement length.

5.0   SUMMARY OF PULLOUT DESIGN PARAMETERS

The pullout capacity of all reinforcement systems is estimated using the general equation:

$$P_r = F^* \cdot \alpha \cdot \sigma_v{}' \cdot L_e \cdot C \tag{16}$$

$$F^* = F_q \cdot \alpha_\beta + K \cdot \mu^* \cdot \alpha_f \tag{17}$$

The pullout capacity design parameters for the generic soil reinforcement systems considered in this manual are summarized in table 7 of Volume I.

6.0   EVALUATION OF ALLOWABLE DISPLACEMENTS FROM PULLOUT TESTS

The soil to reinforcement relative movement required to mobilize the design tensile force depends upon the load transfer mechanism, the extensibility of the reinforcement material, its creep characteristics and soil type. As illustrated in figure 40, for extensible geotextile sheet reinforcements, geogrids or plastic parallel strips, the peak pullout displacement is primarily a function of the reinforcement length. Extrapolation of pullout test results, to reinforcement of different dimensions requires a careful evaluation of the scale effect as it relates to the load transfer along the length of the reinforcement. Estimate of the scale effect requires an adequate estimate of the confined stress-strain properties of the reinforcement and the appropriate soil to geotextile (or geogrid) interaction mechanism.

An analytical solution for the front displacement-pullout force relationship for extensible reinforcements was derived assuming:[70]

   (a)   Reinforcement is linearly elastic.

   (b)   The interface layer is elastic perfectly plastic.

The front edge displacement y_0 is given by:

$$Y_0 = \frac{1}{2} Y_c \left[1 + \left(\frac{\lambda}{Y_c}\right)^2 \left(\frac{T_0}{EA}\right)^2 \right] \tag{18}$$

where: T_0 is the pullout force

   $\lambda = \sqrt{EA/kCb}$ is a reference "transfer length"

   E is the elastic modulus of the reinforcement, as measured in a tension test.

A is the area of the solid portion in the cross section of the reinforcement,

C is the effective unit perimeter of the reinforcement,

b is the gross width of the reinforcement,

k is the shear modulus of the interface,

y_c is the shear displacement required to mobilize the limit interface shear stress: $\tau_{max} = k \cdot y_c$.

The interaction parameter k can be derived either from direct shear tests with soil-geotextile (or geogrid) interface or from pullout tests. Figure 41 illustrates the interpretation procedure for pullout tests on extensible reinforcements to obtain the interaction parameters k and λ.

This procedure consists of drawing the pullout curve in the plane of $(T/EA)^2$ vs. y_0. For $y_0 > y_c$ the experimental curve can be assimilated to a straight line. The linear regression of the experimental results will provide:

. An initial y_0 intercept equals $y_c/2$.

. A slope equals $\lambda^2/(2y_c) = \eta$.

The soil-reinforcement interaction parameters can then be calculated as:

$$\lambda = [2y_c \, \eta]^{1/2} \; ; \; k = \frac{EA}{Cb} \cdot \frac{1}{\lambda^2}; \; \tan \rho = \frac{k \cdot y_c}{\sigma'_v} \, .$$

7.0 SOIL NAILING - ESTIMATE OF PULLOUT CAPACITY

The load transfer mechanism between the nail and the subsurface soil (or rock) and the ultimate pullout capacity depend upon several parameters including: installation technique, drilling and grouting method, grout pressure, size and shape of the grouted inclusion, engineering properties of the in-situ soil and specifically its relative density (or overconsolidation ratio), hydraulic conductivity, and shear strength characteristics.

a. Grouted nails

Grouted nails are generally gravity grouted. Their pullout resistance is therefore expected to be approximately the same as that of an equivalent straight-shafted anchor, tremie-grouted under low (or no) grout pressure. The pullout capacity of these anchors if often estimated by:

74
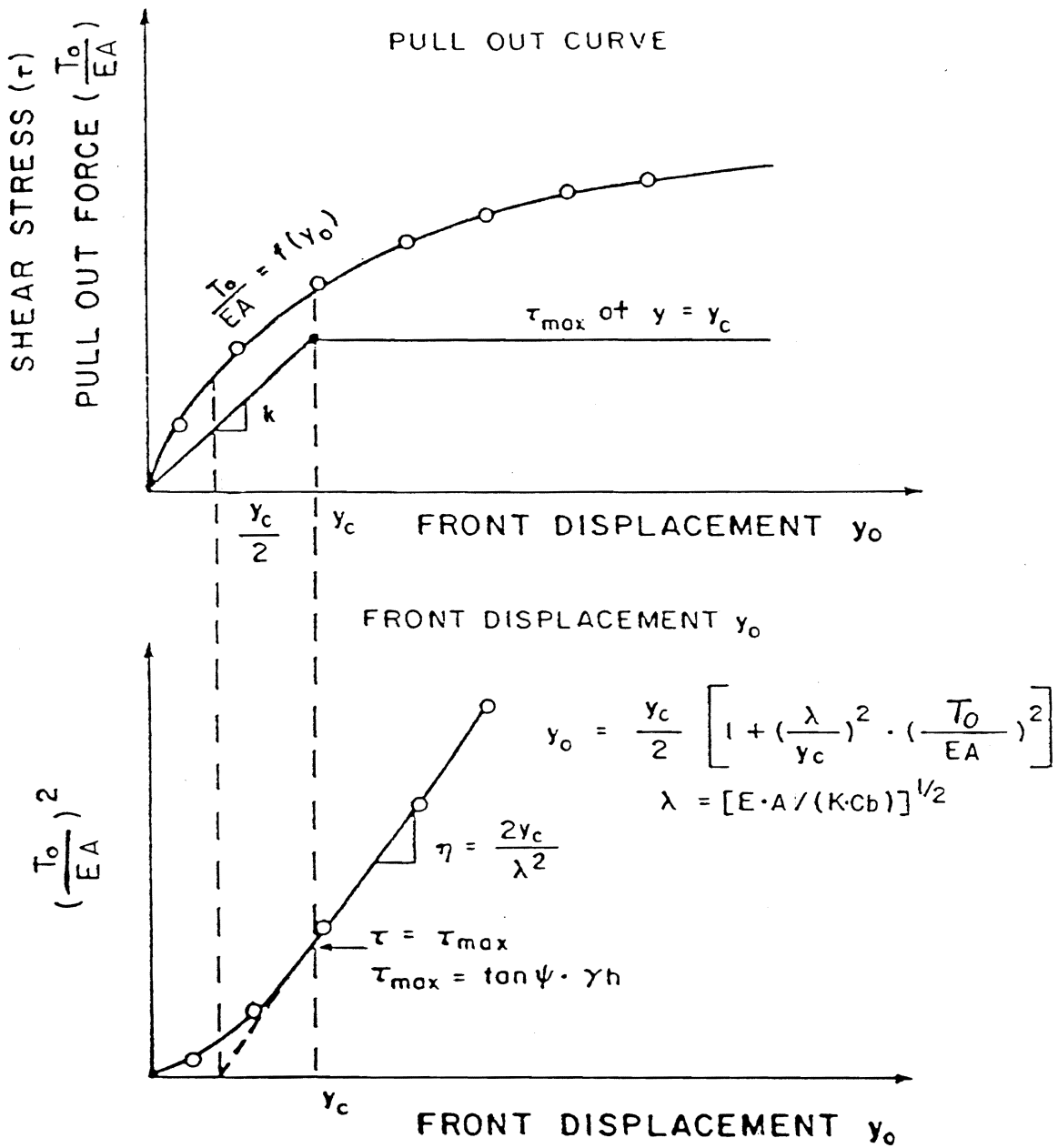
Figure 41. Interpretation procedure for pullout tests on extensible inclusion.

$$P = \pi \, D \, L \, \tau_{ult} \qquad (19)$$

where: τ_{ult} is the ultimate lateral shear stress at the ground - grout interface (also called shaft friction),

D and L are, respectively, the effective diameter and length of the grouted anchor.

It is commonly assumed that:

In competent rocks:

$$\tau_{ult} = 10\% * S_a \text{ for } S_a < 600 \text{ psi} \qquad (20)$$

where: S_a is the uniaxial compressive strength.[71]

In cohesive soils:

$$\tau_{ult} = \alpha \cdot S_u \qquad (21)$$

where: (α) is an adhesion factor,

S_u is the average undrained shear strength of the soil.

The adhesion factor (α) generally varies within the range of 0.3 to 0.75 with the lower values obtained for stiffer and harder clays.[45, 72, 73]

In granular soils an "apparent friction coefficient" is generally used to take into account the restrained dilatancy effect on the soil-nail frictional resistance:

$$\tau_{ult} = \gamma' \, h \, \mu^* \qquad (22)$$

where: γ' is the effective unit weight of the soil,

h is the overburden height above the nail at the mid point of its adherence length,

μ^* is the apparent friction coefficient.

It should be indicated that the effective diameter D of the grouted nail is difficult to estimate since it is highly dependent upon the installation process, ground porosity and grout conductivity.

The drilling of the borehole for the grouted nail produces an unloading of the disturbed surrounding soil that can significantly affect its mechanical properties. The soil-nail interaction is primarily dependent upon soil recompaction due to grouting. In cohesionless soils, grouting pressures of 50 to 100 psi are commonly used to prevent caving as the casing is

withdrawn. This pressure grouting will induce ground recompaction associated with grout penetration into permeable gravelly seams, thereby increasing substantially the pullout resistance of the nail. In a fine grained cohesive soil the tremie-grouting results in a rather smooth soil – inclusion interface. The presence of water at the interfaces, specifically in plastic soils, will generate a lubrification effect decreasing substantially the pullout resistance of the nail. Figure 42 shows a summary of pullout test results obtained with low pressure grouted nails in different types of soils.[74] In the majority of these projects, the nails were installed in preaugered boreholes. The results illustrate the variability of pullout resistance and the difficulty in extrapolating pullout information from one site to another. The results support the need for pullout testing, even for preliminary design evaluation.

b. Driven nails

Pullout tests on driven nails in a granular nailed wall reported by Cartier and Gigan have shown that the apparent friction coefficient μ^* values correspond to the design values generally used for the ribbed metallic strips in Reinforced Earth walls (figure 43).[37] At relatively low depth, due to the restrained dilatancy effect, the value of μ^* is significantly greater than tan ϕ and it decreased with depth to tan ϕ. However, the construction process will significantly affect pullout capacity. Laboratory scale pullout tests in a medium dense sand illustrated that Reinforced Earth (i.e., placing the inclusion during the construction and compacting the sand around it) produces a substantially higher apparent friction coefficient than nailing by driving the inclusion into the compacted sand embankment.[42] In the latter case, nail driving will significantly reduce the retained dilatancy effect on the pullout resistance. Therefore, design guidelines for Reinforced Earth walls cannot be safely extrapolated to soil nailed structures.

c. Jet grouted nails

These nails are installed under a grout pressure than can exceed 20 MPa and is sufficiently high to cause hydraulic fracturing of the surrounding ground.[73] Similar to high pressure grouted anchors, the jet grouting installation technique produces a mechanical interlocking between the penetrating grout and the surrounding ground which results in a substantial increase of the effective nail diameter. It also provides recompaction of the surrounding ground that significantly improves the pullout resistance of the composite nailed soil inclusion. Field pullout tests on jet grouted nails yielded ultimate lateral shear stress values as high as 400 kPa in sands and 1000 kPa in sandy gravels.[74]

d. Estimate of the pullout resistance

To date, estimate of the pullout resistance of nails (or ground anchors) is mainly based upon empirical formulas (or ultimate
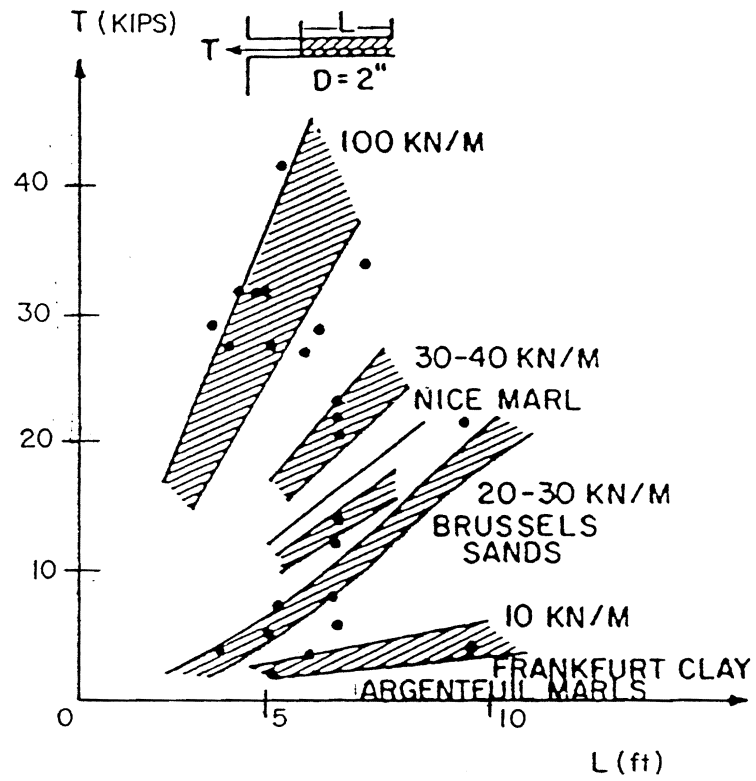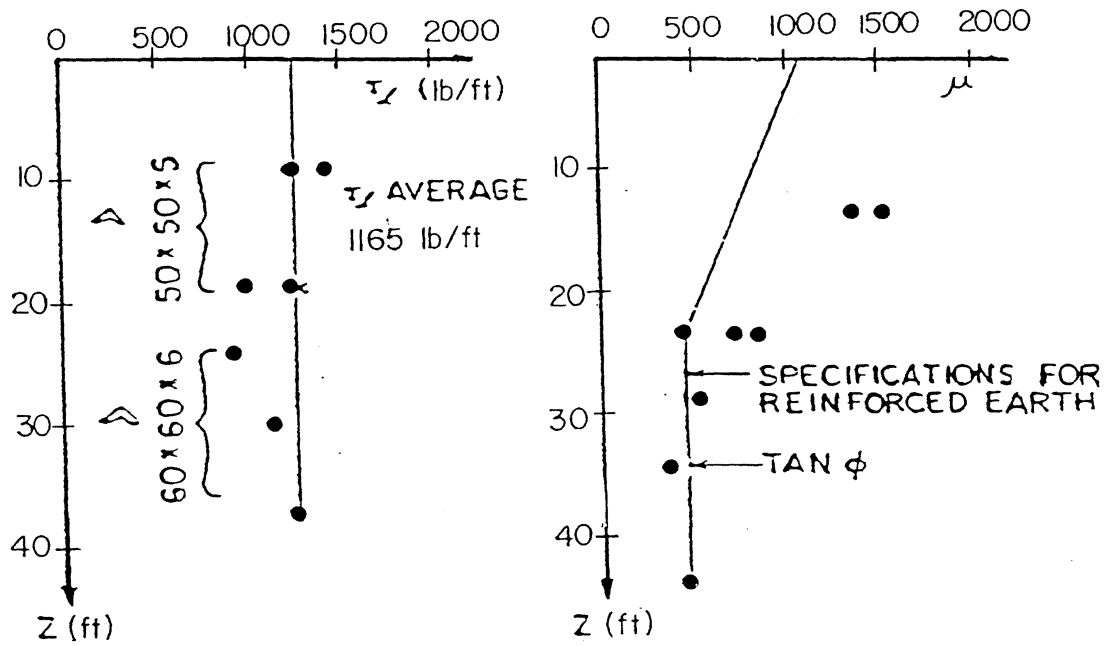
Figure 42. Pullout test results.

Figure 43. Pullout test results on driven nails
in granular soils.

lateral interface shear stress values) derived from field experience. These formulas are useful for feasibility evaluation and preliminary design. Table 2 provides a summary of ultimate interface lateral shear stress values as a function of soil (or rock) type and installation technique.[76]

Recently an increasing attempt has been made to develop field correlations between the ultimate lateral shear stress τ_{ult} mobilized along anchors and nails and the engineering properties of soils obtained from commonly used in-situ tests, specifically the Standard Penetration Test and the self boring pressuremeter test. The available field data pertaining to the pullout capacity of nails is presently still too limited to substantiate development of reliable correlations. An attempt has been made to predict the pullout capacity of both driven and grouted nails using the French recommendations for the determination of lateral shaft friction on bored and driven concrete piles from pressuremeter test results.[77] Figure 44 shows that in fine grain soils (i.e. fine sands, silts, non plastic clays) predicted τ_{ult} values correlate reasonably well with pullout test results while in dilatant gravely soils, compacted moraine or fissured rocks they generally underestimate the measured ultimate lateral shear stress.

It appears that further research and particularly field testing could significantly improve the data base for estimating the pullout capacity of soil nails. However, in light of the large variability of parameters affecting the load transfer mechanism, specifically in heterogeneous soils, empirical correlations can only be used for preliminary design. Pullout tests are required to provide reliable data for final design and to verify the design during construction by testing non-service witness nails.

8.0 LONG TERM PERFORMANCE AND CREEP CONSIDERATIONS

Long term performance of the reinforced soil system depends primarily upon the creep potential of the reinforcement and the soil. In order to assess long term pullout capacity of soil nails in the fine grain soils and geosynthetic reinforcements and to evaluate the potential of the ground inclusion system to creep, the pullout tests should be load controlled.

a. Soil Nailing

The field testing procedure currently used for soil nailing is similar to anchor loading test. It usually consists of 10 to 20 min. sustained load increments of $0.15 f_y$ (where f_y is the yield strength of the steel nail). Each load increment is maintained until measured deflection is negligible (i.e., displacement rate smaller than a specified displacement increment per log cycle of time). The incremental loading is applied until pullout failure is generated. The tested nail, minimum length 8 ft., should be installed using the same installation process of production nails.

Table 2. Ultimate Lateral Shear Stress Data for Preliminary Design of Soil Nailing.[74, 76]

Soil (or Rock) Type	Construction Method	Ultimate Lateral Shear Stress (psf)
Silty sand Silt Piedmont residual	Rotary drilling	2,000 – 4,000 1,200 – 1,600 1,500 – 2,500
Sand Sand/gravel	Driven casing	6,000 8,000
Granular Soils Dense moraine Colluvium		8,000 – 12,000 2,000 – 4,000
Sand Sand/gravel	Jet grouted	8,000 20,000
Silty sand fill	Augered	400 – 600
Soft clay Still clay Clayey silt	Augered	400 – 600 800 – 1,200 1,000 – 2,000
Cohesive Soils Calcareous sandy clay		4,000 – 6,000
Clayey colluvium	Driven	1,000 – 2,000
Marl/limestone Phillite Chalk Soft dolomite Fissured dolomite Weathered sandstone Weathered shale Weathered shist	Rotary drilling (dry)	6,000 – 8,000 2,000 – 6,000 10,000 – 12,000 8,000 – 12,000 12,000 – 20,000 4,000 – 6,000 2,000 – 3,000
Marl Stily marl	Augered	4,000 6,000

81

Figure 44. Comparison between measured and estimated values for ultimate lateral shear stress.

LEGEND:

1. Driven bars in fine grained soil
2. Grouted bars in fine grained soil
3. Driven bars in granular soil
4. Grouted bars in weathered rock
5. Grouted bars in soft clay
6. Grouted bars in stiff clay
7. Grouted bars in marl
8. Grouted bars in still marl
9. Grouted bars in clayey silt
10. Drilled & Grouted bars in silt
11. Drilled & Grouted bars in silty sand
12. Driven casing grouted bars in sand
13. Driven casing grouted bars in Moraine
14. Driven casing grouted bars in Colluvium clays
15. Drilled & Grouted bars in marl-limestone
16. Drilled & Grouted bars in soft rock
17. Drilled & Grouted bars in fissured rock

In soils susceptible to creep, the critical creep load should be established, following a procedure similar to that used for ground anchors which is illustrated in figure 45.[33]   For each load increment the measured nail displacement (s) is plotted versus Log. Time (T). An upward concavity of the creep curve indicates an accelerated creep inducing failure. The slope of the (s) vs. (Log. T) line is plotted against the applied pullout load to determine the critical creep load T_c.

The time dependent nail displacement under a constant load can be consistently described using Singh and Mitchell's creep model.[78] For ground anchors, the creep displacement of the nail under a sustained load can be estimated using Singh and Mitchell's type equation:

$$\Delta l = \Delta l_0 + \frac{Ae^{\alpha T}}{1 - m} (t^{1-m} - 1) \text{ for } m \neq 1 \tag{23}$$

$$\Delta l = \Delta l_0 + Ae^{\alpha T} \ln t \qquad \text{for } m = 1 \tag{24}$$

where: T and Δl_0 are respectively the applied pullout force and the initial displacement prior to creep,

A, α and m are interface creep parameters that are obtained from the experimental "log Δl – log t" (i.e. displacement versus time under constant load) and "log Δl – T" (i.e. displacement versus applied load) curves, (see Figure 46).

Δl is the displacement rate.

Figure 46 illustrates the creep behavior of an anchor in a plastic clay and the determination of the relevant interface creep parameters.[79]   The "m" parameter which is the slope of the "log Δl – log t" linear relationship indicates the creep potential of the soil. "m" values smaller than one indicate a relatively high potential for accelerated (or tertiary) creep inducing a creep rupture.

Geosynthetic reinforcements

Creep considerations with regard to the long term performance of geosynthetic reinforcements have been outlined in NCHRP Report 290 and are briefly summarized below.[2]

The time dependent stress-deformation behavior of unconfined polymeric materials, schematically illustrated in figure 47, involves instantaneous recoverable primary creep, long term non recoverable secondary creep and tertiary creep to rupture similar to that observed in soils by Singh and Mitchell.[78]   The creep potential depends upon the basic polymer properties, structural aspect (woven vs. nonwoven), manufacturing process (e.g., heat or resin bonding vs. needle punched) and environmental factors, specifically temperature.
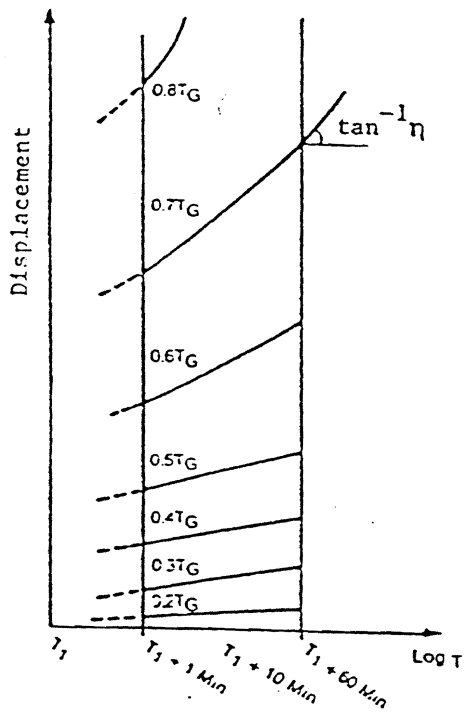
Figure 45.   Anchor tension test for determination
of critical creep load.

Figure 46. Modeling creep of anchors in clays.
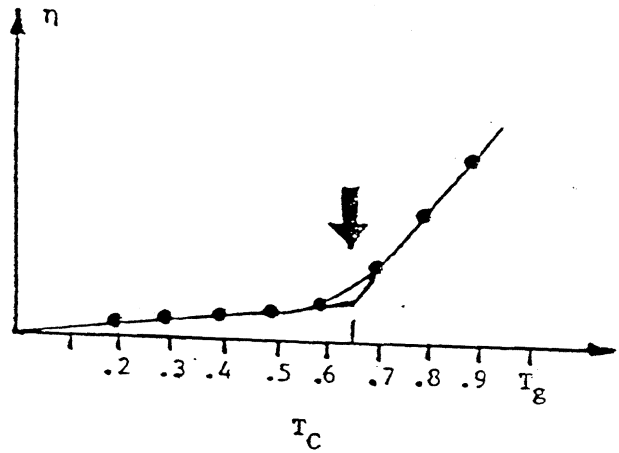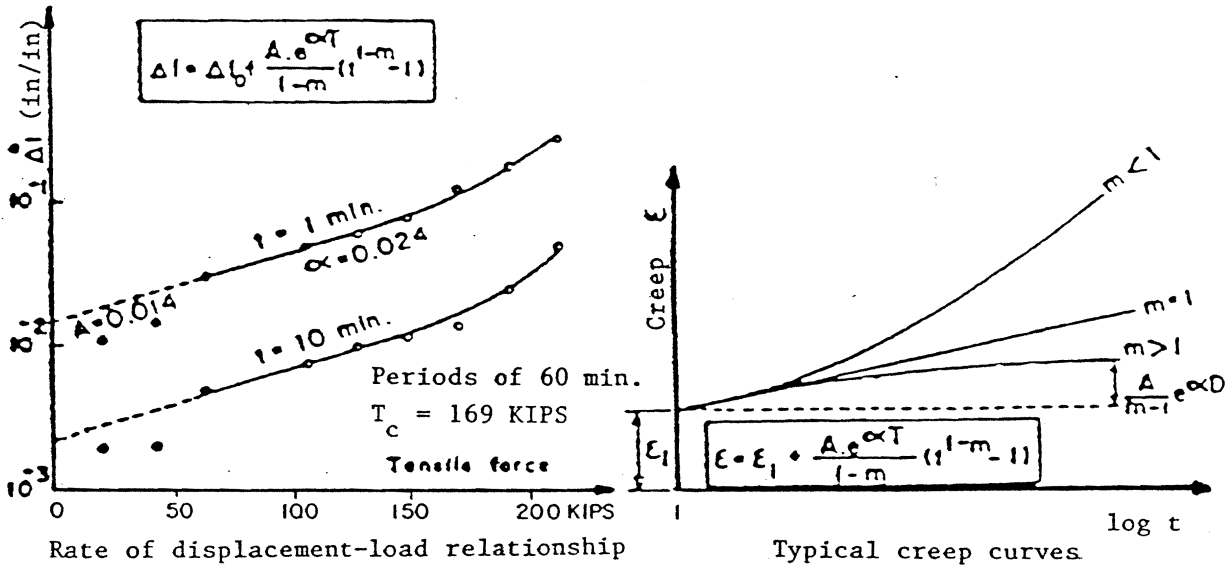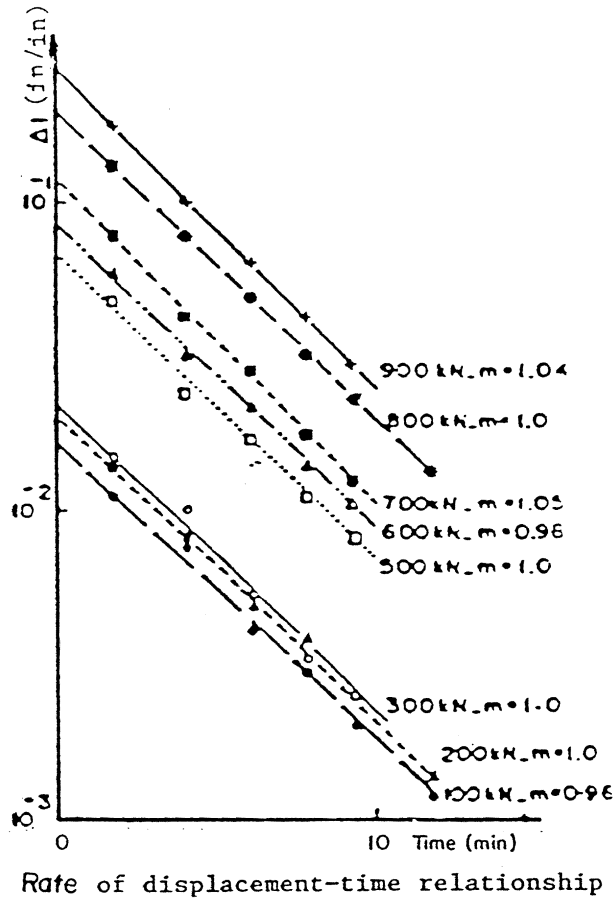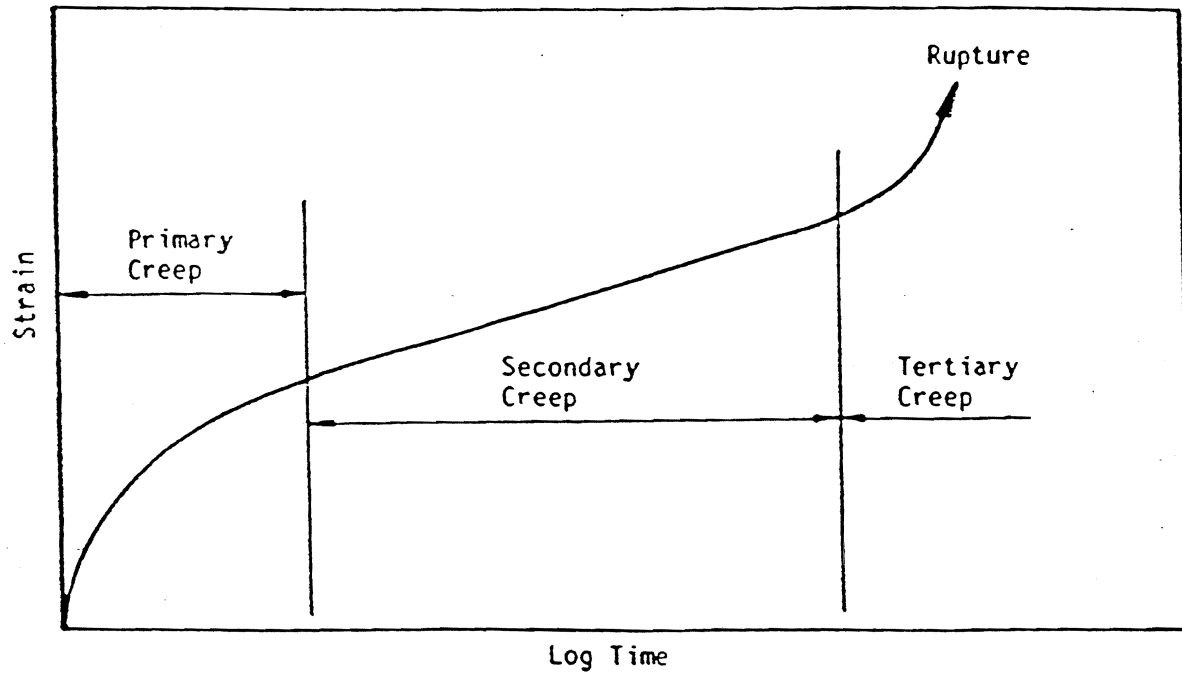
Figure 47.   Phases of creep for a typical geotextile tested
without soil confinement at constant
load and temperature.

The main design concerns are (1) to evaluate the critical creep load or creep strain below which creep rupture is unlikely to occur, and (2) to predict the long-term creep displacement under a constant tensile load.

For design purpose, creep test data may be plotted in the form of isochronous curves to allow extrapolation of the test results to the specified service life of the structure under a given performance limit strain. Figure 48 shows creep tests data obtained for Tensar SR-2 at 20°C. The data may also be plotted as shown in figure 49 is recommended for the determination of the critical creep strain data.[80] The data reported in figure 48 suggest that for Tensar SR2, creep rupture is unlikely to occur for overall strains smaller than 10%. The critical creep strain translates to a critical creep load through the use of stiffness isochrones shown in figure 49 that provide the deformation modulus for the specific service life of the structure.

The creep response of geotextiles confined in the soil may be substantially different from their in-isolation performance. The confinement effect is highly dependent on the structural aspect. It is generally significantly greater with nonwoven geotextile where the combined effect of grain interlocking and soil confinement substantially reduces the short and long term creep deformation. Figure 50 shows the confinement effect on the load-deformation time behavior of nonwoven needle punched polypropylene Terram 1000 and nonwoven polyester Bidim U24.[81] Apparent unconfined creep testing of geotextiles can significantly overestimate the in-soil long term deformation.

Load controlled pullout tests should be conducted to evaluate the in-soil confined creep behavior of geosynthetics. The creep displacement is function of material properties and reinforcement length. Similarly to the evaluation of the scale effect correction factors for extensible reinforcements it is necessary to evaluate the scale effect in extrapolating the results of laboratory creep tests to reinforcement of actual length. This scale effect can be derived from the results of pullout tests on reinforcements with different lengths or assessed using analytical or numerical load transfer models which have to be "calibrated" through numerical test simulations. The Singh and Mitchell creep model can be used in the interpretation of the pullout tests to derive relevant creep parameters for the extrapolation of the laboratory test results to actual reinforcement size.[78]
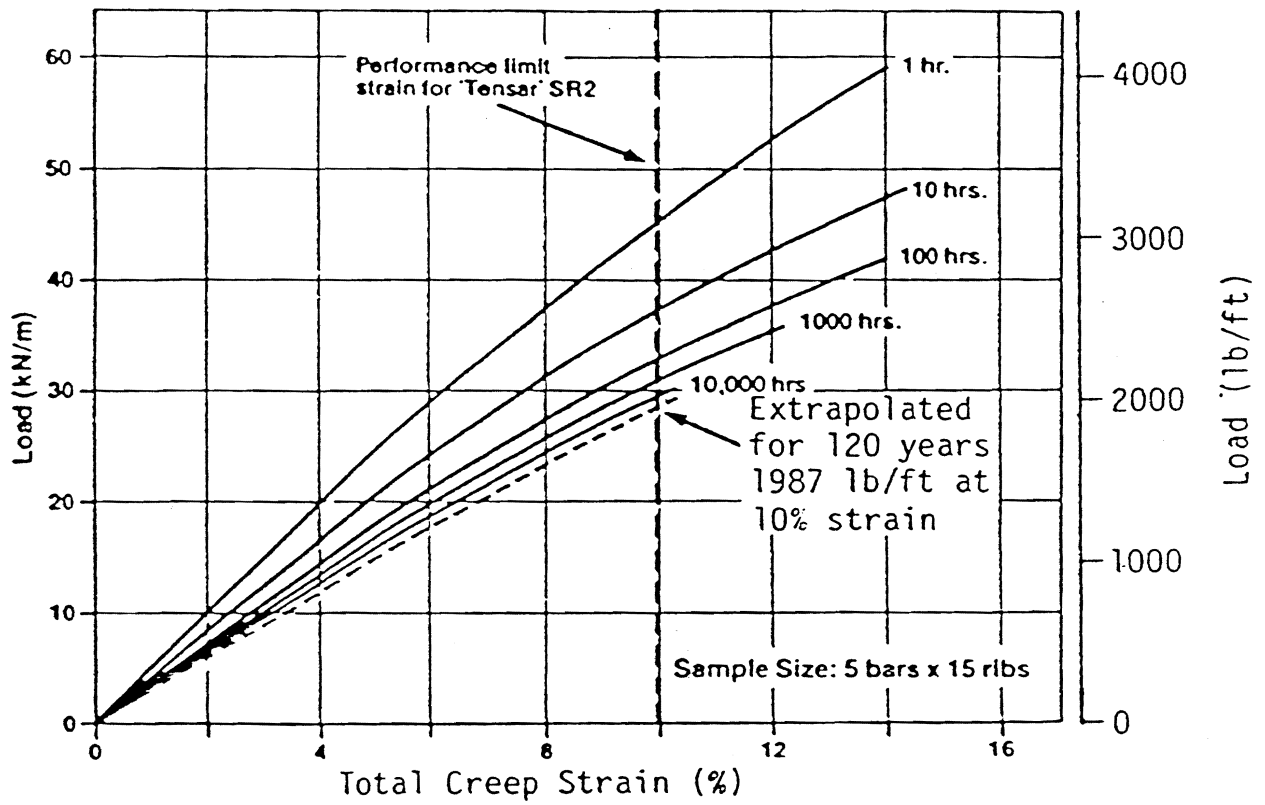
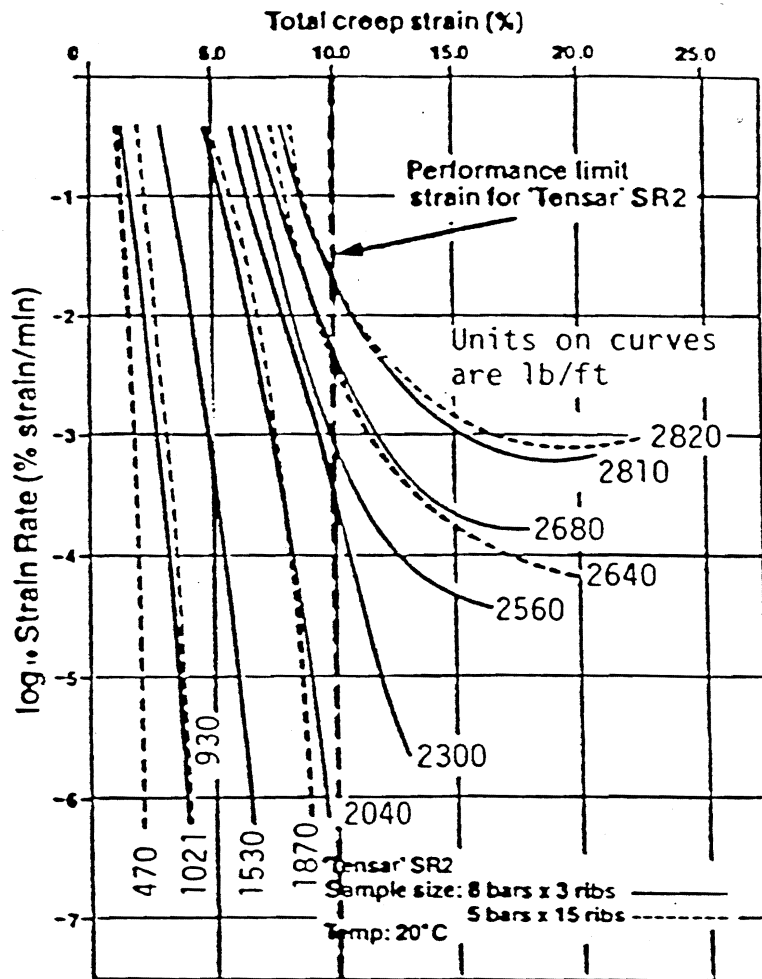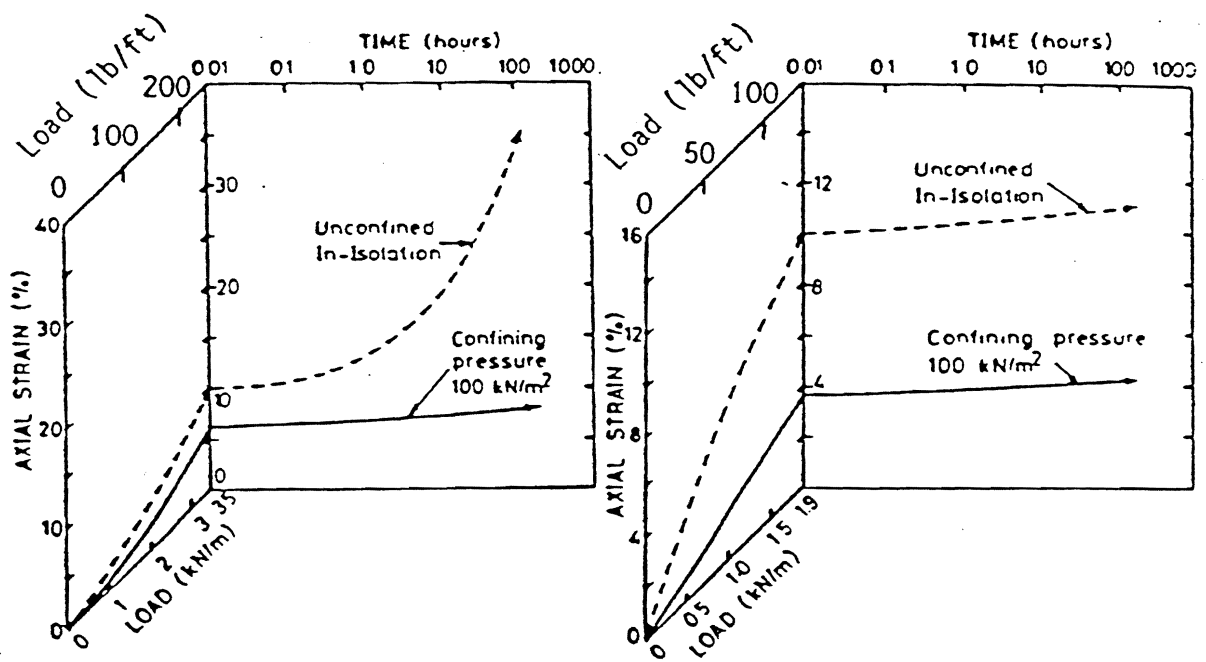Figure 48. Load versus total creep strain for Tensar SR2.

Figure 49. Creep strain rate against total creep strain.

Figure 50.   Confinement effect on creep behavior
of non-woven geotextiles.

CHAPTER 3

REINFORCED FILL WALLS

1.0 INTRODUCTION

As previously indicated in the Introduction section, all the equations and design methods presented in chapter 3 of volume I were based and verified by recent research carried out in this country and abroad. A part of that research was performed in the frame of the present study in order to prepare this manual. This section provides the main results of all that research, as it relates to the design methods in volume I.

2.0 LIST OF RECENT RESEARCHES, INCLUDING FHWA PROGRAM

a. General reports on soil reinforcements

One of the principal variations in reinforced fill wall design is the extensibility of the reinforcement. The first indication of the influence of reinforcement extensibility on reinforced soil wall behavior has been presented by Schlosser, et al., who reported the results of a full scale experimental wall constructed with Paraweb (i.e., extensible) reinforcements and compared it with the behavior of Reinforced Earth walls (inextensible reinforcements).[12, 82] Since that report, several general reports partly or totally devoted to soil reinforcement, have mentioned this aspect of the behavior, most of which are reviewed in NCHRP 290.[2]

b. FHWA research program on reinforced soil wall

The FHWA research program performed for preparing this manual included many types of tests, including:

- Reduced scale three dimensional models of reinforced soil walls with different types of reinforcement: aluminum foil, plastic strips, plastic grids, non-woven and woven geotextiles and anchors.

- Small scale centrifuge testing of reinforced soil walls using the same reinforcements used for the reduced scale model tests.

- Full scale experiments of eight 20-foot high reinforced soil walls, with different types of reinforcements, facings and fill materials (table 3).

- Large scale centrifuge tests on models of the full-scale walls.

- Parametric study of reinforced soil walls using a calibrated finite element computer program.

Table 3. List of full scale reinforced soil walls constructed for the FHWA program.

Wall	Reinforcement	Facing	Fill Material	Geometry
1.	Metallic strips (40×5 mm^2)	Concrete panels	Sandy gravel	Rectangular
2.	Geogrid	Concrete panels	Sandy gravel	Rectangular
3.	Bar mats	Concrete panels	Gravelly sand	Rectangular
4.	Bar mats	Concrete panels	Cobbles	Rectangular
5.	Bar mats	Concrete panels	Silt	Rectangular
6.	Non-woven Geotextile	Geotextile	Gravelly sand	Rectangular
7.	Wire mesh	Gabions	Gravelly sand	Rectangular
8.	Wire mesh	Gabions	Gravelly sand	Trapezoidal

c.   Reinforced Earth Company's Research

The Reinforced Earth Company has performed significant research in the last ten years, the results of which are contained in internal reports. At the onset of the FHWA study, the Reinforced Earth Company agreed to provide results from this research.

The following results were used in the development of this manual:

- Inclination of the thrust at the back of the wall, resulting from a parametric study using a finite element method (F.E.M.) program.

- Full-scale experiments on Reinforced Earth walls with short reinforcement length (L/H = 0.4).

- Behavior of Reinforced Earth walls under seismic loading, resulting from a F.E.M. study using a calibrated computer program.

d.   Research on polymeric reinforcement

In 1987, NATO sponsored an Advanced Research Workshop on the "Application of Polymeric Reinforcement in Soil Retaining Structures".[83] The workshop consisted of reports on case histories from Europe and the United States, evaluation of material properties, analytical techniques and design methods, construction methods and economics, and a research needs summary. A major focus of the workshop was a prediction exercise in which participants were asked to predict the performance of two full scale walls that were constructed, externally loaded and monitored, as part of the program. The information from this workshop provided significant information concerning the predictive capabilities of existing design methods for extensible reinforcement.

3.0 SUMMARY OF FHWA RESEARCH RESULTS

a. Small scale models

Results of all model tests performed in the FHWA project clearly
indicate that reinforcement extensibility and density (amount of
reinforcement) significantly influence the design model. The
small scale model results found:

- For the less extensible reinforcements (red plastic
  strips, plastic grids), distribution of the tensile
  force is close to the K_o line at the top of the wall and
  less than the K_a line at the bottom. This is in good
  agreement with all observations made on metal strip
  model walls.

- For woven geotextile polyester strips, K_o line would be
  still valid at the top but the distribution at the
  bottom is closer to the K_a line.

- For nonwoven geotextile strips, tensile forces would
  agree with the Rankine's distribution (K_a).

- Maximum tension in the more extensible plastic strips
  appears to correspond to the Rankine's distribution on
  the whole height, which is in agreement with
  observations on actual structures built with extensible
  reinforcements (Paraweb strips).

b. Full Scale Field Wall

Similar results in the small scale models have been obtained from
the full scale experiments performed for the FHWA project and by
F.E.M. calculations. For instance, figure 51 shows the comparison
of the K lines for full scale model walls 1 and 2 in which the
only difference is the type of reinforcements. For wall 1 with
metallic strips, the distribution of maximum tension with depth is
close to K_o; for wall 2 with geogrid reinforcements, the
distribution is close to K_a, except in the upper 2 meters.

Likewise, figure 52 shows a comparison of the K line for wall 3
constructed with inextensible bar mats and wall 7 constructed with
extensible woven wire mesh. Again, the distribution of the
maximum tension with depth is close to K_o for wall 3 and close to
K_a for wall 7.

Another interesting result is given by the comparison between
walls 4 and 5. They are both constructed with VSL bar mat
reinforcements with the only difference being the fill material:
cobbles and gravelly sand in wall 4, clayey silt in wall 5.
Distribution of maximum tension with depth in wall 4 was found to
decrease from K_o condition at the top to a K_a condition at the

Figure 51. Effect of the extensibility of the reinforcements on the K coefficient.[84]

a) Distribution of Maximum Tension With Depth in Wall 1. (reinforced earth strips)

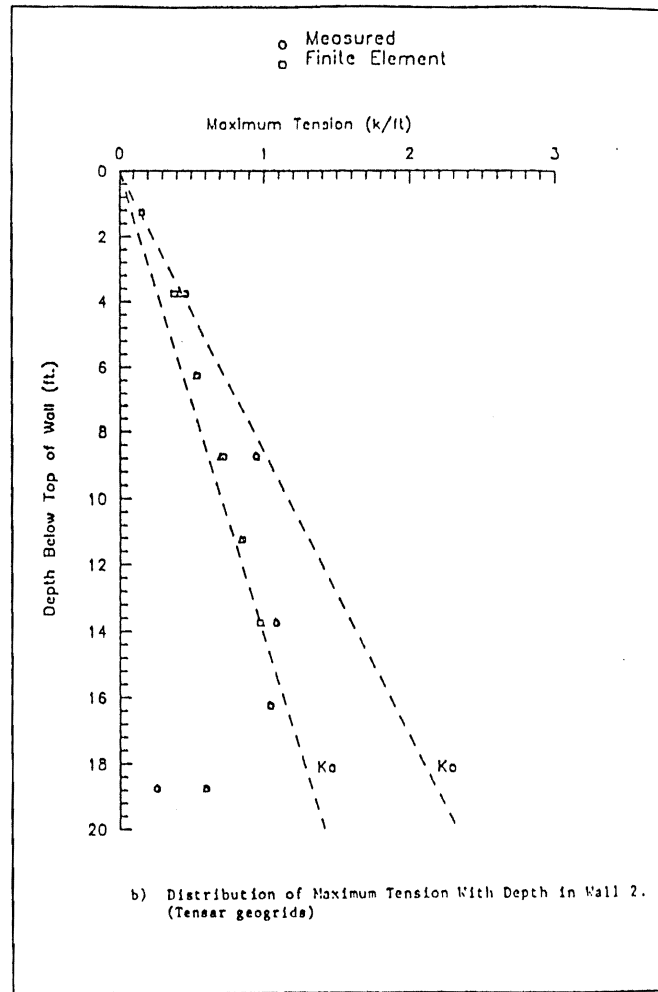b) Distribution of Maximum Tension With Depth in Wall 2. (Tensar geogrids)

94
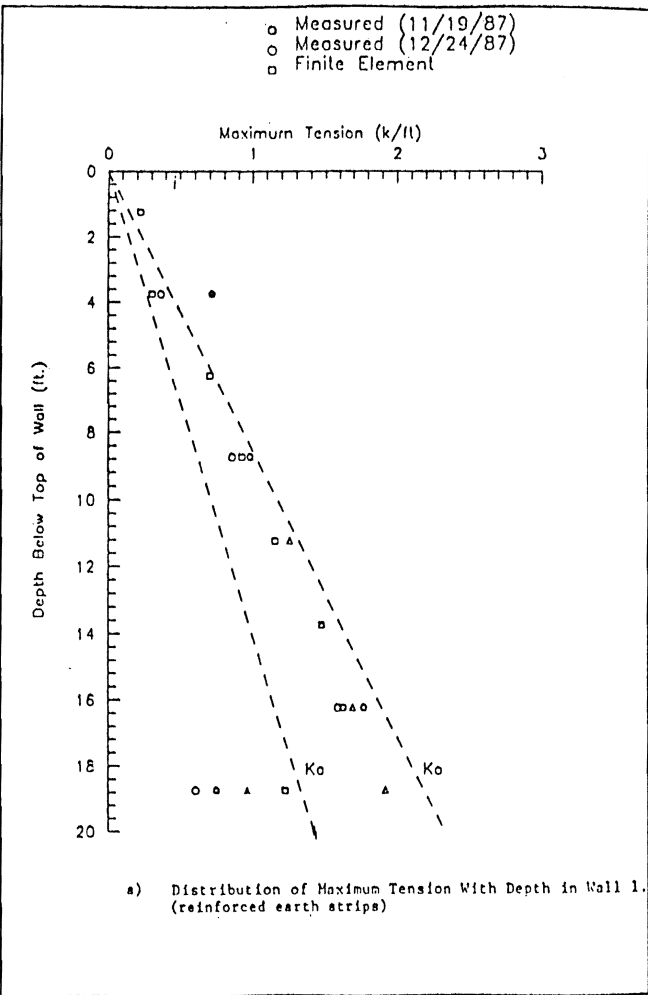
Figure 52. Influence of extensibility on distribution of maximum tension.[84]

a) Distribution of Maximum tension With Depth in Wall 3.
(VSL bar mats)

b) Distribution of Maximum Tension With Depth in Wall 7.
(Maccaferri gabion woven wire mesh)

95
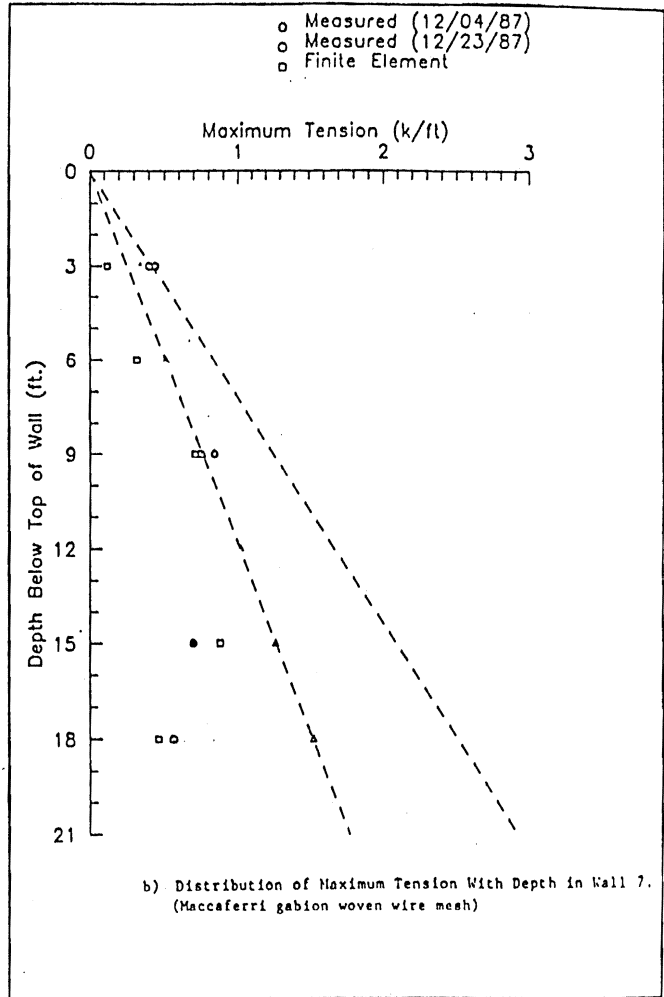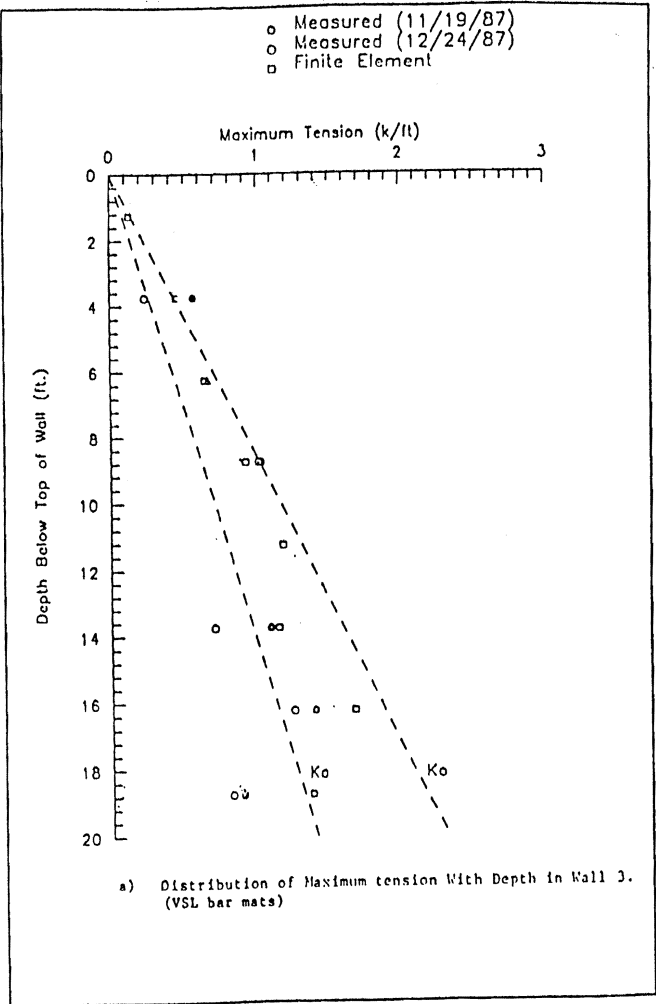
bottom in good agreement with other results on inextensible reinforcements. On the contrary, in wall 5 the distribution is closer to K_a line, indicating that the greater lateral displacements observed in this wall during and following construction directly influenced the K value.

An indepth evaluation of the field results was performed using a finite element computer program.

c.   Summary of Parametric Study on Reinforced Soil Walls

A parametric study of reinforced soil walls was made using a validated, discrete finite element computer program, SSCOMP, to study the effects of wide variations in structure geometry, loading, foundation soil type, wall facing type, and soil compaction on internal stresses and deformations. The computer program was validated during an earlier phase of this research project by showing that it predicted actual stresses in 15 full scale structures with good accuracy. The finite element analysis results were also compared with conventional design/analysis assumptions in an attempt to gain insight into the strengths and weaknesses of the conventional design procedures.

Scope of Study — The study included a range of wall conditions which are variations on a reference wall called the baseline case. All cases that were analyzed are illustrated in table 4. Variations in backfill and reinforcement type were not included in this study. The performance variables evaluated were maximum reinforcement tension, tension distribution along the reinforcement length, and horizontal displacement of the wall facing.

Since the baseline case is representative of a typical highway wall, as described in the following section, the results of this study are expected to be applicable to many common FHWA design situations. As with any analytical study it is uncertain whether the results obtained are applicable to wall conditions outside the range studied.

Computer Program SSCOMP — The program is a plane-strain finite element code which can simulate incremental soil placement, incremental soil compaction, and soil structure interaction. The analyses for this study were performed using the three major types of element models available in the program, namely soil, structure, and interface elements. Soil elements were organized into layers corresponding to construction lift intervals. Structure beam elements (including bending stiffness) were used to model the concrete wall facing and structural bar elements (axial stiffness only) modeled the reinforcement layers. Interface elements with essentially zero thickness were used along the soil/reinforcement and soil/wall facing contacts to allow relative movement between the soil and reinforcement or wall facing.
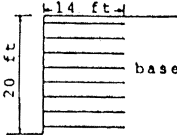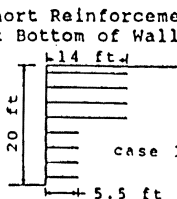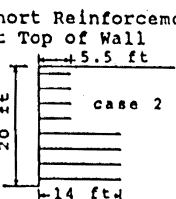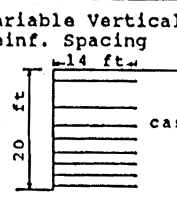
Table 4. Comparison of FEM analysis cases.[61]
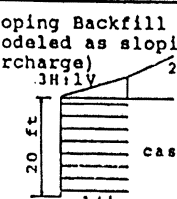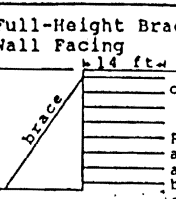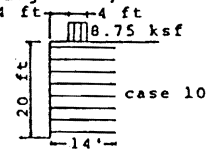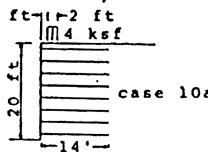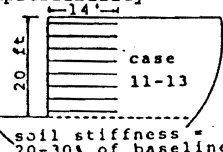
97

Compare FEM results to FEM Baseline Case:	Short Reinforcement at Bottom of Wall (case 1)	Short Reinforcement at Top of Wall (case 2)	Variable Vertical Reinf. Spacing (case 3)	Sloping Backfill (modeled as sloping surcharge) (case 5)	Full-Height Braced Wall Facing (case 6)
A. Reinforcement tension 1. Max. Reinf. Tension 2. Distribution along reinf. length 3. Sum of max. tension for all levels	1. Increase of 0-70% in upper 4 reinf. levels. Decrease of 30-50% in bottom 4 levels. 2. Location of max. tension shifts distinctly toward wall face for bottom 4 levels. Pattern in top 4 levels becomes irregular. 3. Value 15% lower than Baseline case.	1. Change of ±70% in top 3 reinf. levels - greatest increase in 2nd level from top. Less than ±10% change in bottom 5 levels. 2. Location of max. tension shifts distinctly toward wall face for top 4 reinf. levels. 3. Value 5% less than Baseline case.	1. Values are similar but direct level-by-level comparison not possible since reinf. elevations differ from Baseline case. Max. tensions in bottom half of wall are more uniform than in Baseline case (See Figure 41(b)) 2. Location of max. tension same as Baseline. 3. Value 3% smaller than Baseline case.	1. Increase of approx. 25% at all reinf. levels. 2. Location of max. tension is further away from wall face for most reinf. levels. 3. Value 20% greater than baseline.	1. Decrease of 0-350% in lower 7 reinf. levels. Increase of about 100% in top level. 2. Location of max. tension unchanged in lower 6 levels; shifts to wall face for top 2 levels. 3. Value 15 % less than Baseline case.
B. Lateral Wall Face Deformation	Max. deformation 150% greater than Baseline with most of the increase occurring in the shortened layers. Deformation profile has a distinct bulge 12 ft. below the top of the wall.	Deformation same as Baseline in lower half of wall, but greater in upper half with location of max. shifted downward. Max. deformation 60% greater than Baseline.	Max. deformation 60% greater than Baseline. Location of max. deformation shifted downward to about 7 ft. below the top of the wall.	Similar to Baseline but max. deformation 70% greater.	Location of max. deformation shifted down to near wall mid-height. Max. deformation 30% less than Baseline case.
Compare FEM Reinf. tension to value predicted by conventional design methods 1. Max. tension for individual levels 2. Sum of max tension for all levels	No conventional calculations performed.	No conventional calculations performed.	Used Conv. Method A 1. FEM values generally 110-170% of conventional, though 80% at bottom level. Conventional values almost uniform at all reinf. levels. 2. FEM value 120% of conventional.	No conventional calculations performed.	Used Conv. Method A 1. FEM values for middle 6 levels 85-120 % of conventional; for top level about 500 % of conventional. 2. FEM value same as conventional.

Table 4. Comparison of FEM analysis cases.[61]

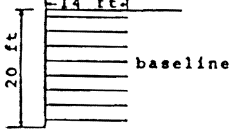| (baseline diagram)	Strip Loading #1 (Bridge Seat)	Strip Loading #2 (Crane Load)	Increased Foundation Compressibility
Compare FEM results to FEM Baseline Case:	4 ft—4 ft 8.75 ksf case 10	1 ft—2 ft 4 ksf case 10a	case 11-13 soil stiffness = 20-30% of baseline
A. Reinforcement tension 1. Max. Reinf. Tension 2. Distribution along reinf. length 3. Sum of max. tension for all levels	1. Large increase at all levels equal to 100-250% of max. value in 2nd level from bottom in Baseline. Max. tensions are fairly uniform in middle 2/3 of the wall - near yield for 60 ksi steel bar mat. 2. Locations of max. tension near the center of the strip load. 3. Value 300% greater than Baseline case.	1. Large increase in upper 2 levels about equal to max. value in 2nd level from bottom in Baseline. Fairly uniform increase in lower 6 levels of magnitude of about 30% of the above max. value. 2. Locations of max. tension shift toward the center of the strip load. 3. Value 80% greater than Baseline case.	1. No change, except slight increase in tension in the lowest layer. 2. Essentially same as Baseline case. 3. Values 0-5% greater than Baseline case.
B. Lateral Wall Face Deformation	Similar to Baseline but deformation increasing all the way to top of wall. Max. deformation 40% greater.	Deformation same as Baseline in lower 13' of wall height, but greater in upper 7'. Max. deformation 25% greater than Baseline.	Deformation at all points on wall face (including bottom of wall) greater than Baseline case by a constant increment. See Table 4 for values.
Compare FEM Reinf. tension to value predicted by conventional design methods 1. Max. tension for individual levels 2. Sum of max tension for all levels	Used Conv. Methods B, C, and D. Comparisons given in Figure 40 and in Table 4.	Used Conv. methods B, C, and D. Comparisons given in Figure 40 and in Table 4.	Used Conv. Method A 1. FEM values for bottom 7 levels 100-135 % of conventional; for top level 250 % of conventional. 2. FEM values about 125% of conventional values.

Definition of Conventional Methods:

A. Conventional Meyerhof procedure for bar mat reinforced soil walls, as in Mitchell and Villet (1987), chapter 5.
B. Increase in vertical stress due to strip loading calculated by 1H:2V load dispersion within reinforced zone, as in Mitchell and Villet (1987), appendix A, chapter 1.
C. Increase in vertical stress due to strip loading calculated by Boussinesq elastic load dispersion within reinforced zone.
D. Laba and Kennedy (1986) load-sharing procedure for strip loading effects.
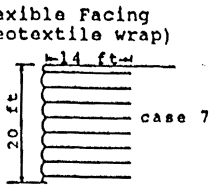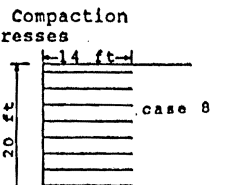
98

Table 4. Comparison of FEM analysis cases.[61]
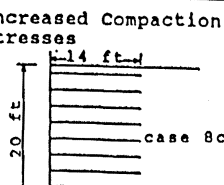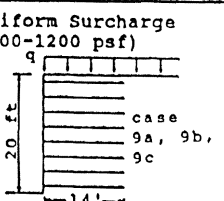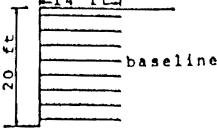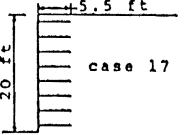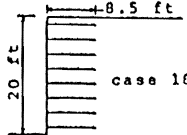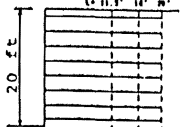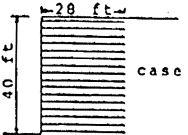
	Flexible Facing (Geotextile wrap)	No Compaction Stresses	Increased Compaction Stresses	Uniform Surcharge (400-1200 psf)
Compare FEM results to FEM Baseline Case: baseline (20 ft)	case 7 (14 ft, 20 ft)	case 8 (14 ft, 20 ft)	case 8c (14 ft, 20 ft)	case 9a, 9b, 9c (14', 20 ft)
A. Reinforcement tension 1. Max. Reinf. Tension 2. Distribution along reinf. length 3. Sum of max. tension for all levels	1. Increase of 5-35% in all levels. 2. Locations of max. tension are 2-3 ft. closer to the wall face for all but the top reinf. level. Reduction in tension at the wall face is more pronounced. 3. Value 20% greater than Baseline case.	1. Decrease of 10-30% in all levels. 2. Location of max. tension same as Baseline case. 3. Value 15% less than Baseline case.	1. Increase of 0-20% in all levels. 2. Location of max. tension same as Baseline case. 3. Value 10% greater than Baseline case.	1. Relatively uniform increase at all reinforcement levels. Magnitude of increase close to qs_vK_o. 2. Distribution shape similar to Baseline but location of max. tension further from wall face in upper 3 reinf. levels. 3. Value increases by 33% of Baseline value for each 400 psf increase in surcharge.
B. Lateral Wall Face Deformation	Similar to Baseline case but max. deformation 20% greater.	Similar to Baseline but location of max. deformation shifted downward to about 6 ft. below the top of the wall, and max. deformation 25% smaller.	Similar to Baseline but max. deformation 10% greater.	Deformed shape similar to Baseline but max. deformation greater by about 25% per 400 psf surcharge.
Compare FEM Reinf. tension to value predicted by conventional design methods 1. Max. tension for individual levels 2. Sum of max tension for all levels	Used Conv. Method A 1. FEM values 125-250 % of conventional. 2. FEM value 145% of conventional.	Used Conv. Method A 1. FEM values for middle 4 levels 100-105% of conventional; 85-125% of conv. at other levels. 2. FEM value same as conventional.	Used Conv. Method A 1. FEM values 100-140 % of conventional. 2. FEM value 130% of conventional.	Used Conv. Method A 1. FEM values 100-140 % of conventional. 2. FEM values about 120% of conventional values. Value of $[0.5(\gamma)H^2+qH]K_o$ is within 3% of FEM sum.

Table 4. Comparison of FEM analysis cases.[61]

Compare FEM results to FEM Baseline Case:	Reinforcement Length, L= 5.5 ft	Reinforcement length, L= 8.5 ft	Reinforcement length, L= 11.5, 16, 20 ft. case 19-21	Wall Height = 40 ft.
A. Reinforcement tension 1. Max. Reinf. Tension 2. Distribution along reinf. length 3. Sum of max. tension for all levels	1. Increase of 30% in upper two reinf. levels. No change in next two layers. Decrease of 20-50% in bottom 4 levels to values near $z(\gamma)s_vK_A$. 2. Location of max. tension shifts to wall face at all levels. 3. Value 25% smaller than Baseline case.	1. Change of -40% in top reinf. level, +50% in next level, and +30% to -15% in bottom 6 levels. 2. Locations of max. tension are 2-5 ft closer to the wall face. 3. Value 5% greater than Baseline case.	1. Change of ±10% at all reinforcement levels for all three lengths. 2. For L= 16' and 20' distribution similar to Baseline case. For L= 11.5' the locations of max. tension are 1-2 ft closer to wall face. 3. Value within 5% of Baseline case for all three lengths.	1. Values similar to Baseline case (see Figures 39 and 25A) Uniform surcharge, q, raises max. tensions by about qs_vK_o. 2. Location of max. tension 0.25H-0.3H behind wall face except at extreme top and bottom of wall. 3. Value 320% greater than Baseline case (2x wall height gives 4x reinf. tension sum.)
B. Lateral Wall Face Deformation	Max. deformation 250% greater than Baseline. Wall is on the verge of overall stability failure. Several reinforcement levels on the verge of pullout failure.	Location of max. deformation shifted downward to about 6' below top of wall. Max. deformation 100% greater than Baseline.	Deformed shape similar to Baseline. Max. deformation for L=11.5' 25% greater than Baseline, for L=16' 10% less, and for L=20' 25% less.	Similar to Baseline but ratio of max. deformation to wall height greater by 10%.
Compare FEM Reinf. tension to value predicted by conventional design methods 1. Max. tension for individual levels 2. Sum of max tension for all levels	Used Conv. Method A 1. FEM value for top level is 330% of conventional; for next 5 levels 60-140% and for lower 2 levels 15-25 %. 2. FEM value 40% of conventional.	Used Conv. Method A 1. FEM values 95-150 % of conventional. 2. FEM value 110% of conventional.	Used Conv. Method A 1. FEM values for bottom 7 levels 90-140% of conventional; for top level about 200% of conventional. 2. FEM values about 120% of conventional values.	Used Conv. Method A 1. FEM values for upper 7 levels 135-170 % of conventional; for bottom level 70%. 2. FEM value 150% of conventional. Value of $0.5*(\gamma)*H^2*K_o$ is within 2% of FEM sum.

The program employs different stress-strain models for each of the three major element types. Soil elements are modeled with a hyperbolic stress-strain path for primary loading and a linear path for unload/reload response. In addition, a hysteretic unload/reload model is used to model compaction stress effects. Soil elements become essentially plastic upon failure. The structure elements are modeled as completely linear elastic materials. Interface elements are formulated with a linear elastic stress-strain path in the direction normal to the physical boundary being modeled, and with a hyperbolic path in the shear direction. The hyperbolic path is used during primary loading and reloading, and a linear path is substituted during unloading.

Baseline Case - The structure chosen as the reference, or baseline, case for this study is shown in figure 53a. It is a 20 ft high bar mat (VSL) wall with a segmental concrete facing, constructed with eight layers of reinforcement and compacted gravelly sand backfill. Moderate compaction stresses, believed to be representative of typical construction practice, were included. This wall was selected as a baseline for the following three primary reasons:

- It is very similar to wall #3 of the "FHWA Field Walls," a wall that had been successfully modeled during an earlier phase of the project.

- It has a reinforcement system of medium stiffness, i.e., between that of the stiffest (welded wire) and most flexible (geotextile) wall systems.

- Its height, reinforcement length and construction sequence are typical of a large number of actual reinforced soil highway walls.

Some of the F.E.M. results for the baseline case are presented in figure 53a and b and briefly summarized below. The results for the baseline case are compared with the results for other analysis cases in table 4.

The maximum reinforcement tensions versus depth predicted by the F.E.M. analysis (figure 53b) generally fall near the K_o line shown on the plot. The tension in the bottom level, however, is between the K_o and K_a lines.

If the baseline case is analyzed without soil compaction stresses, then the predicted maximum reinforcement tensions fall between the K_o and K_a lines at almost all reinforcement levels. This sort of reinforcement tension pattern is very similar to that assumed in conventional design procedures for steel strip walls which use a lateral stress coefficient that varies linearly between K_o and K_a from the top of the wall to a depth of 20 ft. It is possible that the relatively slow time required for construction of field wall may have influenced the results. Of course, another possible explanation for the discrepancy is that the F.E.M. model did not accurately model the compaction conditions used for construction of the baseline case.

101

8 Reinforcement Layers

Reinforcement Type :
   VSL — 0.5"x2'
    4 longitudinal Bars (W11)

Reinforcement Spacings :
   S_h = 4.92 ft.
   S_v = 2.5 ft.

Segmental Concrete Facing

Height of Wall = 20 ft.

Reinforced Zone
14 feet

8 Compacted Soil Layers

Backfill Material : Gravelly Sand
γ = 130 pcf
ϕ = 40 degrees
c = 0.0 psf

Foundation Soil :
Medium Dense Sand With Gravel Traces
(SP—SW)

Physical Conditions
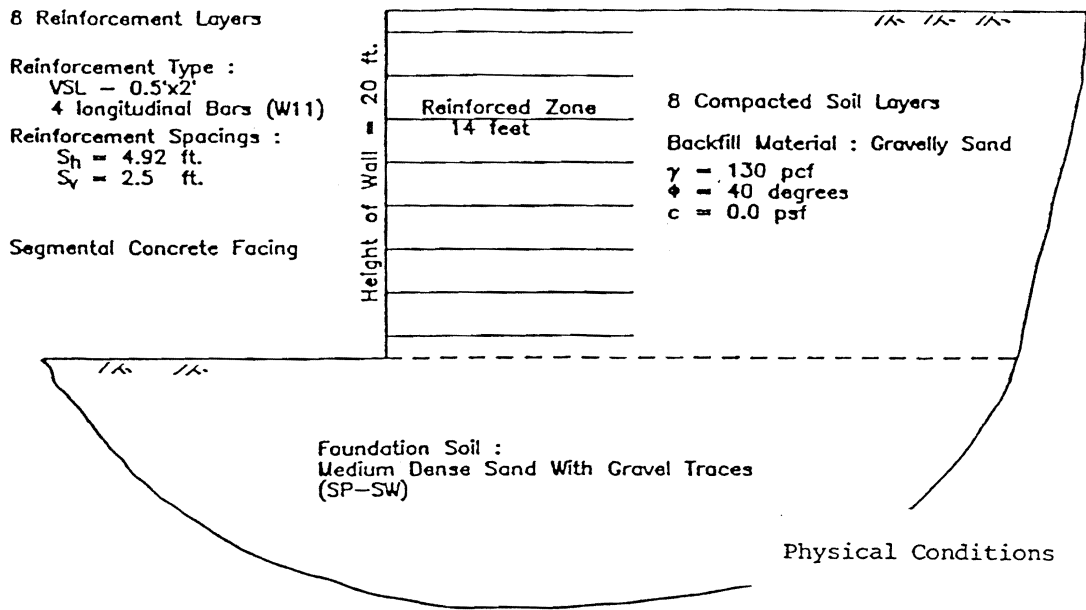
Displacement at Wall Face
Baseline Case

Depth Below Top of Wall (ft)

Lateral Displacement
at Wall Facing

Total Lateral Displacement (in)
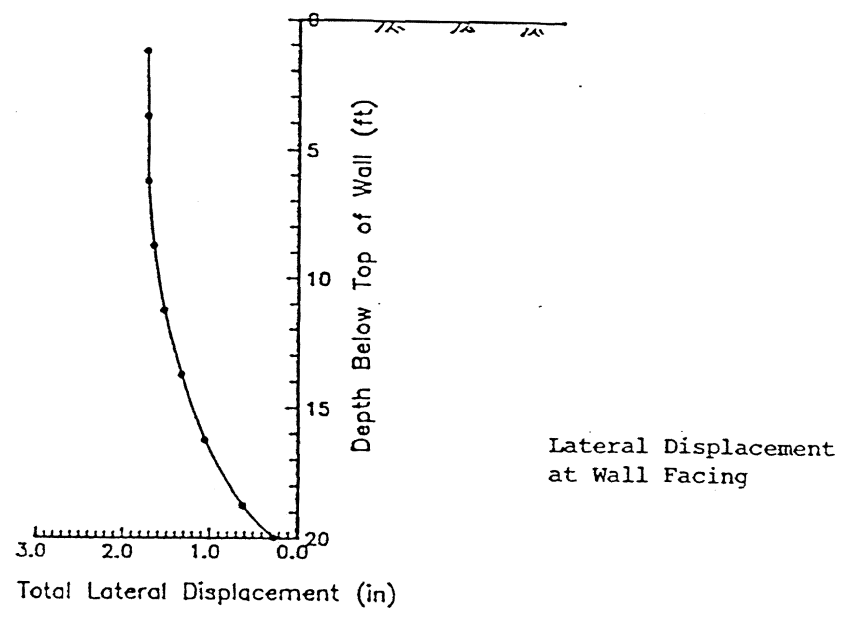
Figure 53a.   Geometry and F.E.M. results for the
baseline case.[85]

102

Distribution of Tension In Reinforcements
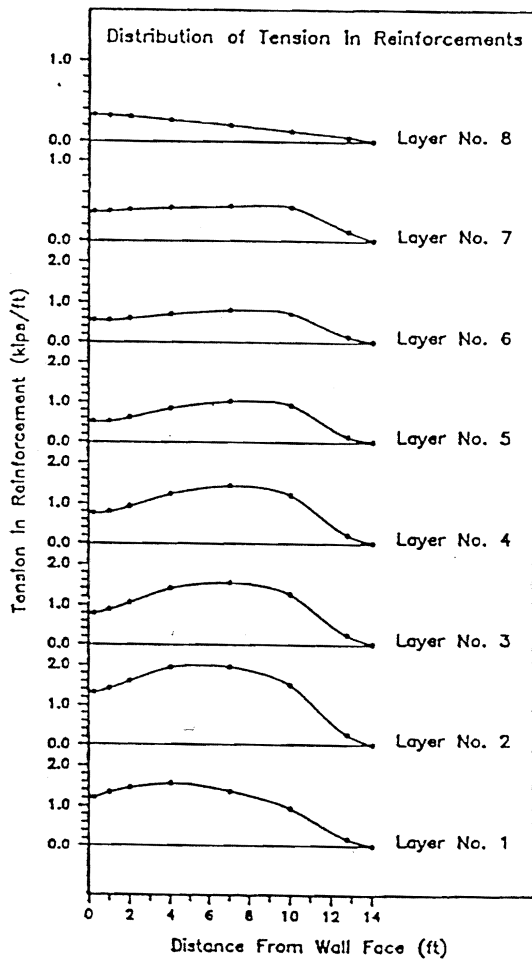
Reinforcement Tension
Distribution

Maximum Reinforcement
Tensions
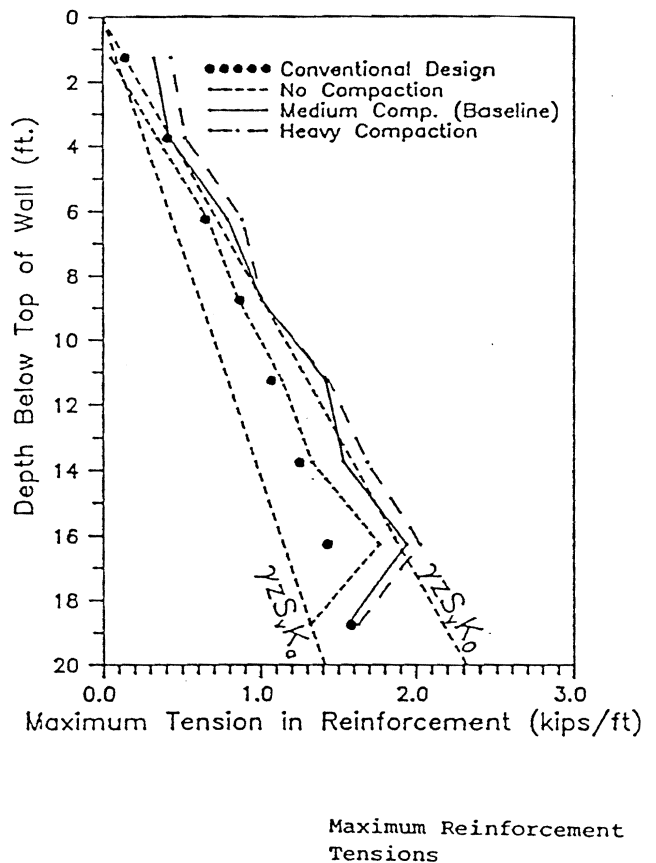
Figure 53b. F.E.M. results continued for the baseline case.[85]

The predicted tension distribution along the reinforcement levels generally has an intermediate value at the wall face, a peak behind the wall face, and a value of zero at the free end (figure 53b). This is a characteristic pattern found by many investigators.

The predicted pattern of wall face deformation (taking into account the construction sequence) increases curvilinearly from the wall base up to the top of the wall (figure 53a).

Conventional Design/Analysis – The conventional design methods used for comparison in table 4 are taken from the sources listed at the end of the table. The conventional method "A," used for comparison for all but the strip loading cases, features the Meyerhof vertical stress distribution procedure, a bilinear assumed failure plane, a lateral soil stress coefficient varying linearly from K_o at the wall top to K_a at the wall base, and an empirical pullout capacity based on VSL bar mat behavior. This method does not take into account facing type, compaction stresses, or foundation soil type and therefore gives the same results for cases where these variables are altered. The method differs from the method proposed in volume I of this report. Conventional Methods "B," "C" and "D" are used only in the strip loading cases and are all superposition methods that add incremental stresses due to the strip loading onto stresses calculated by method "A."

Results and Implications of Study – The predictions, by F.E.M. as well as by conventional methods, of reinforcement tension and wall face deformation for the cases studied are compared and summarized in table 4. Detailed results are included in the FHWA project final report along with F.E.M. results for the magnitude and distribution of vertical soil pressures.

If the F.E.M. results are assumed to be accurate then the results in table 4 have at least three major implications for conventional design practice. The first is that the conventional design methods may underpredict reinforcement tensions when there is significant compaction of the backfill during construction. A possible explanation for this is that the conventional methods may have been calibrated against instrumented walls that were meticulously constructed, and therefore may not represent a typical highway wall.

The second implication is that in a few cases the predictions by conventional and F.E.M. methods differ by magnitudes too great to be explained by the compaction effects discussed above. These differences are often unconservative in nature, i.e., the conventional analysis predicts lower tensions than the F.E.M. A possible explanation for these observations is that the conventional method may not be reasonable for non-standard wall conditions. Results indicating these unconservative conditions are marked by stars in Table 4. One example is that the prediction of reinforcement force increases due to strip loading appear quite unconservative in the lower half of the wall (figure 54). On the other hand, overconservative conventional design is also undesirable.

104

Parametric Study — Strip Loading Case

Maximum Tension in Reinforcement (kips/ft)
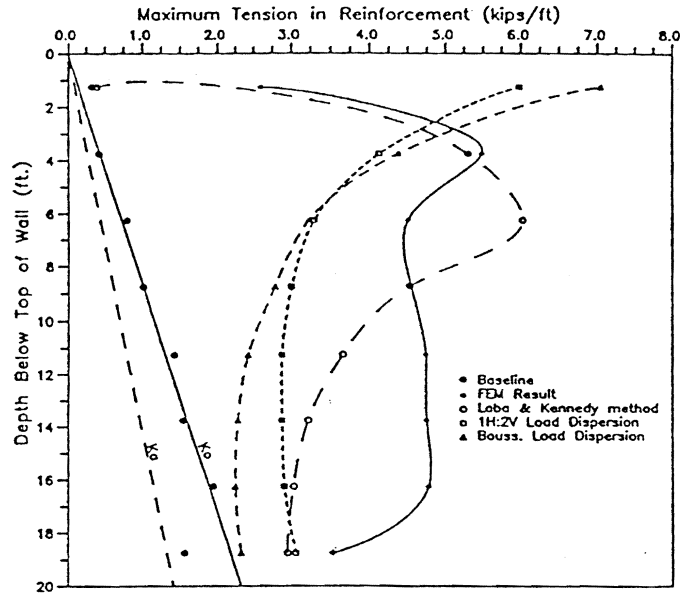
a) Bridge Seat

Parametric Study — Strip Loading Case #2

Maximum Tension in Reinforcement (kips/ft)
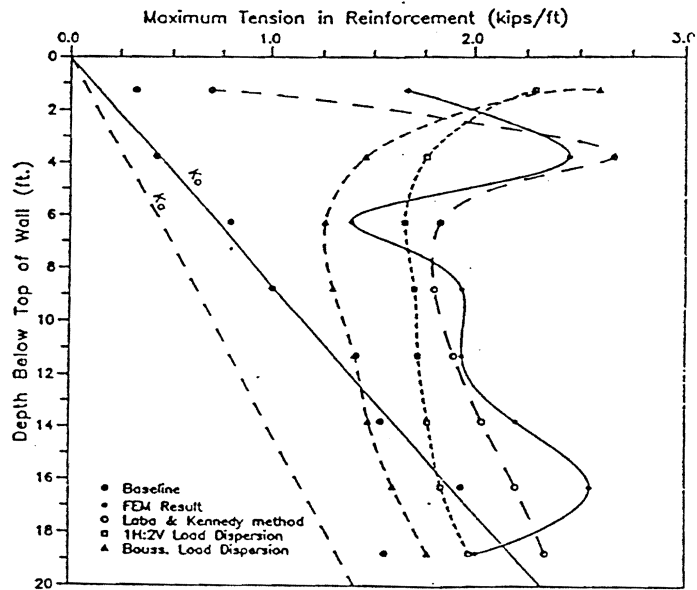
b) Crane Load

Figure 54. Maximum reinforcement tensions for strip loading cases by F.E.M. and conventional methods.[85]

The _third_ implication is that wall face deformations, an important performance criterion, may change significantly due to factors that conventional design practice does not consider. For example, the baseline wall deformation can be decreased by 25 percent by increasing the reinforcement length to 20 ft, or can be increased by 60 percent using a variable reinforcement spacing.

4.0   INCLINATION OF THE THRUST AT THE BACK OF THE WALL

A large F.E.M. parametric study using a calibrated computer program was performed from 1982 to 1984 by the Reinforced Earth Company to specifically evaluate the inclination of the thrust at the back of the wall.

More recently, the French Administration and the Reinforced Earth Company conducted a large research program including full scale experiments in order to have a better knowledge on the critical value of the L/H ratio.

The results of both studies showed that the thrust at the back of inextensibly reinforced soil walls is inclined downwards and that the inclination angle λ agrees fairly well with the empirical relation:

$$\lambda = (1.2 - L/H)\phi_b \qquad (25)$$

where L is the length of the reinforcements, H is the height of the wall, and ϕ_b the friction angle of the retained backfill.[86]

There are several reasons for the inclination of the thrust:

1)   The reinforced fill section is stiffer than the nonreinforced backfill.

2)   The relative settlement of the backfill has been found to be greater than the reinforced section creating downdrag at the back of the stiffer reinforced section.

3)   The smaller the L/H ratio, the greater the tilting of the reinforced soil wall and the relative settlement of the retained fill.

However, these findings have not been validated for reinforced soil walls with extensible reinforcements. Furthermore, since the stiffness of the reinforced section of walls constructed with extensible reinforcement is not that dissimilar to the backfill, the relative movement of the reinforced fill and the unreinforced backfill are approximately the same. Therefore, inclination of the thrust is not assumed to occur and a value of $\lambda = 0$ has been conservatively recommended for walls constructed with extensible reinforcement.

Figure 55 illustrates this new inclination concept for reinforced fill walls.

$$\lambda = \left[1.2 - \frac{L}{H}\right]\phi$$
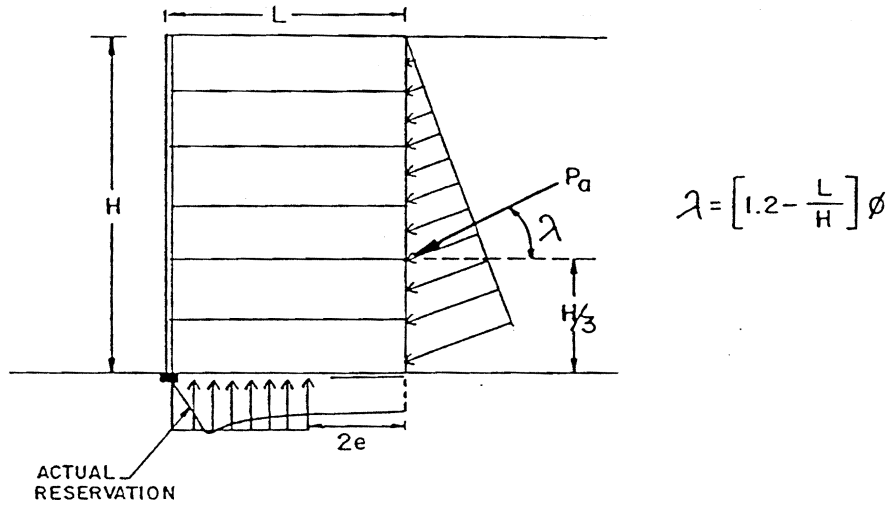
a) Inextensible reinforcement.
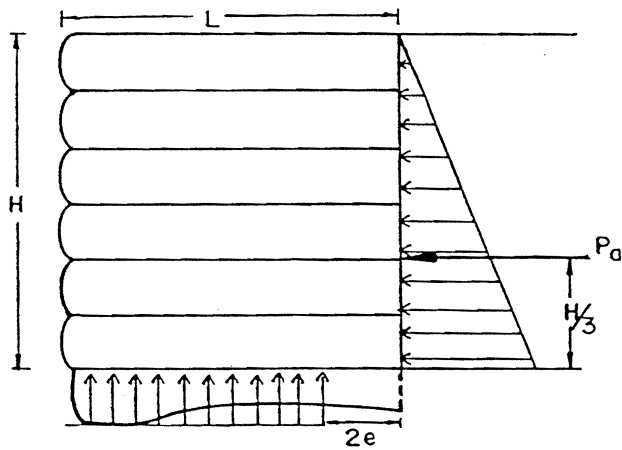
Figure 55.   Thrust at the back and vertical stress distribution
at the base of reinforced soil walls.

107

5.0 DISTRIBUTION OF THE VERTICAL STRESS σ_v AT THE BASE

Since the early development of the Reinforced Earth technique, a
Meyerhof distribution has been used to analyze the vertical stress
σ_v at the base of a reinforced soil wall. Field instrumentation,
as well as F.E.M. studies, have shown that this distribution is a
fairly good and simple approximation of the actual value of
maximum pressure (figure 55). No difference has to be made
between walls with inextensible and extensible reinforcements.

6.0 INFLUENCE OF SYSTEM STIFFNESS ON THE HORIZONTAL STRESS IN THE REINFORCED SOIL SECTION.

In reviewing the small scale model and finite element results, it
became apparent that the relative stiffness of the reinforced soil
system has a direct influence on the tension developed in the
reinforcement. To further evaluate this relationship, the lateral
stress ratio K was back calculated from available field data and
compared to the active earth pressure coefficient K_a as shown in
figure 56. K values were calculated from:

$$K = \frac{T_{max}}{\sigma_v \, S_v \, S_H} \tag{26}$$

where: $\sigma_v = \gamma Z$

T_{max} is the measured maximum tension in the
reinforcement at depth Z.

S_v, S_H are the vertical and horizontal spacing of
reinforcements.

The data was then grouped according to the relative stiffness of
the reinforcement system S_r, as shown in figures 57, 58, and 59,
where

$$S_r = \frac{EA'}{H/n} \text{ as defined in figure 26, of volume I.} \tag{27}$$

The K/K_a relationships shown by the solid line in each plot
correspond fairly well to the K values used in conventional
analysis of the specific reinforcement systems represented by each
set of data. The results show clearly that for most of the
reinforced soil structures for which data was available, in which
S_r is between 600 and 2,000 k/ft^2, the K/K_a value is close to 2 at
the top of the wall and becomes 1 at depth of 20 ft (figure 58).
The other set of field data (figure 59) clearly indicates that for
S_r > 2,500 k/ft^2, the K/K_a value is close to 3 at the wall top and
1.5 at a depth of 20 ft.

The relationships developed from the analysis were subsequently
used to develop figure 26 in volume I. Analysis of the predicted
horizontal stress in a 20 ft high wall using figure 26, volume I

Figure 56. Variation of K/K_a versus depth for some field wall.
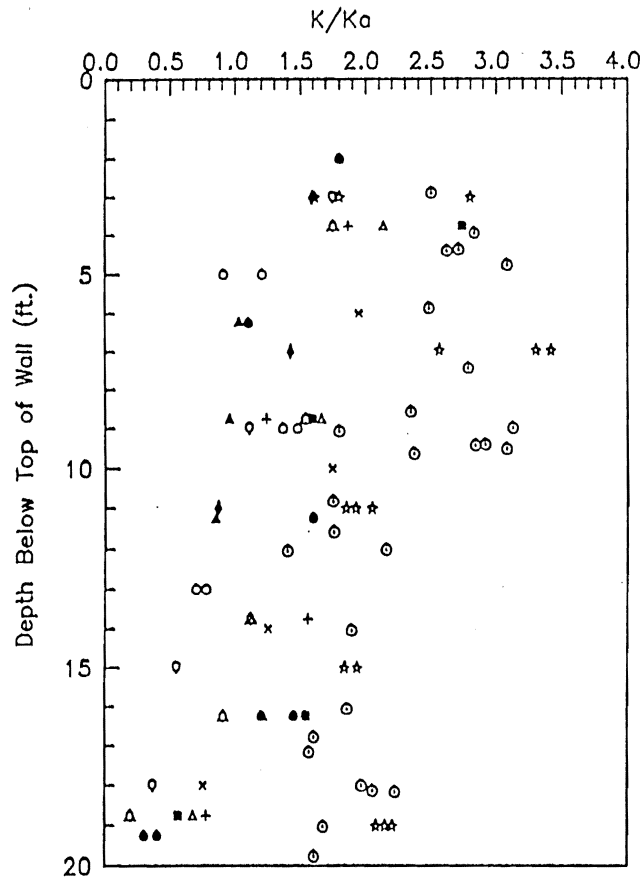
Variation of K with depth
For all value of Sr

Backfill: Sand or Sandy Gravel

	H (ft)	S_f (k/ft²)	System
●●●●● UCLA Wall	20	2160	RE
▲▲▲▲▲ Dunsmuir	16	1390	RE
■■■■■ STS Wall 1	20	1500	RE
♦♦♦♦♦ WES Wall	12	622	RE
○○○○○ Baxter	16	1858	MSE
△△△△△ STS Wall 3	20	1037	VSL
+++++ STS Wall 4	20	1037	VSL
××××× CalTran	20	997	MSE
☆☆☆☆☆ Hayward Wall	20	2342	VSL
◉◉◉◉◉ Seattle WW	47	3010	Welded Wire
△△△△△ STS Wall 2	20	56	Geogrid
♀♀♀♀♀ STS Wall 7	21	20	Gabion

109

Figure 57. Variation of K/K_a versus depth for S_r = 20-100 k/ft².

Figure 58. Variation of K/K_a versus depth for S_r = 500-2000 k/ft².
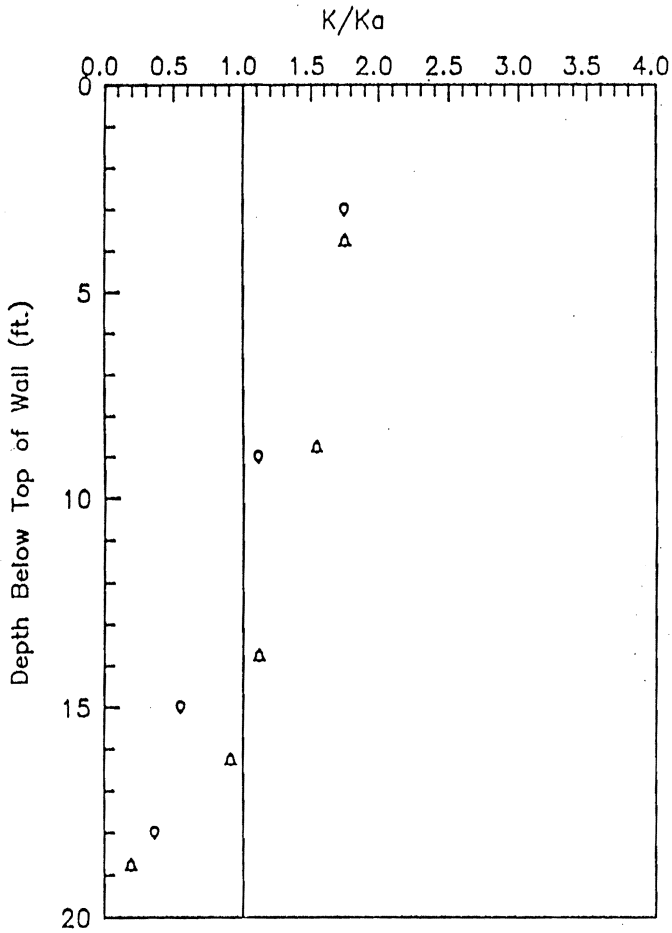
Variation of K with depth
Sr = 500 — 2000 k/ft²

Backfill: Sand or Sandy Gravel

	H (ft)	S_r (k/ft²)	System
●●●●● UCLA Wall	20	2160	RE
▲▲▲▲▲ Dunsmuir	16	1390	RE
■■■■■ STS Wall 1	20	1500	RE
◆◆◆◆◆ WES Wall	12	622	RE
○○○○○ Baxter	16	1858	MSE
△△△△△ STS Wall 3	20	1037	VSL
+++++ STS Wall 4	20	1037	VSL
××××× CalTran	20	997	MSE
—— Proposed FHWA K/Ka—Z Line			

111

Figure 59. Variation of K/K$_a$ versus depth for S$_r$ > 2500 k/ft^2.

Fig. 59 Variation of K/K$_a$ vs. depth for S$_r$ > 2500 k/ft^2

112

is compared to the conventional Reinforced Earth method and the New French Recommendations in figure 60. The $K/K_a - Z$ relationship corresponding to S_r = 500-2000 k/ft^2 was used. Similar comparison for a high wall (40 ft) is shown in figure 61.

From these plots, it appears that the horizontal stress is comparable for the FHWA Manual method and the New French Recommendations. The FHWA Manual method may give slightly more conservative values near the wall top, but gives a less conservative value near the bottom of the wall. Notice, however, that the field data in figure 58 show measured K/K_a data in the upper wall levels exceed the proposed values in several cases and at depths greater than 15 ft, all data is less than the proposed value. Thus, the proposed FHWA Manual method is still on the safe side.

7.0   INFLUENCE OF THE LENGTH OF THE REINFORCEMENTS

Initially, for Reinforced Earth walls, the ratio of the reinforcement length to the wall height L/H was taken equal to 1 for preliminary design. At the end of the 70's, based on account the results of about 15 instrumented Reinforced Earth walls and a number of model tests, the recommended L/H ratio value was reduced to 0.7 (French Specifications on Reinforced Earth, 1979). In volume I, an L/H ratio value of 0.5 is considered for preliminary evaluation of reinforced fill walls.

The L/H value of 0.5 results from the model tests, parametric F.E.M. studies and full scale experiments discussed in section 2. A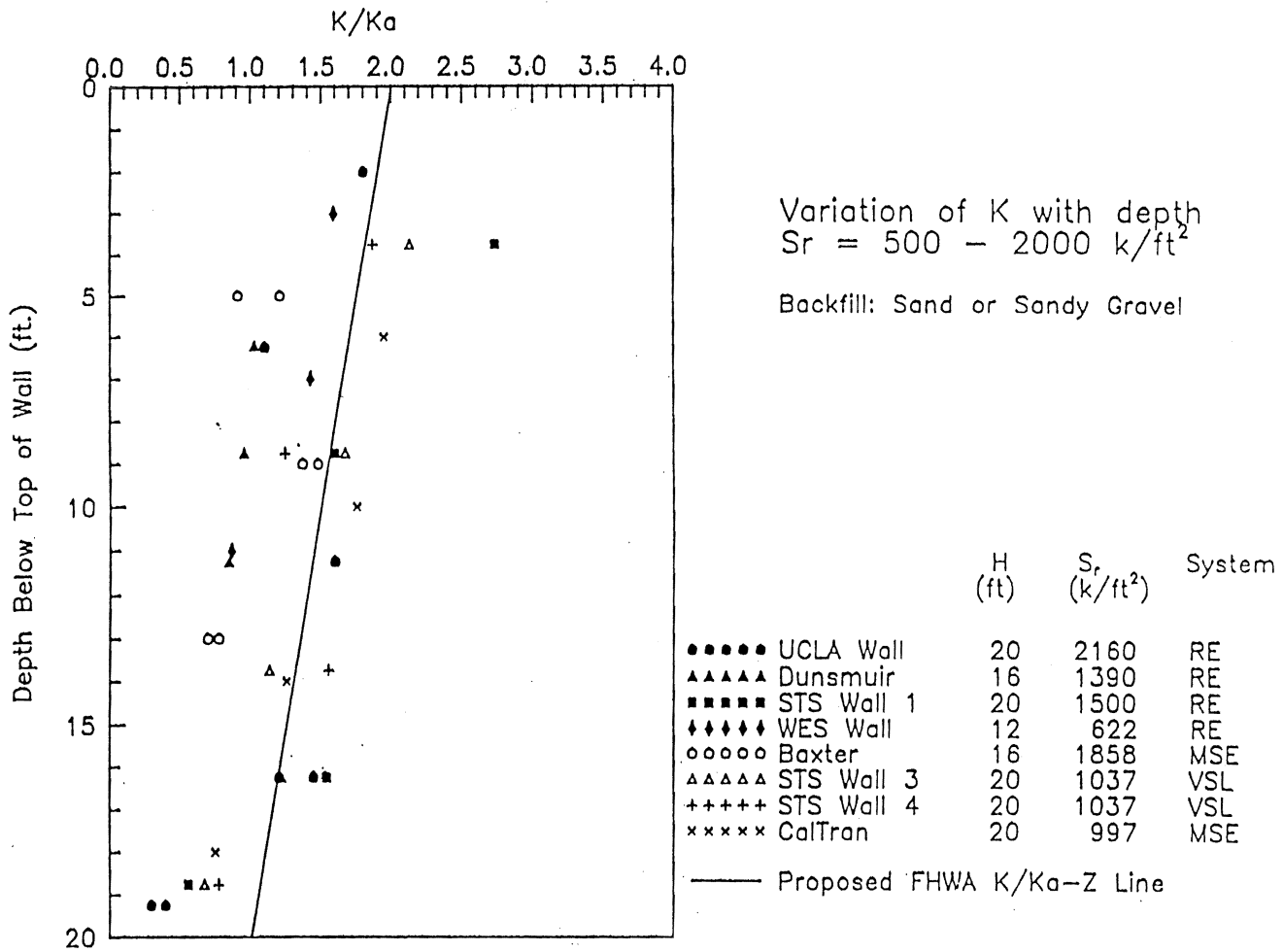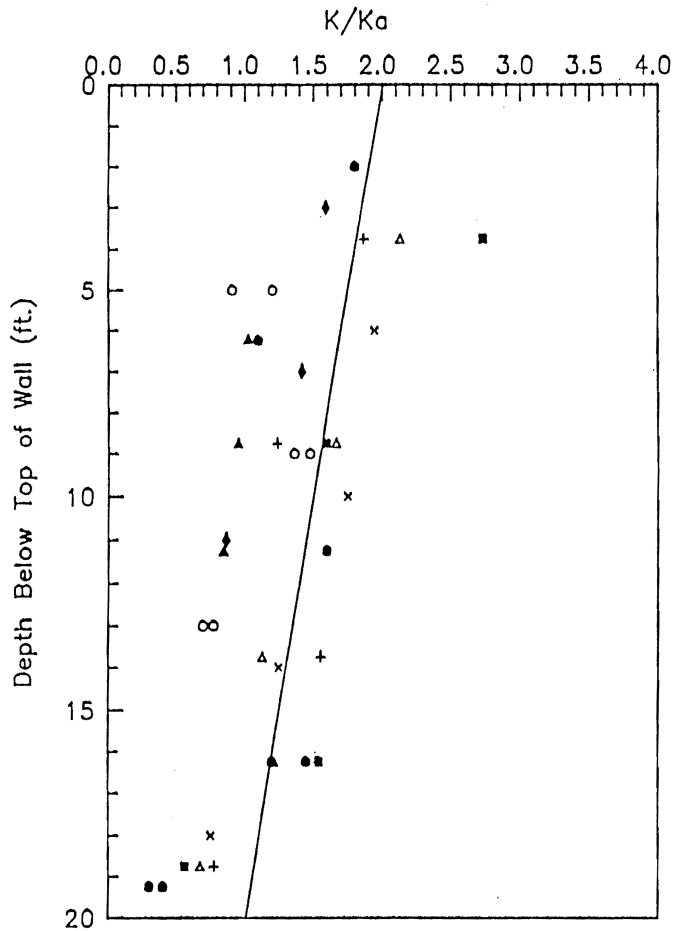s the similitude is not respected in classical reduced scale models, centrifuge model results were given more consideration than the reduced scale model results.

The F.E.M. results in section 2.c., Table 4, corresponding to the extreme case of L/H equal to 0.275 clearly shows the influence of a reduced L/H on the wall system. The main conclusions concerning the behavior are:

   .   F.E.M. calculated tensions are less than the ones
       calculated using the design method proposed in this
       manual, indicating that the tension analysis method is
       conservative for a decreased L/H ratio.

   .   The horizontal displacements were found to be 250
       percent greater than with a L/H ratio equal to 0.7
       (Baseline) and the wall appeared to be at the verge of
       the overall stability failure. At an L/H ratio of
       0.425, the wall was found to be stable, but had a
       corresponding horizontal displacement of 100 percent
       greater than the baseline case.

These conclusions indicate the importance of evaluating lateral deformation response for reduced L/H ratios.

Figure 60. Typical Reinforced Earth Wall. [42]

Typical Reinforced Earth Wall, H=20 ft.

γ_r=129 pcf, ϕ_r=39°
γ_b=129 pcf, ϕ_b=39°

——— Original Reinforced Earth Method: Meyerhof + K=K$_0$ to K$_a$
------ New French Recommendation: Meyerhof + λ + K=K$_0$ to K$_a$
·— — FHWA Manual Method: γZ + K=K(Sr)

L/H = 0.5

(a)

L/H = 0.7

(b)

L/H = 1.0

(c)

High Wall H=40 ft.

——— Original Reinforced Earth Method: Meyerhof + K=K$_0$ to K$_a$
········ New French Recommendation: Meyerhof + λ + K=K$_0$ to K$_a$
·— — FHWA Manual Method: γZ + K=K(Sr)

γ_r=129 pcf, ϕ_r=39^0
γ_b=129 pcf, ϕ_b=39^0
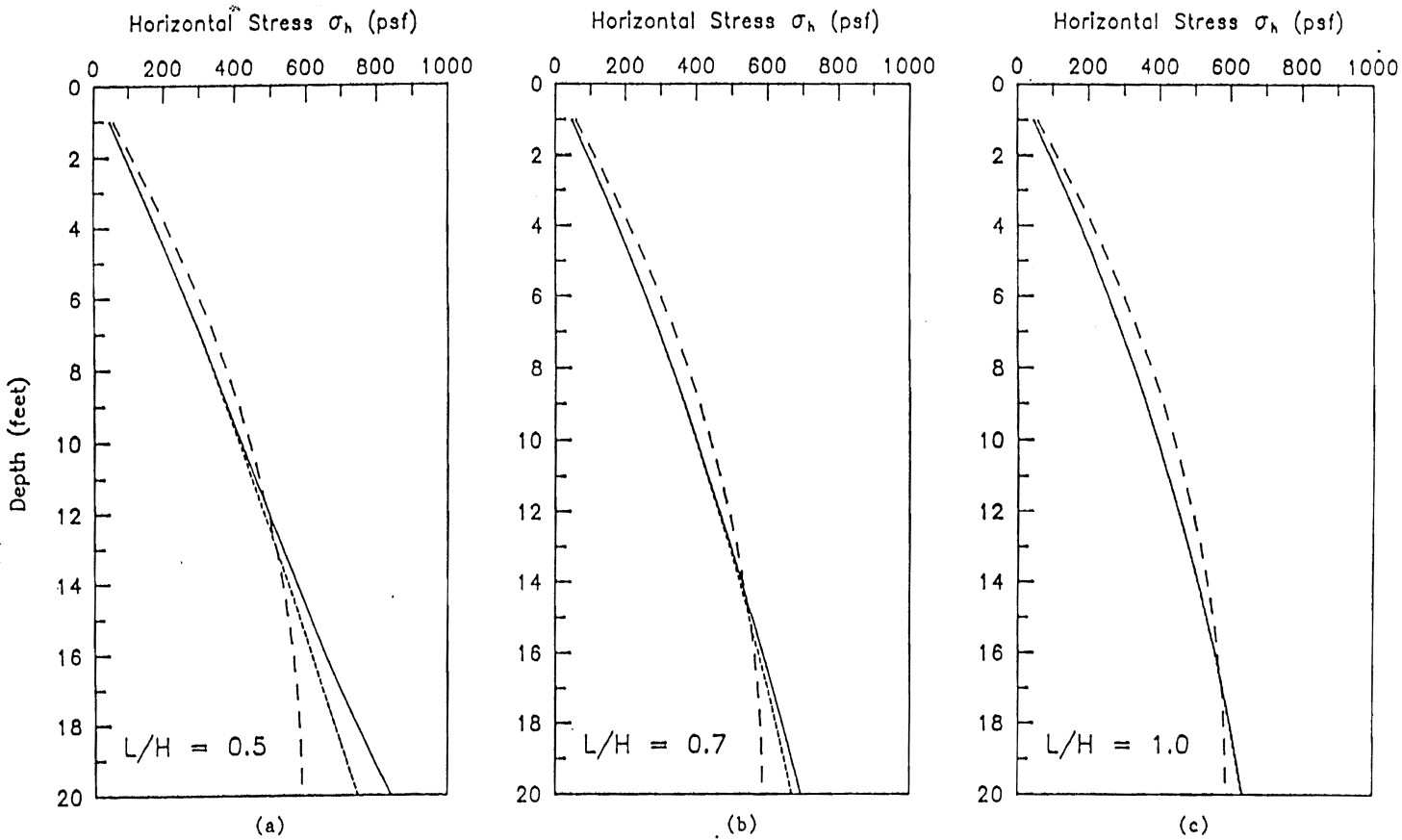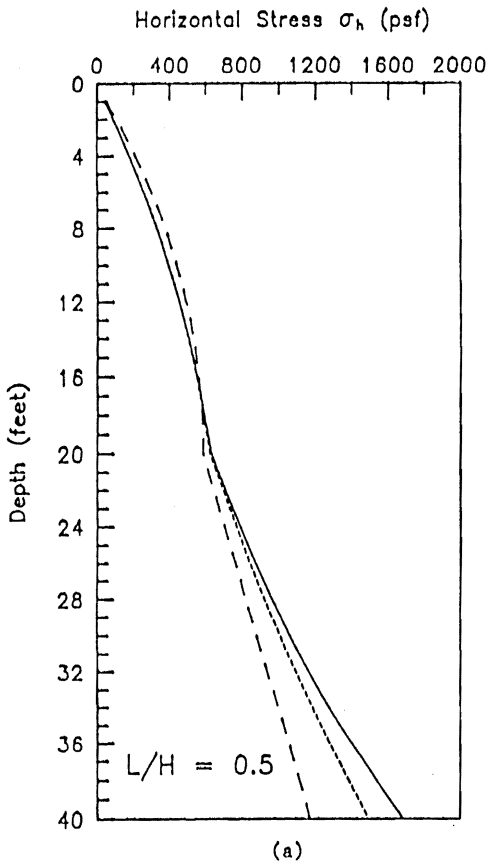
Figure 61. Horizontal stress comparison for high wall. [42]

115
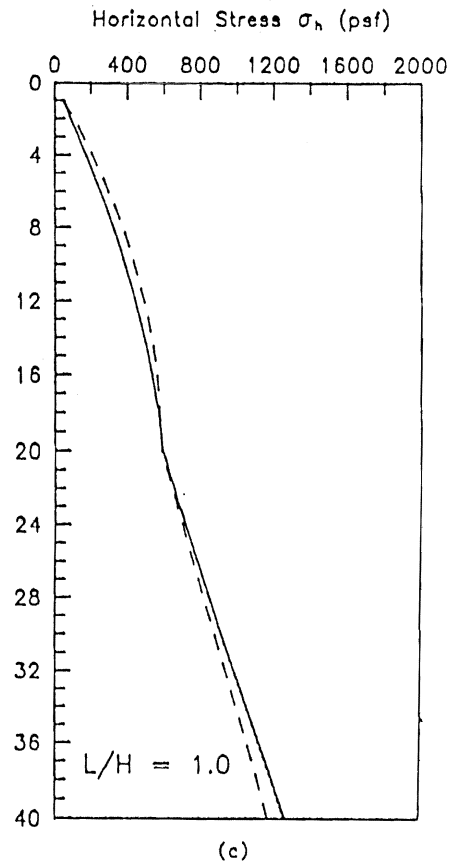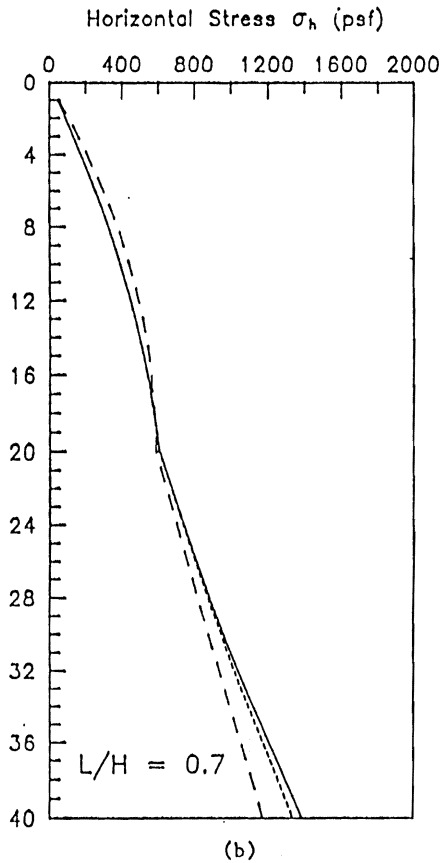
Full scale experiments performed recently by the French Administration and by the Reinforced Earth Company have found that carefully constructed reinforced soil walls with inextensible reinforcement and a L/H value equal to 0.5 behave satisfactorily.[86] Until the L/H ratio was reduced to less than 0.5, the location and shape of the maximum tensile force line was not affected.

8.0 LATERAL DEFORMATION AT WALL FACE

As indicated in chapter 3 of volume I, the current design method for evaluating the lateral displacements at wall face is handled empirically based on the results of the F.E.M. study (section 2.c.) and the results of the eight instrumented full-scale walls (section 2.b.). The L/H ratio of the field walls was 0.7, so that tilting and sliding movements were very small. As indicated in the previous section and as illustrated in figure 62, the F.E.M. results showed that the L/H ratio has a significant influence on the lateral deformation at the wall face.

Measurements of the lateral displacements on wall 2 of the FHWA study as compared to the other walls found that the rigidity of the reinforcement connections at the face has a large influence on tilting deformations.

It should be realized that all lateral movement due to design stress conditions should take place during construction. Postconstruction movement should only occur due to settlement of the reinforced soil section. Therefore, lateral deformation is mainly a construction problem that can be handled by proper batter. Excessive postconstruction movement may be an indication of foundation problems or an overstressing of the reinforcement due to an inadequate design.

9.0 RECENT RESULTS ON SEISMIC BEHAVIOR OF REINFORCED SOIL WALLS

The basis for seismic design in volume I is an internal report to the reinforced earth company by seed and mitchell in 1981 as updated, based on an extensive f.e.m. study and half-scale shaking table model tests performed by the Reinforced Earth Company.[19, 87]

the results of recent research has found that the maximum tensile force line in a reinforced soil wall under seismic loading is essentially the same as under static loading, even for strong accelerations ($\alpha \geq 0.4$). in addition, the lower strips are the most affected (i.e., required to withstand the greatest dynamic increment) under a seismic loading. the use of a pseudo-static dynamic thrust p_{ae} was proposed by seed and whitman.[21]

the design principle considers that the total tensile forces in the reinforcements results from the vertical overstresses due to the seismic thrust p_{ae} and from the inertia force p_i acting on the active zone. the forces are then distributed among the different layers of strips based on the area of the resistant zone and the distribution of reinforcement in the resistant zone.
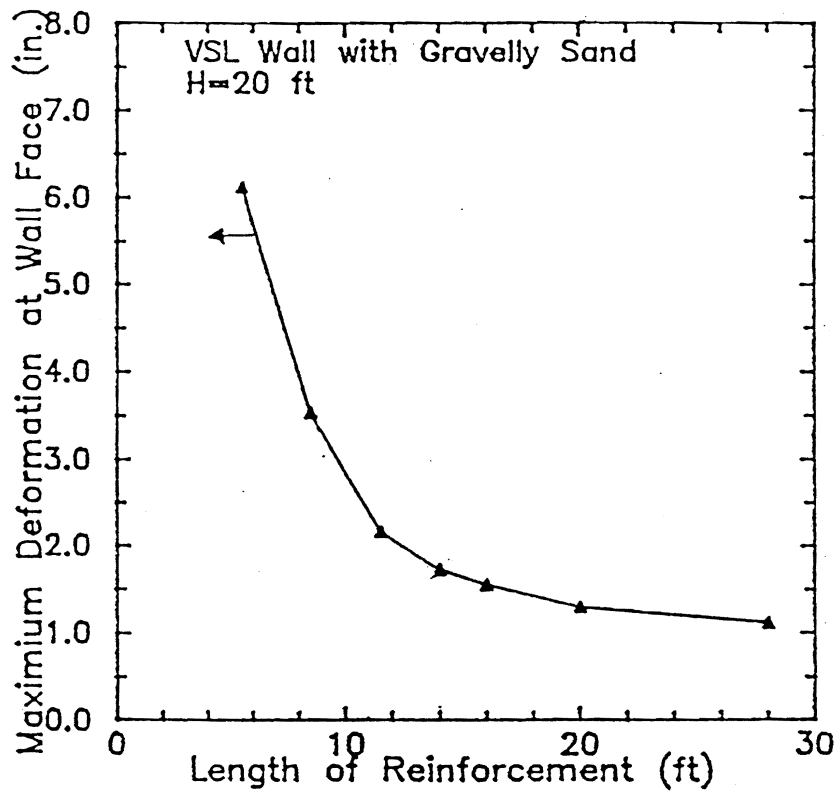
Figure 62. Influence of change in reinforcement length on lateral
deformation at the face of the wall anticipated
during construction.

117

Results of finite element calculations have shown that this simple design method represents very well the total tensile forces developed in the strips under a seismic loading. The safe behavior of numerous reinforced fill walls designed using this approach which have been subjected to seismic loading, particularly in Japan, is additional proof of the validity of this method.

CHAPTER 4

REINFORCED ENGINEERED SLOPES

1.0 INTRODUCTION

The methods for internal stability analysis at working stresses described in chapter 3 of volume I have been developed for vertically and quasi-vertically faced walls. They are empirical methods and they cannot be easily generalized to sloped structures. Consequently, the internal stability of reinforced engineered slopes is better analyzed using the limit equilibrium analysis.

Although several limit equilibrium approaches have been formulated (see reference 25 for summary of approaches) and successfully utilized to design numerous reinforced engineered slopes, very little research has been performed to substantiate these methods. A parametric study using a computer program was performed by Jewell and used to develop design charts for the Tensar Corporation (as modified by Schmertmann, et al) in figure 43, chapter 4, volume I.[26, 69] Other substantive numerical, laboratory, or field research does not appear to be available. In a study of polymeric reinforced soil structures constructed in North America, no instrumented field projects were identified.[48] Therefore, an important aspect of the FHWA Behavior of Reinforced Soil Study was to construct and instrument field structures to verify the limit equilibrium design approach.

For the FHWA project, two 25 ft high, 1 horizontal to 1 vertical slopes and two 25 ft high 0.5 horizontal to 1 vertical reinforced soil slopes were constructed as summarized in Table 5.

Table 5. Full scale reinforced slope experiments constructed for the FHWA program.

Slope	Reinforcements	Fill Material
1. 0.5 H:1V	Polypropylene Geogrid (T_{ult} = 145 lb/in)	Silt (ϕ = 35°)
2. 0.5 H:1V	Polypropylene Woven Geotextile (T_{ult} = 214 lb/in)	Silt (ϕ = 35°)
3. 1H:1V	Polypropylene Geogrid (T_{ult} = 145 lb/in)	Silt (ϕ = 35°)
4. 1H:1V	Polypropylene Woven Geotextile (T_{ult} = 214 lb/in)	Silt (ϕ = 35°)

All slopes were designed using the rotational failure limit equilibrium analysis approach in chapter 4, volume I and checked using Jewell's design charts. For all structures, eight layers of reinforcement with a uniform spacing of 2.5 feet (0.76 m) and a

119

total length of 14 ft (4.3 m) were used. Using an allowable
tension T_a of 60 lb/in (10.5 kN/m) assumed for both materials,
this arrangement provided a design factor of safety FS approaching
1.0 for slopes 1 and 2 and a FS of 1.3 for slopes 3 and 4.

The complete results of the field program are contained in a
separate report to the FHWA. Figures 63 through 66 show the
tension measured in each reinforcing layer as compared to the
computed maximum tension from the limit equilibrium method
(chapter 4, volume I) and from finite element analysis. As can be
seen from the figures, the limit equilibrium methods are somewhat
conservative for estimating the maximum tension.

Figure 67 shows a representative plot of the distribution of
tension measured in the reinforcement as compared to that
predicted by the finite element method. Also shown is the
predicted location of maximum tension in the reinforcement from
the limit equilibrium method which appears to be in close
agreement with the measured values.

Figure 68 provides an example of the measured and predicted
deformation response. For all slopes, the measured deformation
was much less than the estimated deformation. Most likely, this
was due to the inherent additional factor of safety for the
material tension (i.e. T_a versus T_{ult}) used for design.

As a result of the field study, a rotational limit equilibrium
analysis method is proposed for the design of reinforced
engineered slopes.

Embankment 1
Slope = .5 H/1 V
Geogrid (EA=90 kips/ft)

Embankment Height = 20 ft.

o   Measured (12/4/87)
△   Finite Element (c=50 psf, Φ=35 deg.)
- - - - - Limit Equil.   (based on Φ=35 deg.)
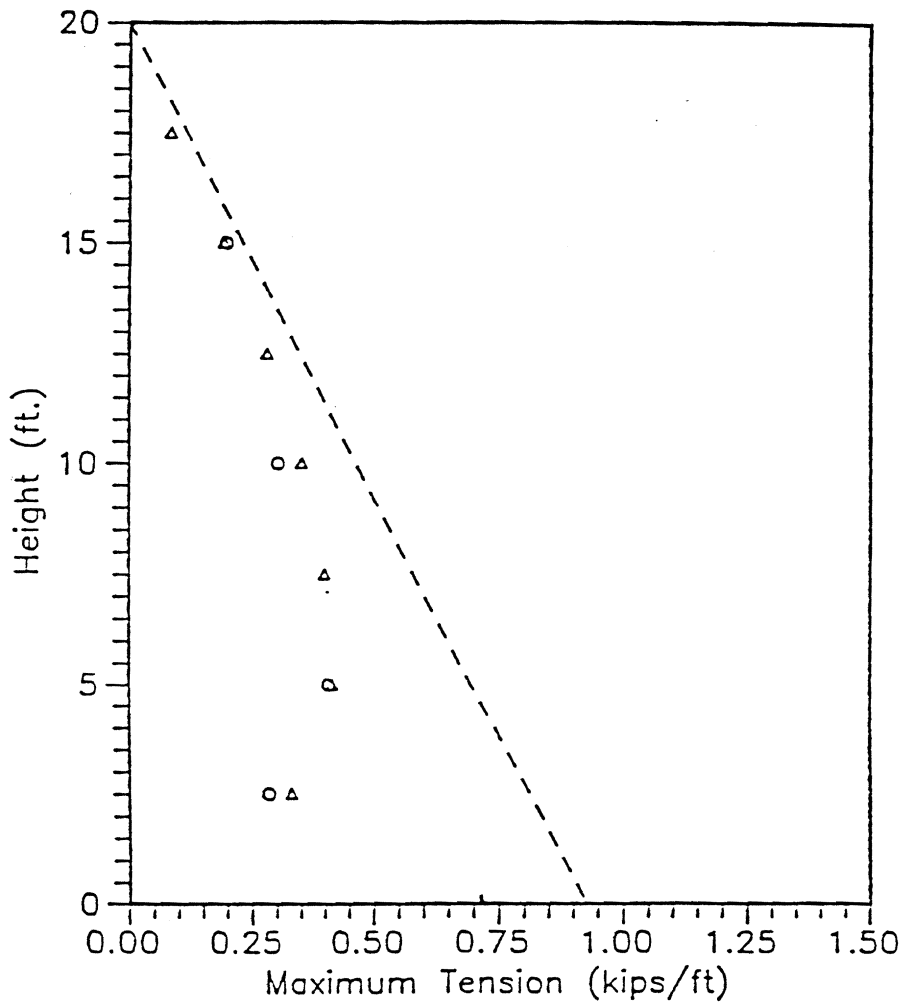
Figure 63.   Distribution of maximum tension with
             depth in embankment 1.

Embankment 2
Slope = .5 H/1 V
Geotextile (EA = 96 kips/ft)

Embankment Height = 20 ft.

o   Measured
△   Finite Element (c=50 psf, ϕ_i=35 deg.)
---- - Limit Equil.   (based on ϕ=35 deg.)
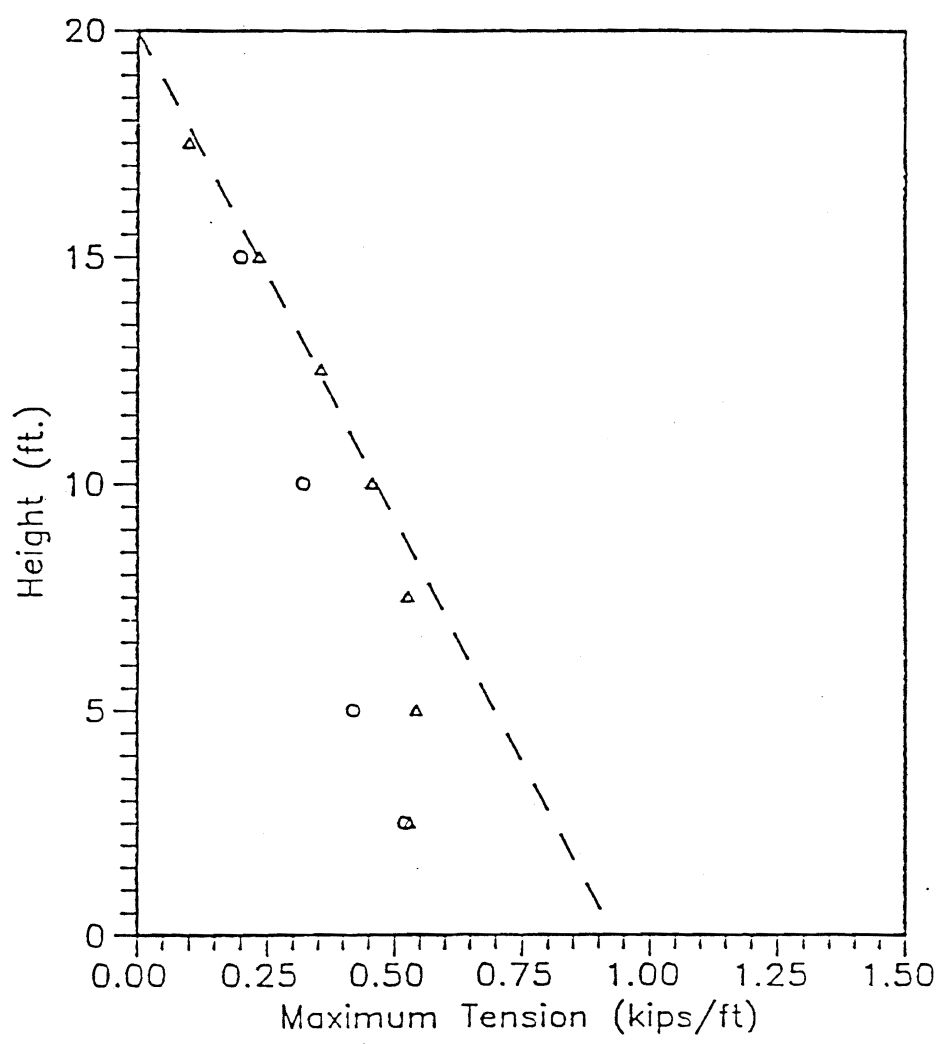
Figure 64.   Distribution of maximum tension with
depth in embankment 2.
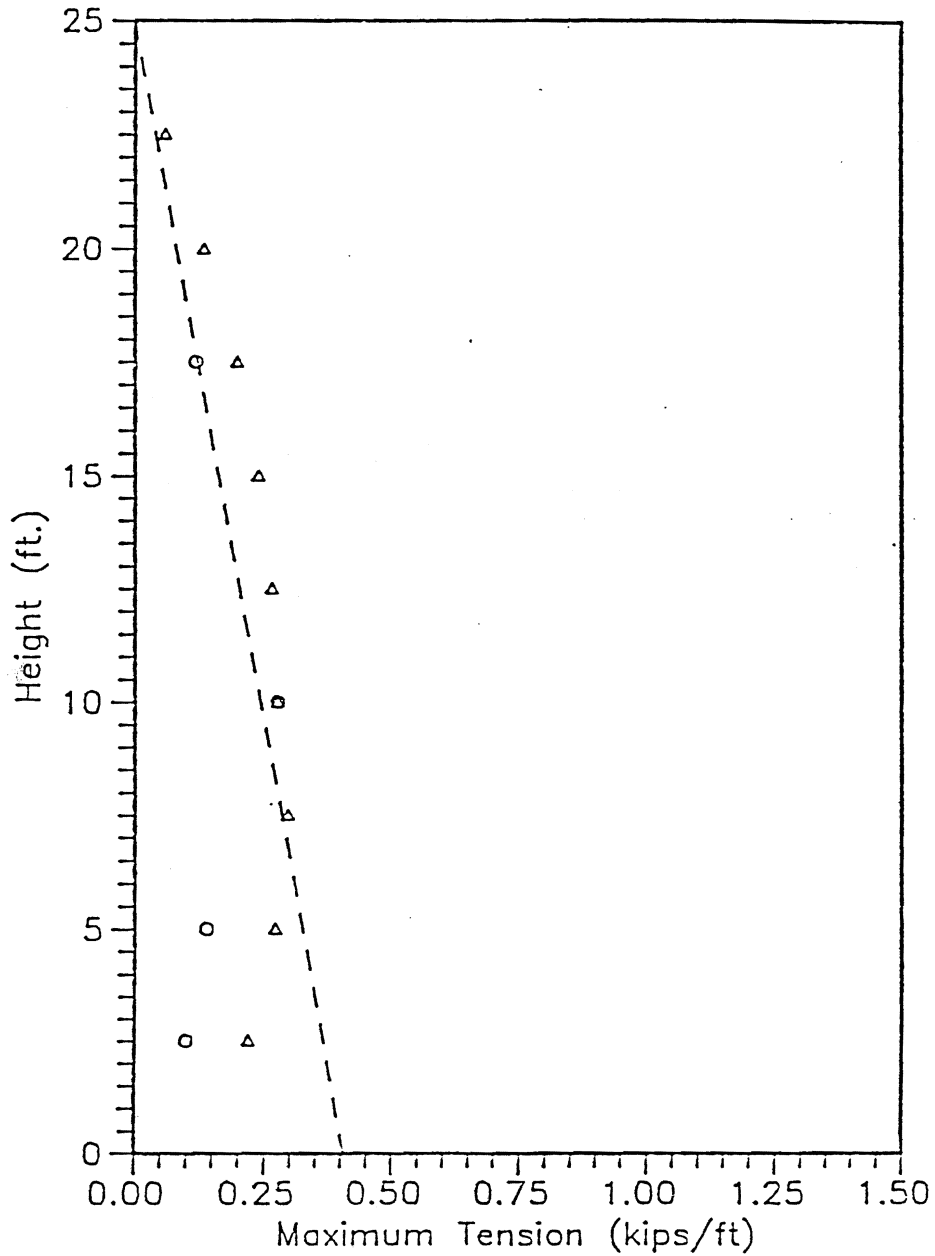
Figure 65. Distribution of maximum tension with
depth in embankment 3.
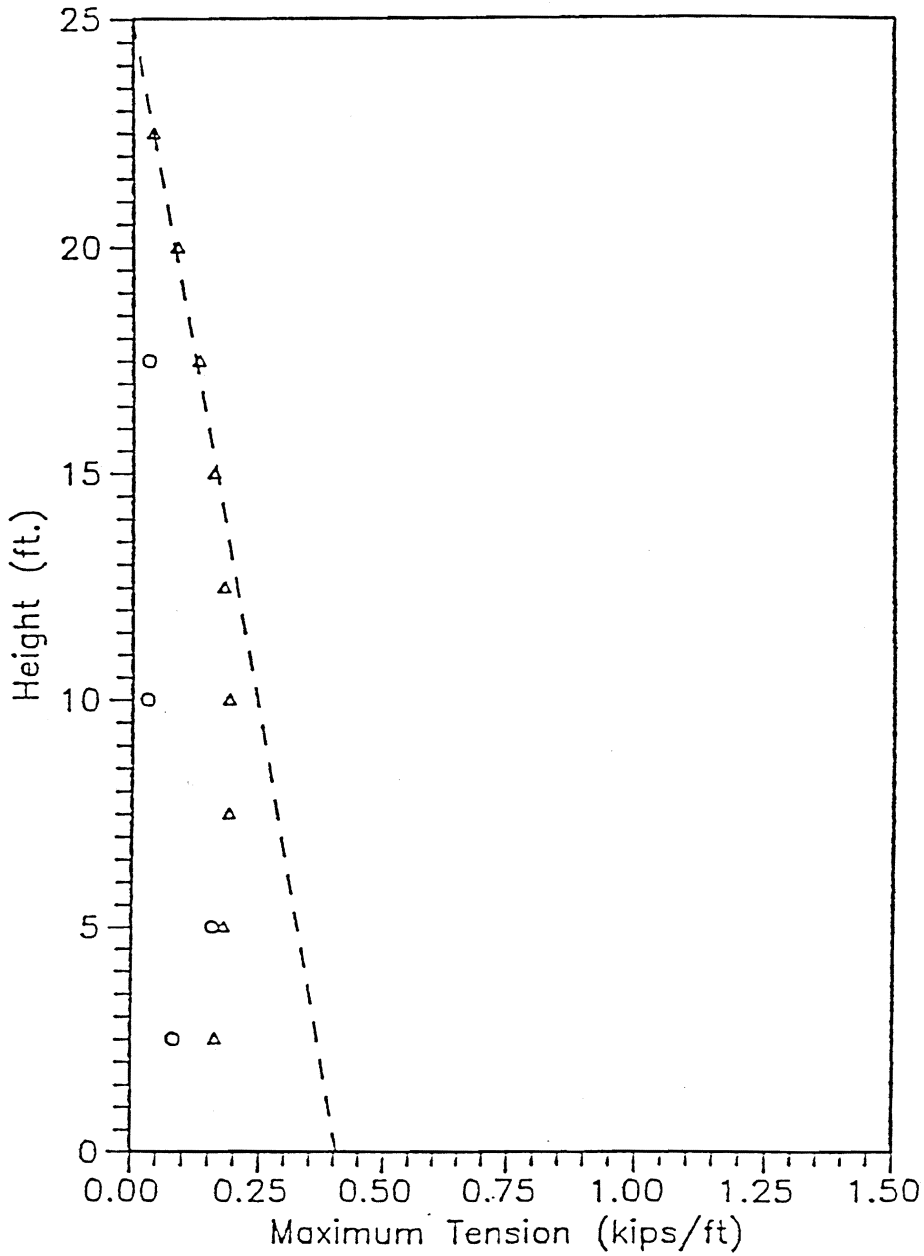
Figure 66. Distribution of maximum tension with
depth in embankment 4.

Figure 67. Distribution of tension along different levels
of reinforcement in embankment 1.

Embankment 1
Geogrid and Clayey Silt
Deformation at 12.5 ft. From Toe
Height of Fill = 16.25 ft.
○ Field Data
□ Finite Element

12.5'

Height
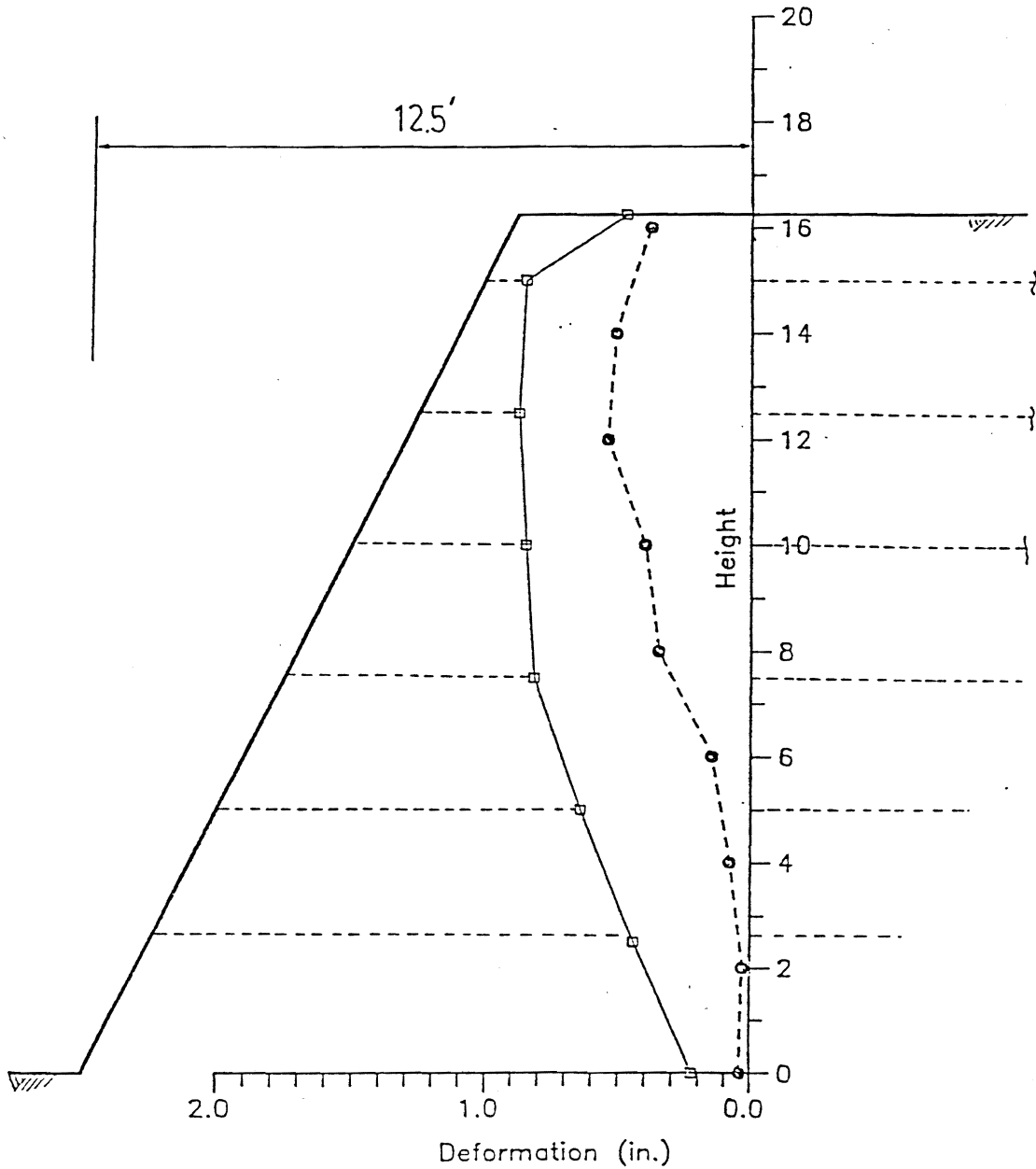
Deformation (in.)

Figure 68. Deformation at 12.5 feet from the toe of embankment 1.

CHAPTER 5

SOIL NAILING

1.0 INTRODUCTION

Several approaches have been developed to estimate the resisting forces required to restrain ground displacements in cut slope retaining structures such as bracing supports, tiedback walls or soil nailed systems. They can be broadly classified into three main categories:

  (1) Empirical design earth pressure diagrams.

  (2) Finite element analyses.

  (3) Kinematical limit analysis method.

2.0 EMPIRICAL DESIGN EARTH PRESSURE DIAGRAMS

Selection of an appropriate earth pressure diagram for the determination of nail forces should be consistent with the anticipated level of the structure and ground movements. Measurements of facing displacements in nailed soil cut slopes illustrate (figure 69) that in non plastic soils these displacements are comparable to those measured in braced excavations. Therefore, design diagrams proposed by Terzaghi and Peck and Tschebotarioff for the design of braced excavations, provide a rational estimate of working tensile forces generated in the nails.[39, 44, 88, 89] These diagrams are schematically illustrated in figure 70. Note that Terzaghi and Peck's design diagram for sands has been slightly modified in order to calculate nail forces. The maximum tension force mobilized in the nail is expressed as a normalized, non-dimensional parameter:

$$T_N = \frac{T_{max}}{\gamma H \cdot S_h \cdot S_v} \quad \text{at the relative depth of } z/H \quad (28)$$

T_N is the working tensile force generated in the reinforcement.

T_{max} is the maximum tension force mobilized in the nail.

  where: H is the total structure height (or excavation depth)
  S_h and S_v are, respectively, the horizontal and vertical spacings between the nails

For sands ($c/\gamma H < 0.05$, where c is an apparent soil cohesion):

$$T_N = 0.65 K_a \quad (29)$$

where the active lateral earth pressure coefficient

$$K_a = \tan^2 \left(\frac{\pi}{4} - \frac{\phi}{2}\right). \quad (30)$$
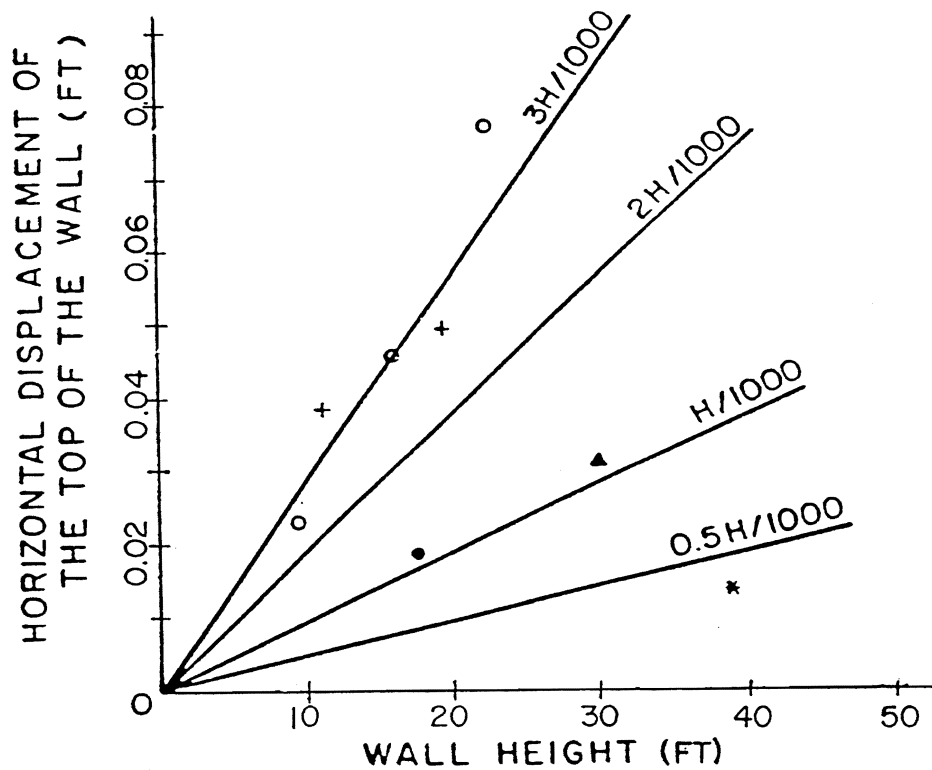
	SOIL	NAIL	REFERENCE
+	Medium sand	driven	38
▲	Silty sand (SM)	grouted	11
●	Fine sand (SP) to clayey sand (SC)	driven	37
✶	Residual clayey silt weathered shale, sandstone	grouted	39
○	Fontainbleau Sand (SP)	grouted	40

Figure 69. Horizontal displacement of nailed soil walls.

128

NOTES:

— Vertical cut slope

— Horizontal upper surface.

σ_h = lateral earth pressure

γh = overburden pressure
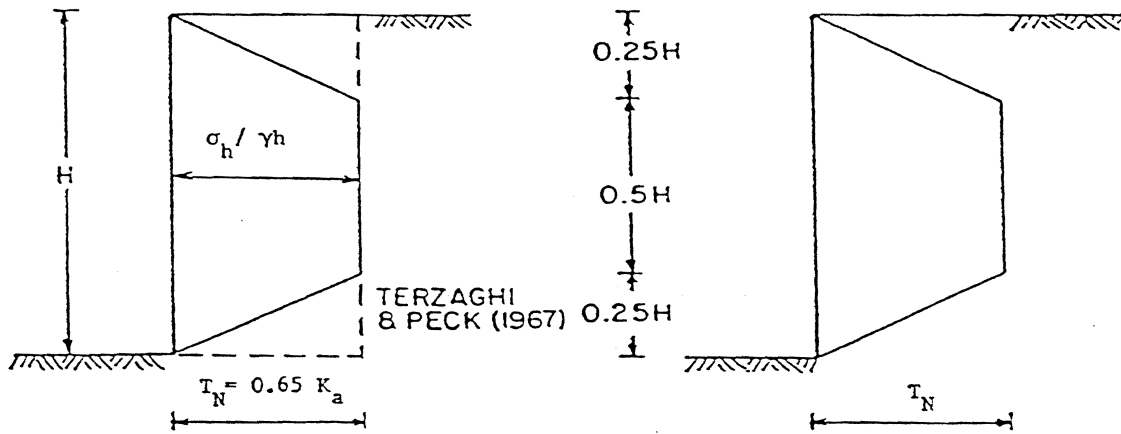
SAND : $\dfrac{c}{\gamma H} \leqslant 0.05$

$K_a = \tan^2 (\pi/4 - \phi/2)$

CLAYEY SAND : $T_N = K_a (1 - \dfrac{4c}{\gamma H} \dfrac{1}{\sqrt{K_a}}) \leqslant 0.65 \ K_a$

CLAY : $T_N = 0.2 \ \gamma H \rightarrow 0.4 \ \gamma H$

Figure 70. Empirical earth pressure design diagram.

and for a cohesive soil with both cohesion (c) and friction angle:

$$T_N = K [1 - \frac{4c}{\gamma H} (\frac{1}{K_a})^{0.5}] < 0.65 \, K_a . \tag{31}$$

Figure 71 shows nail forces and structure displacements measured in four instrumented soil nailed structure.[11,37,39,40] The measured nail forces, specifically in grouted nails, were found to agree fairly well with the assumed earth pressure design diagrams. These results illustrate that the observed behavior of nailed cut slopes is similar to that of braced excavations.

The use of the empirical earth pressure diagrams in the design of soil nailed retaining structures presents some severe limitations. In particular, these diagrams correspond to conventional cases of bracing supports with simple geometry of a vertical wall, horizontal ground surface and lateral braces. Therefore, they cannot be used to assess the effect of design parameters such as inclination of the facing, inclination and rigidity of the inclusions, surcharge, etc. on the working forces in the inclusions and structure displacements. They do not provide any data with regard to the shear forces and bending moments that can develop in the nails. In addition, as shown in figure 72, in cohesive soils the empirical earth pressure diagram is highly sensitive to small variations in soil properties.

3.0 FINITE ELEMENT ANALYSES

The finite element method has been used by several investigators to analyze the behavior of soil nailed retaining structures.[11, 90, 91] These analyses involve different constitutive equations for the soil and interface elements to simulate soil-facing and soil-inclusion interaction. Attempts have been made to compare finite element predictions with observed behavior of instrumented structures.[11, 91] However, the use of finite element method in design is currently limited by the relatively high costs and raises significant difficulties with regard to:

- The actual construction stages and installation process of the inclusions are difficult, if not practically impossible, to simulate.

- The complex soil-inclusion and soil-wall interaction is difficult to model. Several interface models have been developed but their implementation in design requires relevant interface properties which are difficult to properly determine.[92, 93]

130

HORIZONTAL DISPLACEMENT
(mm)

$K = \dfrac{T_{max}}{\gamma \cdot H \cdot S_H \cdot S_V}$

$\dfrac{c}{\gamma H} = 0.114$
$\phi = 33°$

$\dfrac{c}{\gamma H} = 0.124$
$\phi = 34°$

EMPIRICAL DESIGN METHOD

● INCLINOMETER AT 1.5 m FROM THE FACING

○ INCLINOMETER AT 4.5 m FROM THE FACING

END OF CONSTRUCTION
● EXPERIMENTAL RESULTS
H = 9.2 m

Z/H
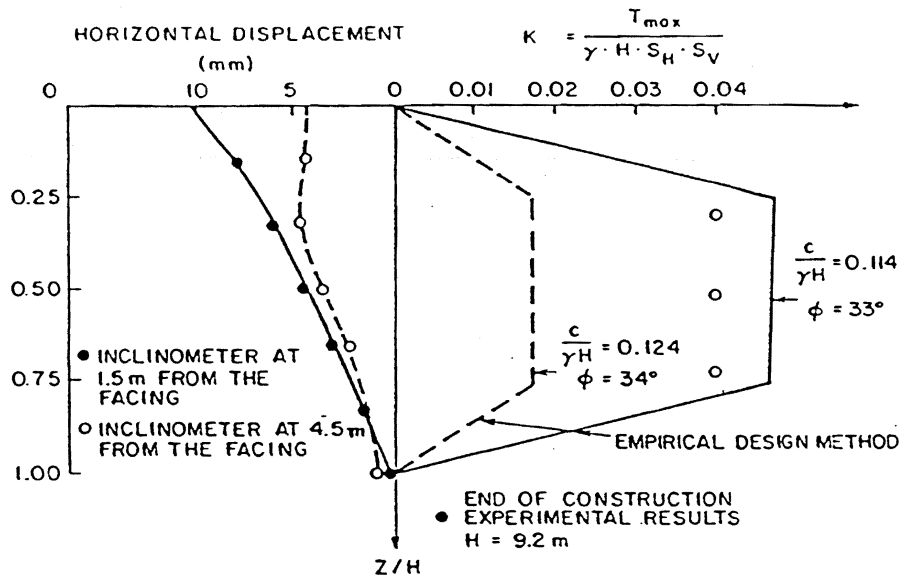
a. DAVIS WALL (Shen et al., 1981)

HORIZONTAL DISPLACEMENT
(mm)

$K = \dfrac{T_{max}}{\gamma \cdot H \cdot S_H \cdot S_V}$

END OF CONSTRUCTION
EXPERIMENTAL RESULTS
○ H = 3 m
● H = 5 m
▲ H = 7 m

KINEMATICAL APPROACH

$(\phi = 38°, c = 0)$

$(\phi = 35°, c = 0)$

EMPIRICAL DESIGN METHOD

● FACING DISPLACEMENT (H = 7 m)

○ FACING DISPLACEMENT (H = 3 m)

Z/H
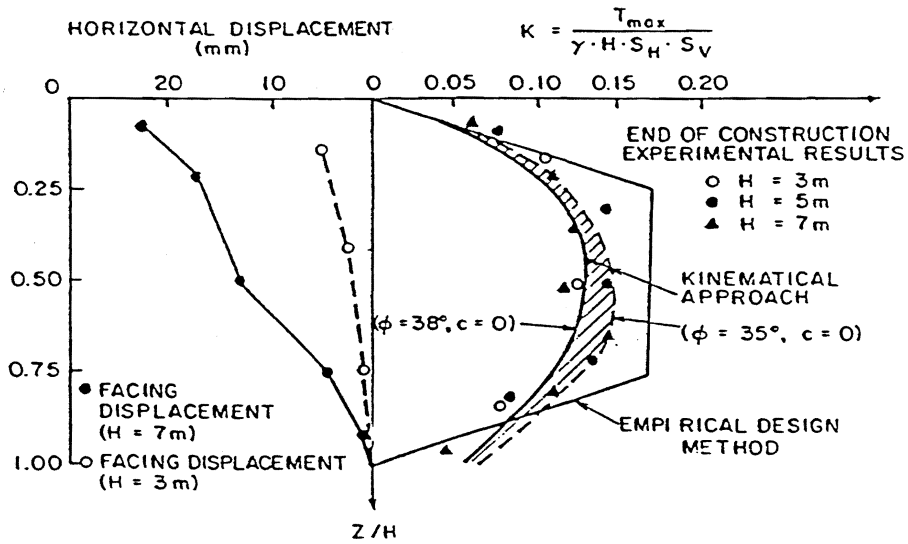
b. CEBTP FULL SCALE EXPERIMENT (Plumelle, 1986)

Figure 71.   Experimental data and theoretical
predictions of tension forces.

131

K = $\frac{T_{max}}{\gamma \cdot H \cdot S_H \cdot S_V}$

HORIZONTAL DISPLACEMENT (mm)

$\phi = 35°$
$\frac{c}{\gamma H} = 0.05$

KINEMATICAL APPROACH

($\phi = 40°$, c = 0)

EMPIRICAL DESIGN METHOD

• INCLINOMETER AT 1.5m FROM THE TOP OF THE WALL

○ INCLINOMETER AT 3.9m FROM THE TOP OF THE WALL

Z/H

END OF CONSTRUCTION EXPERIMENTAL RESULTS
▲ H = 12.0m
● H = 9.0m
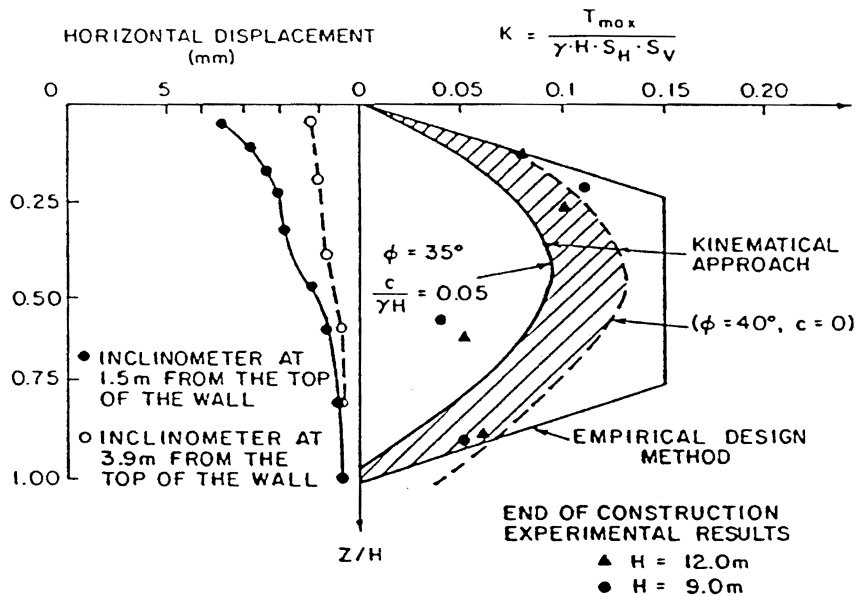
c. CUMBERLAND GAP WALL (FHWA, 1985)

HORIZONTAL DISPLACEMENT (mm)

K = $\frac{T_{max}}{\gamma \cdot H \cdot S_H \cdot S_V}$

EMPIRICAL DESIGN METHOD

$\phi = 35°$
c = 0

$\phi = 30°$
c = 0

• INCLINOMETER AT 3M FROM THE FACING

○ INCLINOMETER AT 7M FROM THE FACING

KINEMATICAL APPROACH

$K_c = 0.65 K_o$

$K_c = 0.8 K_o$

END OF CONSTRUCTION
• EXPERIMENTAL RESULTS

H = 5.6m

Z/H
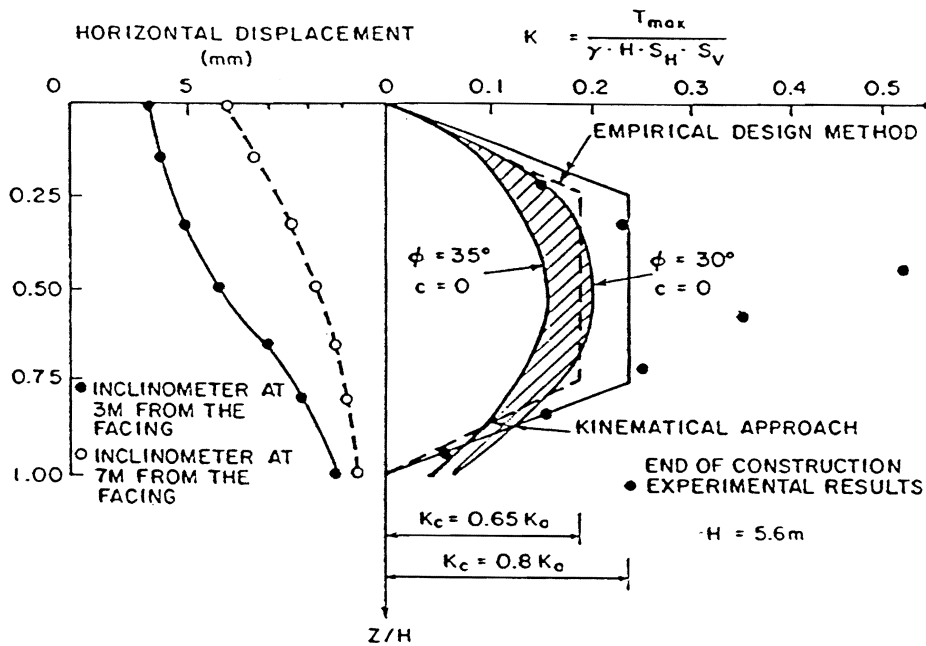
d. PARISIAN WALL (Cartier and Gigan, 1983)

Figure 71. Experimental data and theoretical predictions of tension forces (continued).

132
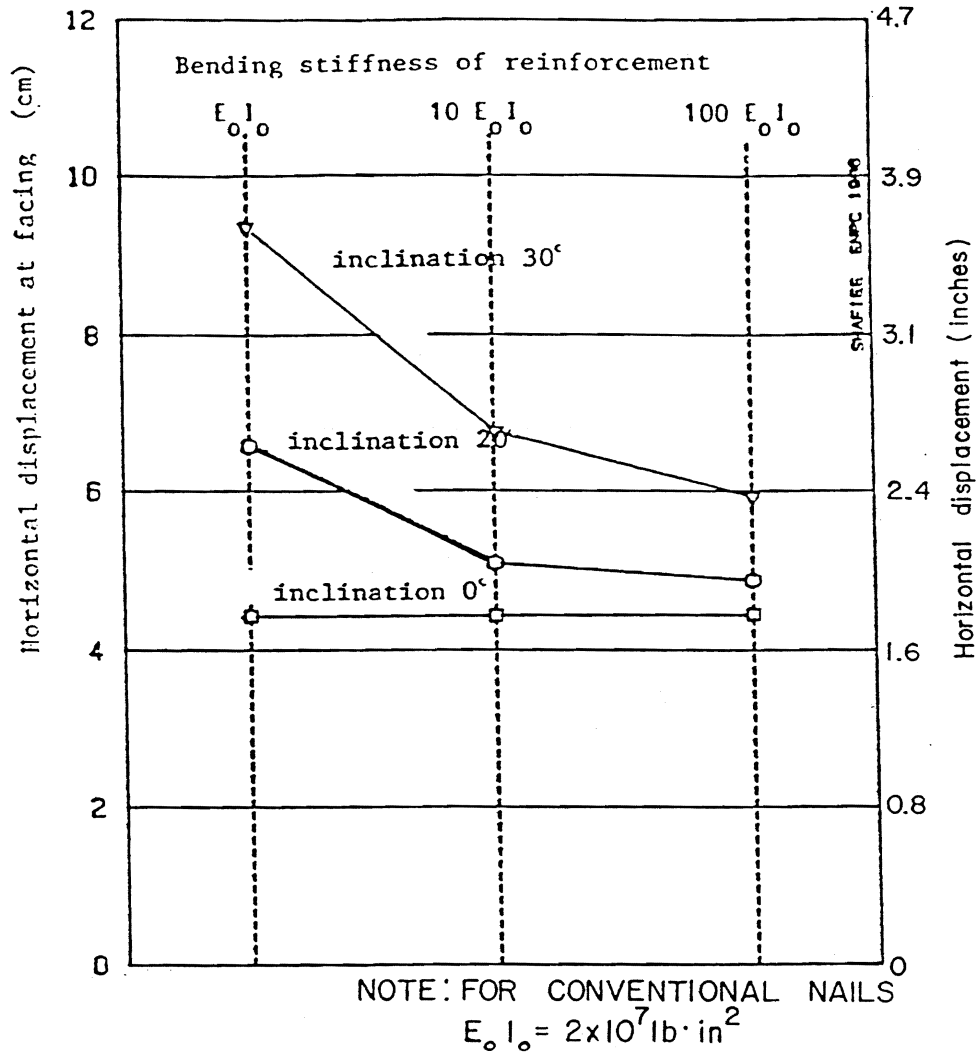
Figure 72. Effect of the bending stiffness and the inclination of reinforcement on the facing displacements.[91]
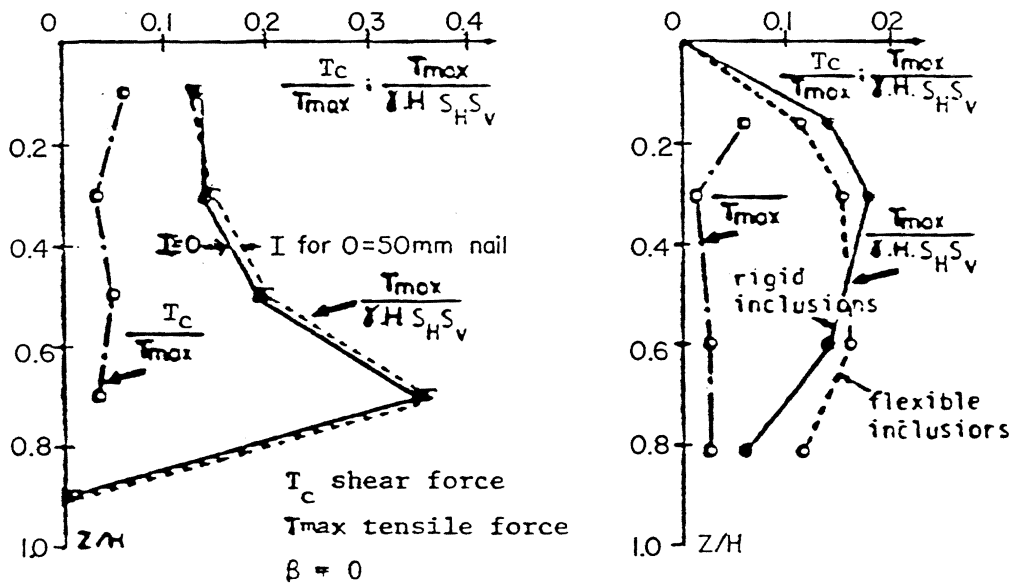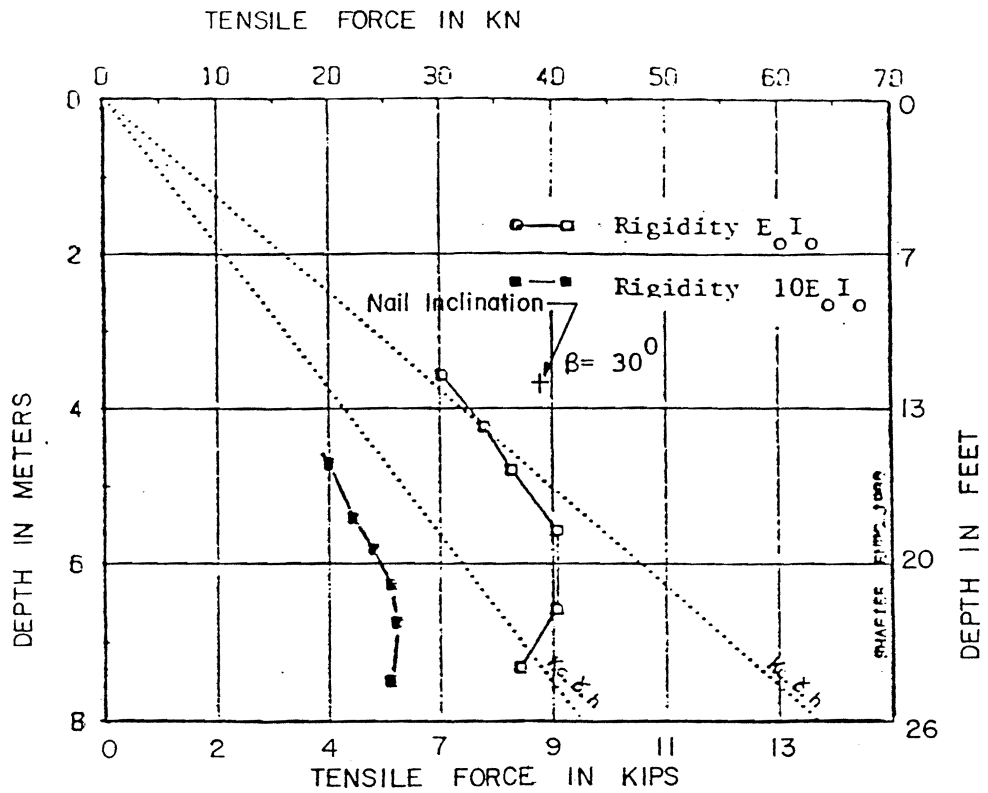
Figure 73. Effect of bending stiffness of the inclusions on nail forces.

134

- Various elasto-plastic soil models can presently be used to predict soil behavior during excavation. However, determination of soil model parameters generally requires specific and rather elaborated testing procedures limiting the practical use of these models.

The finite element method has therefore been used mainly as a research tool to evaluate the effect of the main design parameters on the behavior of the structure, ground movement, and working forces in the inclusions.

Figure 72 shows the results of a parametric study using the finite element method to evaluate the effect of bending stiffness and nail inclination on facing displacement in vertical nailed cut slopes.[40, 91] These results illustrate that, for nail inclinations used in practice (10 to 15 deg.), the greater the nail bending stiffness is, the smaller is the facing displacement. As shown is figure 73a, for inclined nails an increase in the bending stiffness results in a decrease of the maximum tensile forces. The behavior of inclined nails is substantially different from that of horizontally placed nails.

During construction, inclined nails tend to undergo a local deformation approaching the horizontal direction of maximum extension strain in the soil. This local deformation which is controlled by the bending stiffness of the nails, results in an increase of the structure/facing displacements. For horizontal nails, as illustrated by both reduced scale model tests and numerical test simulations (figures 72 and 73), the bending stiffness has practically no effect on the mobilized nail forces and structure displacements. Although the finite element results are rather qualitative, they provide a significant insight into the fundamental understanding of the system behavior and relevant input into the selection of the main design parameters.

4.0 KINEMATICAL LIMIT ANALYSIS DESIGN METHOD

This limit analysis approach was developed for the design of nailed soil retaining structures.[41, 42] It permits an evaluation of the effect of the main design parameters (i.e., structure geometry, inclination, spacing, and bending stiffness of nails) on the tension and shear forces generated in the nails during construction. The main design assumptions, shown in figure 74, as reviewed in volume I, chapter 6 are:

- Failure occurs by a quasi-rigid body rotation of the active zone which is limited by either a circular or a log-spiral failure surface.

- The locus of the maximum tension and shear forces at failure coincides with the failure surface developed in the soil.

135

- The shearing resistance of the soil, defined by Coulomb's failure criterion, is entirely mobilized along the sliding surface.

- The shearing resistance of stiff inclusions is mobilized in the direction of the sliding surface in the soil.

- The horizontal components of the interslice forces E_h (figure 74) are equal.

- The effect of a slope (or horizontal surcharge F_h), at the upper surface of the nailed soil mass, on the tension forces in the inclusions in linearly decreasing along the failure surface.

The effect of the bending stiffness is analyzed using a conventional "p – y" analysis procedure, assimilating the relatively flexible nail to a laterally loaded infinitely long pile. The solution involves a non dimensional bending stiffness parameter, defined as:

$$N = \frac{K_h \cdot D \cdot L_o^2}{H \cdot S_h \cdot S_v} \tag{32}$$

where: $L_o = [\frac{4\ EI}{K_h\ D}]^{1/4}$

is the transfer length which characterizes the relative stiffness of the inclusion to the soil; note that the length of the inclusion L is substantially greater than three times the transfer length L_o and it can therefore be considered as infinitely long,

D is diameter of the nail,

E and I are the elastic modulus and the moment of intertia of the nail, respectively,

K_h is the modulus of lateral soil reaction.

As provided in volume I, the charts shown in figure 75 can be used to obtain K_h values as a function of soil shear strength parameters.
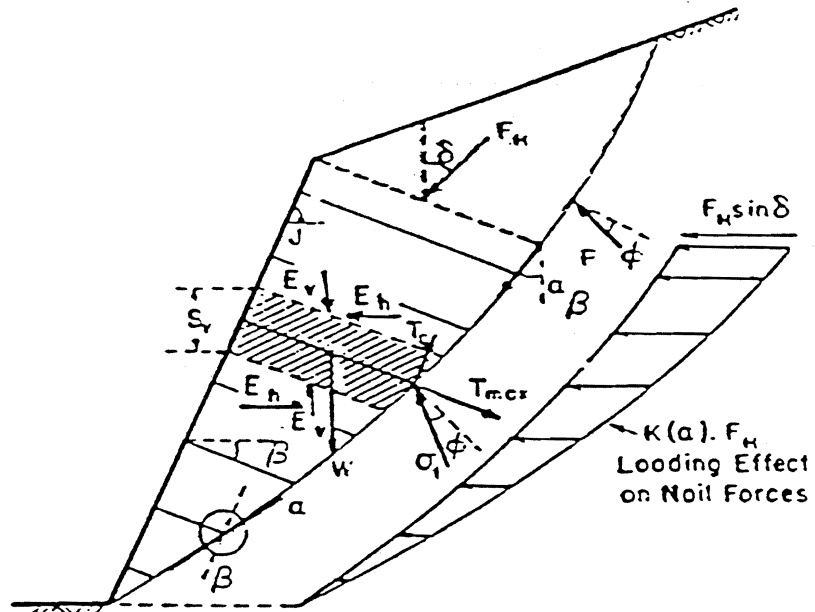
a) MECHANICS OF FAILURE AND DESIGN ASSUMPTIONS
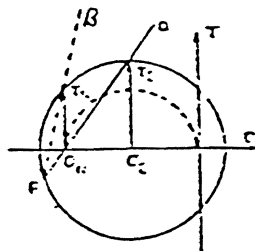
$$T_{max} = \sigma_N \cdot A_S ; \quad T_C = T_N \cdot A_S$$
$$A_S : \text{SECTION AREA OF NAIL}$$

b) STATE OF STRESS IN THE INCLUSION
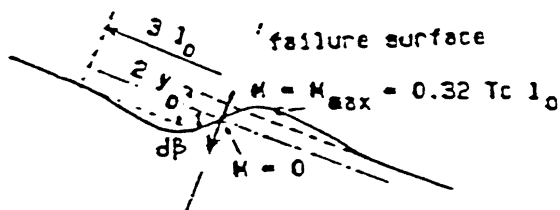
c) THEORETICAL SOLUTION FOR INFINETELY
LONG BAR ADOPTED FOR DESIGN PURPOSES

Figure 74.   Kinematical limit analysis approach.
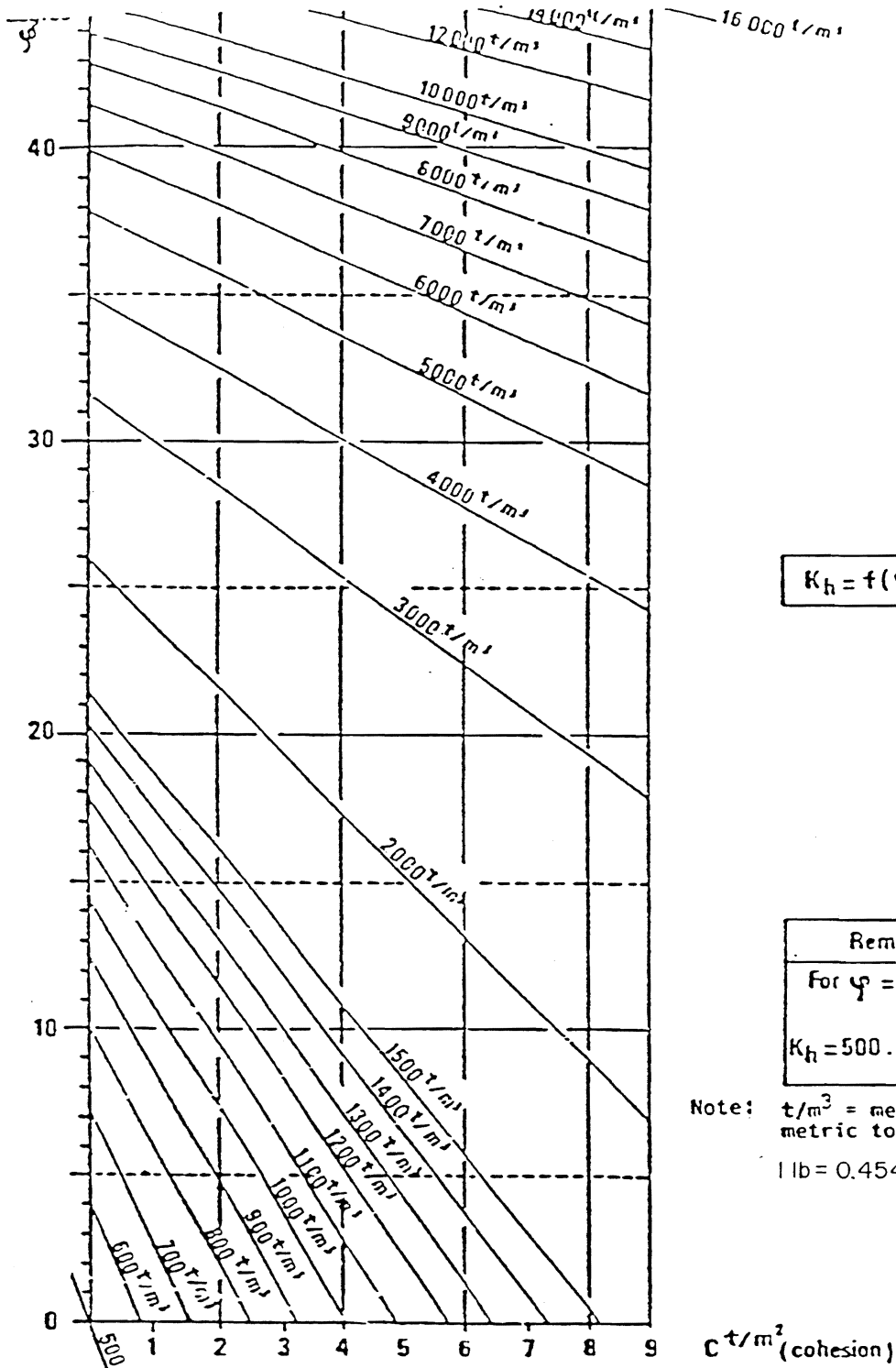
Figure 75. Horizontal subgrade reaction as a
function of the soil shear parameters.

138

A failure surface which verifies all the equilibrium conditions of the active zone can be defined. In order to establish the geometry of this failure surface it is necessary to determine its inclination a_o with respect to the upper ground surface. Observations on both full scale structures and laboratory model walls show that for the relatively flexible nails the failure surface is practically vertical at the upper part of the structure ($a_o = \phi$).[12, 36]

The normal soil stress along this failure surface is calculated using Kotter's equation. The maximum tension force (T_{max}) in each inclusion is calculated from the horizontal force equilibrium of the slice comprising the inclusion. Following the mobilization of shearing stress assumption, analysis of the state of stress in the inclusion yields the ratio of the mobilized shear T_c to tension T_{max} forces as a function of the inclination of the inclusion with respect to the failure surface.

Figure 71 shows a comparison between predicted and measured values of maximum tension forces in soil nailed retaining structures. It illustrates that the kinematical design approach provides a reasonable estimate of tension forces mobilized in the inclusions. Specifically, the results of the full scale experiment conducted in France on a 7m deep granular soil nailed wall (field data reported by reference 40) which are reported in figure 71c for several excavation depths, illustrate that the total excavation depth has only a negligible effect on both the normalized tension forces in the nails and the geometry of the active zone. Therefore, at any relative depth (Z/H) the maximum nail tension forces are approximately proportional to the total excavation depth. The predicted distribution of the maximum tension forces agrees fairly well with the earth pressure design diagrams proposed for braced excavations.

5.0 STABILITY ANALYSIS OF SOIL NAILED RETAINING STRUCTURES

The design of soil nailed retaining structures should verify:

. The local stability at the level of each inclusion.

. The global stability of the structure and the surrounding ground with respect to a rotational or translational failure along potential sliding surfaces.

a. Local stability analysis

At the level of each inclusion the design should satisfy the following internal failure criteria:

Pullout failure of the inclusion:

$$\frac{T_{max}}{\pi \cdot D \cdot l_a} < \frac{\tau_{ult}}{F_1} \qquad (33)$$

where: T_{max} is the maximum tensile force in the nail,

l_a is the adherence length, τ_{ult} is the maximum shear resistance at the soil-nail interface, and

F_1 is the safety factor with respect to pullout.

This design criteria implies that for a soil nailed cut slope, the structure geometry defined by the L/H ratio (where L is the total inclusion length) should verify at each reinforcement level:

$$\frac{L}{H} \geq \frac{S}{H} + F_1 \left[\frac{T_N}{\pi \cdot \mu}\right] \qquad (34)$$

where: $T_N = \dfrac{T_{max}}{\gamma \cdot S_h \cdot S_v}$

$\mu = \dfrac{\tau_{ult} \cdot D}{\gamma \cdot S_h \cdot S_v}$

S is the nail length in the active zone

Breakage failure of the inclusion:

For <u>flexible nails</u> which withstand only tension forces:

$$\frac{F_{all} \cdot A_s}{\gamma H \cdot S_v \cdot S_h} > T_N \qquad (35)$$

where: F_{all} and A_s are the allowable tension stress and cross-sectional area of the inclusion, respectively. For <u>rigid nails</u> which can withstand both tension and <u>shear forces</u>, considering Tresca's failure criterion:

$$\frac{F_{all} \cdot A_s}{\gamma H \cdot S_v \cdot S_h} > K_{eq} \qquad (36)$$

where: $K_{eq} = [T_N{}^2 + 4 \cdot T_s{}^2]^{1/2}$

$TS = \dfrac{T_c}{\gamma H \cdot S_h \cdot S_v}$

T_c is the maximum shear force in the inclusion,

Failure by excessive bending of a stiff inclusion:

$$M_p > F_m \cdot M_{max} \tag{37}$$

where: F_m is a factor of safety with respect to plastic bending (usually, $F_m = 1.5$),

M_p is the plastic bending moment of the nail; for a grouted nail, an equivalent plastic bending moment is calculated considering that the grout has a compressive strength f_y of 210 KN/m^2 (3,000 psi), and zero tension strength.

The bending moment M_{max} is derived from the "p - y" analysis:

$$M_{max} = 0.32 \, T_c \cdot L_o , \text{ hence:}$$

$$\frac{M_p \, / \, L_o}{\gamma \, H \cdot S_v \cdot S_h} > 0.32 \, FS_m \cdot T_s \tag{38}$$

Normal interaction between the soil and stiff inclusions: The normal interaction between the soil and relatively stiff inclusion results in a progressive mobilization of the passive lateral soil pressure on the inclusion, as illustrated schematically in figure 76. This soil-inclusion interaction is analyzed using the "p - y" analysis procedure outlined above. In order to prevent plastic flow (or creep) of the soil between the inclusions the maximum lateral soil pressure $p_{(lim)}$ should not exceed half of the ultimate lateral pressure of the characteristic "p - y" curve. In french practice, this lateral soil pressure is limited to the creep pressure obtained from a pressuremeter test. The shear force in the inclusion should therefore not exceed:

$$T_c = P_{(lim)} \cdot L_o \cdot D/2 \tag{39}$$

b.   Global stability analysis

This analysis consists of evaluating a global safety factor of the soil nailed retaining structure and the surrounding ground with respect to a rotational or translational failure along potential sliding surfaces. It requires determination of the critical sliding surface which may be dictated by the stratification of the subsurface soil or, in rock, by an existing system of joints and discontinuities. The potential sliding surface can be located inside or outside the soil nailed retaining structure.

Evaluation of the global safety factor is generally based on the rather conventional approach of limit equilibrium methods. Slope stability analysis procedures have been developed to account for the available limit pullout, tension, and shearing resistance of the inclusions crossing the potential sliding surfaces. The limit
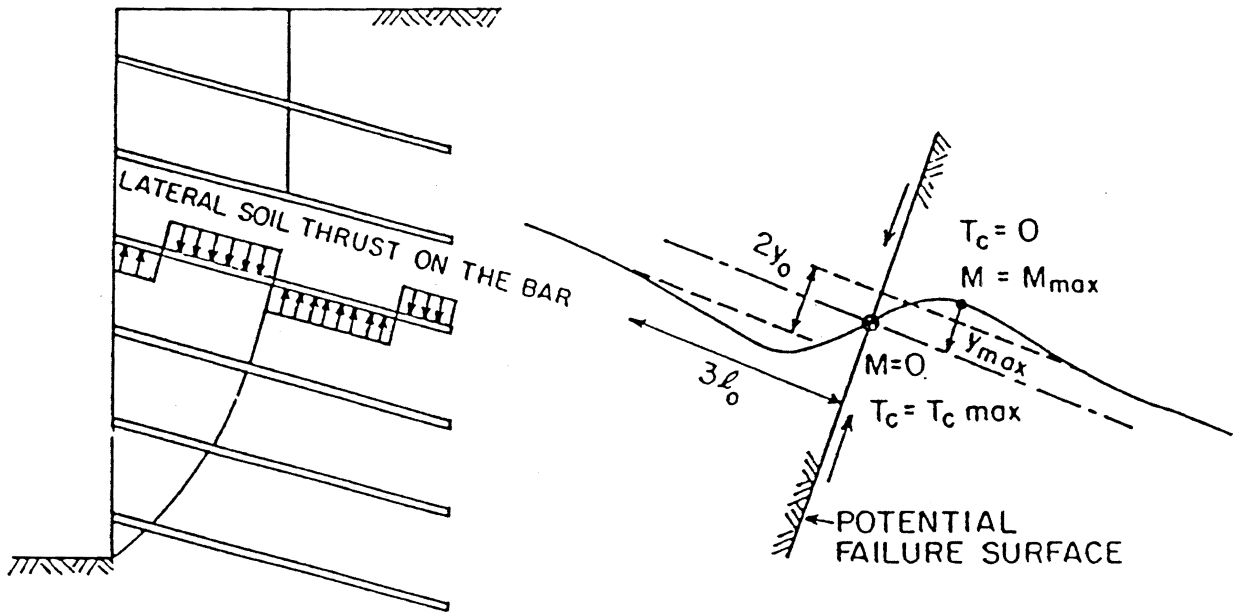
Figure 76. Bending of a rigid inclusion.

142

equilibrium methods commonly used involve different definitions of the safety factors, and a variety of assumptions with regard to the shape of the failure surface, the type of soil-inclusion interaction and the resisting forces in the inclusions.[11, 12, 46]

The German Method: Stocker and coworkers proposed a limit force equilibrium method (figure 77) considering a bilinear sliding surface and assuming that the nails withstand only tension forces.[46] The shearing resistance of the soil, as defined by Mohr - Coulomb's failure criterion, is assumed to be entirely mobilized along the potential failure surface. The global safety factor is defined as the ratio of the sum of the available resisting limit nail forces ΣT_p to the total force ΣT required to maintain limit equilibrium, that is:

$$FS = \Sigma T_p / \Sigma T \qquad\qquad (40)$$

As shown in figure 77, the total force ΣT required to maintain limit equilibrium is readily obtained considering the polygon of forces acting on the rigid soil wedge limited by the potential failure surface. The resisting forces T_p are provided by the pull-out capacity of the nails (i.e., the pullout capacity of the portion of the nail located beyond the potential failure surface). The inclination θ_B of the failure surface is iteratively determined to yield the minimum factor of safety. Gassler and Gudehus have shown through stability analyses that the minimum factor of safety is usually obtained for $\theta_A = [\pi/4 - \phi/2]$ assuming a vertical line at wedge A to be limited by the back of the reinforced soil mass.[38]

The assumed bilinear failure surface is mainly based on a limited number of model tests where failure was caused by substantial surcharge loading. However, it does not appear to be consistent with the observed behavior of nailed soil retaining structures which are subjected mainly to their self-weight. In particular, stability analyses show that this bilinear failure surface is generally not contained in the nailed soil mass and therefore yields an active zone (or potential failure wedge) which is substantially larger than that observed on actual structures.

The Davis Method: Shen et al developed a similar force equilibrium method (commonly called the Davis method).[11] They consider a parabolic failure surface passing either entirely or partially within the nailed soil mass and assume that the nails withstand only tension forces. Failure of the nailed soil system can be generated by either pullout or breakage of the nails or sliding of the soil along the failure surface. The assumed failure surface (figure 78b) is based on the contours of factor of safety derived from finite element simulations, as shown in figure 78b.
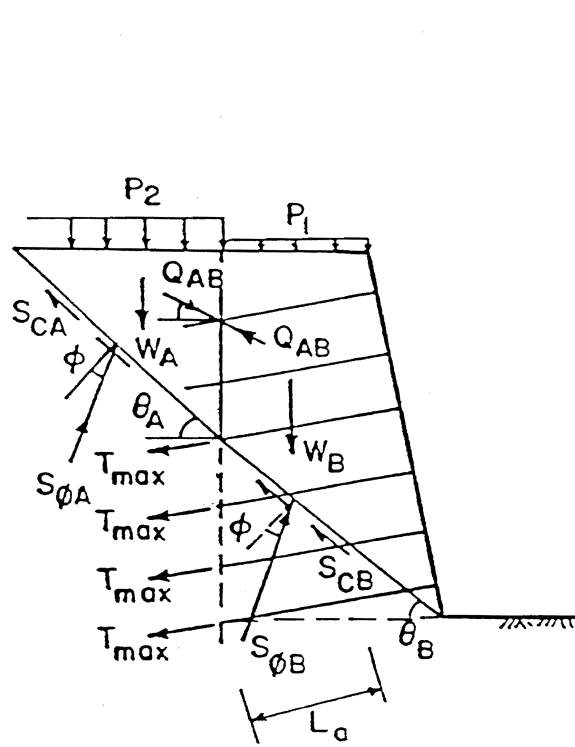
$$\theta_A = \left(\frac{\pi}{4} - \frac{\phi}{2} \right)$$
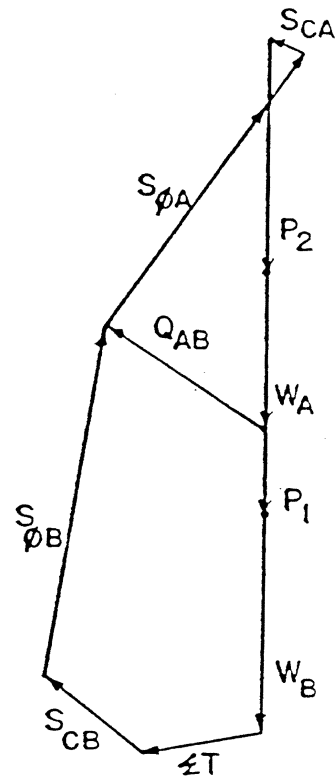
$$F.S. = \frac{\Sigma T_p}{\Sigma T}$$

$$T_p = \tau_{ult} \cdot \pi D \cdot L_a$$

Figure 77.   Force equilibrium method for global stability analysis of nailed soil retaining structure.[46]

144

a   Contours of factor of safety derived from finite
element analysis

$$F_c = \frac{c}{c_m} \quad , \quad F_\phi = \frac{\phi}{\phi_m} \quad , \quad F_L = \frac{Tp}{T} \quad , Tp = \tau_{ult} \pi.D.L_a$$
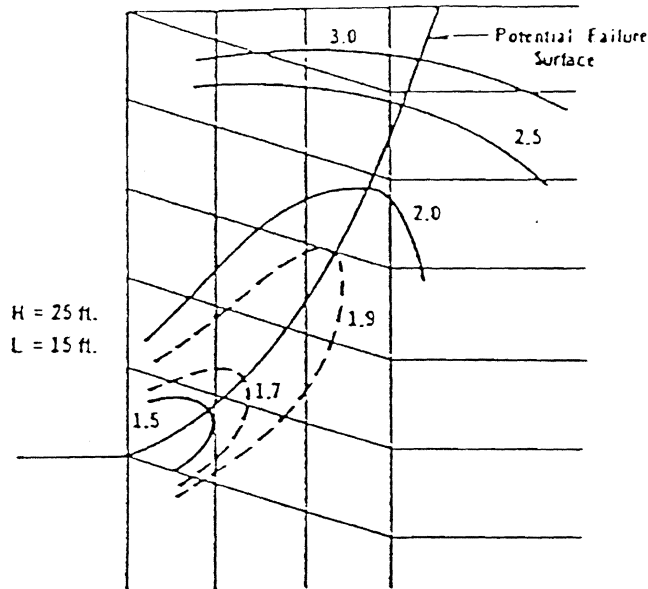
$$F_c = F_\phi = F_L = F_s$$
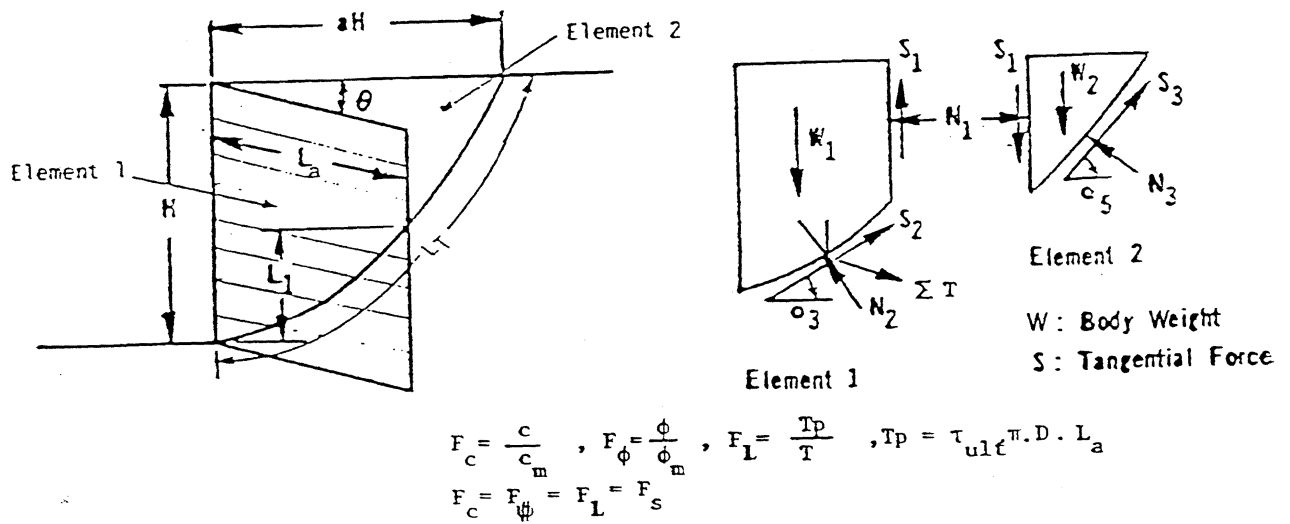
Figure 78.   Location of critical failure surface.[11]

In this analysis it is implicitly assumed that the safety factors with respect to the shear strength of the soil,

$$\text{i.e., } F_c = \frac{c}{c_m} \text{ and } F_\phi = \frac{\tan \phi}{\tan \phi_m} \tag{41}$$

(where c_m and ϕ_m are respectively the soil cohesion and internal friction angle actually mobilized along the critical potential failure surface) and the safety factor with respect to the ultimate interface lateral shear stress,

$$\text{i.e., } F_1 = \tau_{ult}/\tau_m \tag{42}$$

(where τ_m is the lateral shear stress actually mobilized at the soil-nail interfaces) are equal, and the global safety factor is defined as:

$$FS = F_c = F_\phi = F_1 \tag{43}$$

A minimum safety factor of 1.5 is generally required.

The lateral shear stress at the interfaces is calculated according to Mohr-Coulomb failure criterion:

$$\tau_{ult} = N \cdot \tan \phi_m = c_m \tag{44}$$

where N is the average normal stress along the adherence length L_a. This original formulation has been extended under FHWA soil nailing study to input interface limit lateral shear force per unit length of nail as obtained from pullout tests.[76]

A slope stability analysis procedure, using the method-of-slices, has been implemented to iteratively determine the critical sliding surface and the minimum factor of safety. To calculate the interslice forces a stress ratio parameter K (i.e., ratio of the lateral to the vertical stresses at the interslice) is input with K values of 0.4 for frictional soils and 0.5 for cohesive soils. Parametric sensitivity analyses have shown, however, that the safety factor is fairly insensitive to the K value.[76]

Shen et al have evaluated their design procedure through analysis of observed failure surfaces and failure heights of centrifugal soil nailed model walls. The method predictions were found to agree fairly well with the experimental results.[11]

The French Method: Common to all the limit equilibrium methods specified above is the assumption that the inclusions withstand only tension forces. A more general method for the stability analysis of nailed soil retaining structures, considering the two fundamental mechanisms of soil-inclusion interaction (i.e., lateral friction and passive normal soil reaction), has been developed by Schlosser.[12]

his method (commonly called the French method) takes into account both the tension and shearing resistance of the inclusions as well as the effect of their bending stiffness. For an inclusion that withstands both tension (T_{max}) and shear (T_c) forces, the mobilized limit forces are calculated according to the principle of maximum plastic work considering Tresca's failure criterium. The T_c/T_{max} ratio is a function of the inclination, a, of the inclusion with respect to the potential failure surface.

A multi-criteria analysis, illustrated in figure 79, is conducted to evaluate the global stability of the nailed soil system with respect to the four potential failure modes: shear failure of the soil along the critical sliding surface, pullout failure of the soil, nail breakage by either excessive bending or combined effect of tension and shear forces, and creep or plastic flow of the soil between the nails. The global factor of safety is defined by equation: $F_c = f_\phi = F_1 = FS$, and a minimum safety factor of 1.5 is generally required.

For design purpose, input data of interface limit lateral shear force per unit length of nail are obtained from pull-out tests. The tensile strength of the inclusion is defined as the elastic limit f_y and the shear resistance as $f_y/2$. The maximum shear force and bending moments that can be developed in the nail are governed by the soil-nail normal interaction. They are calculated using a conventional "p - y" analysis procedure, simulating the relatively flexible nail by a laterally loaded, infinitely long pile, and are given, respectively, by equations 39 and 38.

This multi-criteria analysis procedure uses a classical slices method (e.g. Bishop's modified method or Fellinius's method) which is modified to take into account the effect of resisting nail forces on the equilibrium of each slice. This analysis procedure which is significantly more elaborated and comprehensive than those outlined above, permits an evaluation of the effect of soil stratification, ground water flow, and seismic loading on the global structure stability. It can also be effectively used for the design of mixed structures combining ground anchor and soil nail systems. Post failure analyses of several nailed soil retaining structures have illustrated that with an appropriate input design value of the ultimate lateral shear stress this design procedure could predict fairly well the pullout failure of the structures.[39]

c. Evaluation of global stability analysis procedures

The Davis and the French design procedures have been evaluated through the analysis of the field data reported in figure 71 which were obtained on four full scale structures.[39] Figure 80 shows that the observed locus of the maximum tension forces in these structures agree fairly well with predicted locations of the potential failure surface.

FORCES IN THE BAR
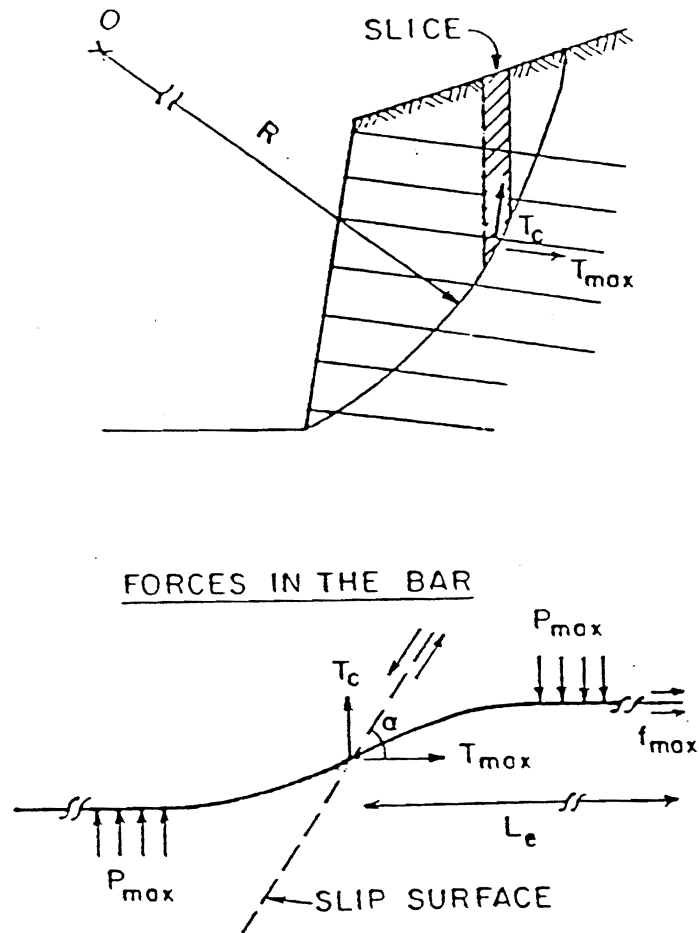
FAILURE CRITERIA

Shear resistance of the bar $T_{max} \leqslant A_s \cdot f_y$, $T_c \leqslant R_c = A_s \cdot f_y/2$

Soil bar friction $T_{max} \leqslant \pi D \tau_{ult} L_a$

Normal Lateral Earth Thrust on the bar $p \leqslant p_{max}$

Shear resistance of the soil $\tau < c + \sigma \tan \phi$

Figure 79.   Multicriteria slope stability analysis method.[12]
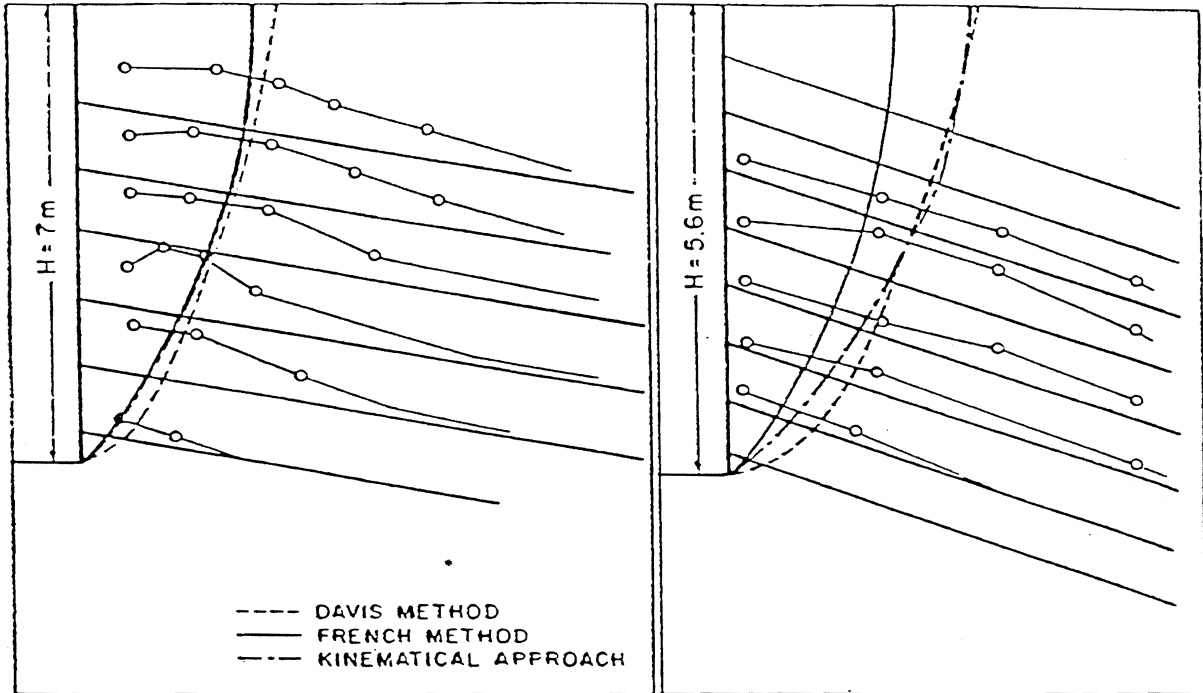
a. FULL SCALE EXPERIMENT CEBTP
(Experimental Results, Plumelle, 1986)

b. PARISIAN WALL
(Experimental Results, Cortier
and Gigon, 1983)

Figure 80. Predicted and observed locus of maximum
tension forces in nails.

The stability analyses of these structures were conducted using the measured tension forces as yield forces of the inclusions and assuming a pullout resistance large enough to prevent any sliding of the inclusion (with $F_1 > 1.5$). This procedure yields, for the mobilized nail forces, the actual value of the safety factor with respect to the shear strength of the soil ($F_c = F_t$). The results of these analyses illustrate that in soil nailed cut slopes the factors of safety with respect to soil strength are generally close to one. Specifically, the safety factors obtained using the Davis method for most of these structures were within the range of 1 ± 10 percent. The Davis method generally yielded safety factor values which were about 15% lower than those predicted using the French method.

It can be concluded, that in soil nailed retaining structures, as well as in braced excavations, due to the staged construction process, the soil resistance to shearing along the potential failure surface is practically mobilized at the early stages of excavation. As the excavation proceeds, the load increments are being entirely transferred to the inclusions. Therefore, for the design of these structures it appears more consistent to assign a safety factor of one with respect to the shear resistance of the soil along potential failure surfaces passing inside the soil nailed system. The global factor of safety of the system, as defined by Stocker et al. (eq. 40), is evaluated with respect to the pullout resistance of the inclusions. Considering this definition of the global safety factor a minimum safety factor of 2 is recommended. Gassler and Gudehus recommend for nailed soil structures the use of residual soil strength parameters factored by 1.25 to comply with statistical evaluation criteria concerning the probability of failure.[38]

The major limitation of the slope stability analysis procedures currently used in design of soil nailed retaining structures lies in the basic definition of a global factor of safety. Observations on both full scale structures and reduced scale laboratory models have illustrated that pullout failure is a progressive phenomenon which is generally induced by the sliding of the upper inclusions. Therefore, this internal failure mechanism cannot be adequately defined using a "global" value of a unique safety factor for all the inclusions. The local stability at the level of the sliding inclusion can be significantly more critical than the estimated "global" stability with respect to general sliding in the retaining system or the surrounding ground.

The main conclusion that can be drawn for a reliable design of these composite nailed – soil systems is that, consistently with most reinforced soil structures, the design engineer should attempt to evaluate both the local stability at the level of each inclusion and the "global" stability of the structure.

REFERENCES

1. AASHTO, "Standard Specifications for Highway Bridges", 13th ed., American Association of State Highway and Transportation Officials, Washington, D.C., 1983.

2. Mitchell, J.K. and Villet, W.C.B., "Reinforcement of Earth Slopes and Embankments", NCHRP Report No. 290, Transportation Research Board, Washington, D.C., 1987.

3. Devata, M.S., "Geogrid Reinforced Embankments with Steep Slopes," Proc. of Conf. on Polymeric Grid Reinforcement, Sponsored by the Science and Engineering Research Council, p82, Telford, London, March, 1984.

4. The Reinforced Earth Company, Arlington, Virginia promotional publication, 1988.

5. Enka Systems, promotional publication.

6. Chang, J.C., Beaton, J.L., and Forsyth, R.A. "Design and Field Behavior of the Reinforced Earth Embankment − California Highway 39" presented at the Jan. 21-25, 1974 ASCE National Water Resources Engineering Meeting, Los Angeles, California, 1974.

7. Jewell, R.A., "Material Requirements for Geotextiles and Geogrids in Reinforced Slope Applications", Proc. 23rd Int. Man−Made Fibres Congress, Dornbirn, Austria, Sept., 1984.

8. Hueckel, S.M. and Kwasniewski, J., "Scale Model Tests on the Anchorage Values of Various Elements Buried in Sand," Proc. 5th International Conference on Soil Mechanics and Foundation Engineering, Paris, 1961.

9. Schlosser, F., Juran, I. and Jacobsen, H.M., "Soil Reinforcement" General Report, 8th European Conf. on Soil Mechanics and Foundation Engineering, Helsinki, 1983.

10. Phan, T.L., Segrestine, P., Schlosser, F., and Long, N.T., "Stability Analysis of Reinforced Earth Walls by Two Slip Circle Methods", Proc. Int. Conf. on Soil Reinforcement, pp 119-123, Paris, 1979.

11. Shen, C.K., Bang, S., Romstad, J.M., Kulchin, L. and Denatale, J.S., "Field Measurements of an Earth Support System", J. Geot. Eng. Div., Vol. 107, GT12, ASCE, 1981.

12. Schlosser, F., "Analogies et Differences Dans le Comportement et le Calcul des Ouvrages de Soutennement en Terre Armee et par Clouge du Sol", Annals de L'Institut Technique du Batiment et des Travaux Publics, No. 418, 1983.

13. DiMaggio, J., "Mechanically Stabilized Earth: Walls and Slopes", Report to Federal Highway Administration, Washington, D.C., 1988.

14. Weatherby, D.E., "Tiebacks", Report No. FHWA/RD-82/047, Federal Highway Administration, Washington, D.C., 1982

15. Elias, V., and Juran, I., "Soil Nailing", Report to Federal Highway Administration, Washington, D.C., 1988.

16. Bastick, M., Schlosser, F., Amar, S., and Canepa, Y., "Monitoring of a Prototype Reinforced Earth Wall with Short Strips," to be published in the Proc. of the 12th ICSMFE, Rio de Janeiro, 1989.

17. Terre Armee Internationale, Finite Element Study of Reinforced Earth Structures, Rosalie, Internal Report, 1983.

18. Meyerhof, G.G., "The Bearing Capacity of Foundations Under Eccentric and Inclined Loads", Proc. 3rd Int. Conf. on Soil Mechanics and Foundation Engineering, pp 440-445, Zurich, Switzerland, 1953.

19. Segrestin, P., Bastic, M.J., Seismic Design of Reinforced Earth Retaining Walls: The Contribution of Finite Element Analysis," Proc. of the Int. Symp. on Theory and Practice of Earth Reinforcement, Kyushu, Japan, Oct, 1988.

20. Seed, H.B., and Mitchell, J.K., "Earthquake Resistant Design of Reinforced Earth Walls", Internal Study for the Reinforced Earth Company, Progess Report, Berkeley, California, 1981.

21. Seed, H.B. and Whitman, R.V., "Design of Earth Retaining Structures for Dynamic Loads", Proc. of the ASCE Specialty Conf., Lateral Stresses and Earth Retaining Structures, Cornell University, pp 103-147, Ithaca, NY, June, 1970.

22. Christopher, B.R., Unpublished, STS Consultants, Ltd. Report on Task C Field Test Wall Construction - Prepared for FHWA, Washington, D.C., Contract No. DTFH61-84-C-00073, "Behavior of Reinforced Soil", 1987.

23. Wichter, L., Risseeuw, P., and Gay, G., "Large Scale Tests on the Bearing Behavior of Woven Reinforced Earth Wall", Proc. of the 3rd Int. Conf. on Geotextiles, Vol. IV, pp 1073-1078, Vienna, Austria, 1986.

24. Christopher, B.R., and Holtz, R.D., "Geotextile Design and Construction Guidelines Manual," Prepared for FHWA National Highway Institute, Under Contract to GeoServices, Inc. Contract No. DTFH61-86-R-00102, 1988.

25. Christopher, B.R. and Holtz, R.D., Geotextile Engineering Manual, STS Consultants, Ltd., Report to Federal Highway Administration, No. FHWA-TS-86/203, pp 1044, Northbrook, Illinois, 1985.

26. Schmertmann, G.R., Chouery-Curtis, V.E., Johnson, R.D., and Bonaparte, R., "Design Charts for Geogrid -Reinforced Soil Slopes", Proc. Geosynthetics, Vol. 1, pp 108-120, New Orleans, 1987.

27. Cheney, R.S., and Chassie, R.G., "Soils and Foundation Workshop Manual", FHWA, Washington, D.C., 1982.

28. Fukuoka, M., "Fabric Retaining Walls", Proc. 2nd Int. Conf. on Geotextiles, pp 575-580, Las Vegas, 1982.

29. Juran, I., Schlosser, F., Legeay, G., and Long, N.T., "Experimentation en Vraid Grandeur sur un mur Soumis a des Surcharges en Tete a Dunkerque", Proc. Int. Conf. on Soil Reinforcement: Reinforced Earth and Other Techniques, Vol II, Paris, 1979.

30. Murray, R.T., "Studies of the Behavior of Reinforced and Anchored Earth", Ph.D. Thesis, Hariot-Watt University, Edinburgh, 1983.

31. Juran, I., "Behavior of Reinforced Soil Structures", Partial Report No.2, FHWA Contract No. 61-84-C-00078, 1985.

32. Winkler, E., "Die Lehre von Elastizitat und Festigkeit:, Prague, 1867.

33. Cheney, R.S., "Permanent Ground Anchors," Federal Highway Administration Report No. FHWA-DP-68-1R, November, 1984.

34. Jewell, R.A., Milligan, G.W., Sarsby, R.W., and Dubois, D., "Interaction Between Soil and Geogrids", Proc. Symp. on Polymer Grid Reinforcement in Civil Engineering, Science and Engineering Research Council and Netlon, Ltd., March, 1984.

35. Gouvenot, D., and Bustamante, M.G., "Mesures In-situ Sur Les Ouvrages Maritimes de Soutenement", Report, Annales de L'Institut Technique du Batiment et des Travaux Publique, Sept, 1979.

36. Juran, I., Beech, J., and Delaure, E., "Experimental Study of the Behavior of Nailed Soil Retaining Structures on Reduced Scale Models," Proc., Int. Symp. on In-situ Soil and Rock Reinforcements, Paris, 1984.

37. Cartier, G., and Gigan, J.P., "Experiments and Observations on Soil Nailing Structures," Proc., Seventh Conf. of the ECSMFE, Helsinki, Finald, 1983.

38. Gassler, G., and Gudehus, G., "Soil Nailing: Some Mechanical Aspects of In-situ Reinforced Earth," Proc., 10th ICSMFE, Vol. 3, pp 665-670, Stockholm, Sweden, 1981.

39. Juran, I., and Elias, V., "Soil Nailed Retaining Structures: Analysis of Case Histories", ASCE, Special Geotechnical Publication No. 12, pp 232-245, 1987.

40. Plumelle, C., "Experimentation en Vraie Grandeur d'une Paroi Clouee," Revue Francaise de Geotechnique, No. 40, pp 45-50, 1987.

41. Juran, I., Beech, J., "Analyze Theorique du Comportement d'un Soutenement en Sol Cloue", Proc. Int. Conf. on In-situ Reinforcement of Soils and Rocks, pp 301-307, Paris, 1984.

42. Juran, I., Baudrand, G., Farrag, F, and Elias, V., "Kinematical Limit Analysis Approach for the Design of Nailed Soil Retaining Structures," Proc. Int. Geotechnical Symp. on Theory and Practice of Earth Reinforcement, Fukuoka Kyushu, Japan, 1988.

43. Terzaghi, K., "Theoretical Soil Mechanics", John Wiley & Sons, Inc., New York, 1943.

44. Terzaghi, K., and Peck, R.B., "Soil Mechanics in Engineering Practice," John Wiley & Sons, Inc., New York, 1948 and 1967.

45. Tschebotarioff, G.P., "Foundations, Retaining and Earth Structures", McGraw-Hill Book Company, 1951.

46. Stocker, M.F., Korber, G.W., Gassler, G., and Gudehus, G., "Soil Nailing", Proc. Int. Conf. on Soil Reinforcement, Vol. 2, pp 469-474, Paris, 1979.

47. Steward, J.E. and Mohney, J., "Trial Use, Results and Experience Using Geotextiles for Low-Volume Forest Roads," Proc., 2nd Int. Conf. on Geotextiles, Vol. 2 pp 335-340, Las Vegas, Nevada, August 1982.

48. Yako, M.A., and Christopher, B.R., "Polymerically Reinforced Retaining Walls and Slopes in North America", The Application of Polymeric Reinforcement in Soil Retaining Structures, P.M. Jarrett and A. McGown, eds. pp 239-282, 1987.

49. Dunnicliff, J., and Green, G.E., "Geotechnical Instrumentation for Monitoring Field Performance," J. Wiley & Sons, New York, 1988.

50. Bell, J.R., and Steward, J.E., "Construction and Observations of Fabric Retained Soil Walls," Proc. Int. Conf. on the Use of Fabrics in Geotechnics, Vol. 1, pp 123-128, Paris, France, April, 1977.

51. Mohney, J., "Fabric Retaining Wall, Olympic National Forest," Highway Focus, Federal Highway Administration, Vol. 9. No. 1, pp 88-103, May, 1977.

52. Chassie, R.G., "Geotextile Retaining Walls, Some Case History Examples," prepared for presentation at the NW Roads and Streets Conf., Corvallis, Oregon, February, 1984.

53. Al-Hussaini, M.M., "Field Experiment of Fabric Reinforced Earth Wall," Proc. Int. Conf. on the Use of Fabrics in Geotechnics, Vol. 1, pp 119-121, April, 1977.

54. Al-Hussaini, M.M., and Perry, E.B., "Effect of Horizontal Reinforcement on Stability of Earth Masses, "Technical Report No. S-76-11, U.S. Army Engineer Waterways Experiment Station, Vicksburg, Mississippi, 1976.

55. Douglas, E.G., "Design and Construction of Fabric Reinforced Retaining Walls by New York State," Transporation Research Board, Transportation Research Record 872, pp 32-37, Washington, D.C., 1982.

56. Bell, J.R., Barrett, R.K. and Ruckman, A.C., "Geotextile Earth-Reinforced Retaining Wall Tests: Glenwood Canyon, Colorado," Transportation Research Board, Transportation Research Record 916, pp 59-69, Washington, D.C., 1983.

57. Barrett, R.K., "Geotextiles in Earth Reinforcement," Geotechnical Fabrics Report, pp 15-19, March/April, 1985.

58. Forsyth, R.A. and Bieber, D.A., "La Honda Slope Repair with Geogrid Reinforcement," Proc. of the Symp. on Grid Reinforcement in Civil Eng., Paper No. 2.2, London, U.K., 1984.

59. Berg, R.R., LaRochelle, P., Bonapart, R., and Tanguay, L., "Gaspe' Peninsula Reinforced Soil Seawall Case History," Proc. ASCE Symp. on Soil Improvement, Atlantic City, New Jersey, April, 1987.

60. Anderson, R.P., "Soil Reinforcement Objective: Polymer Geogrid Replaces Galvanized Metal Strips in Concrete-Faced Retaining Walls," Geotechnical Fabrics Report, January/February, 1986.

61. Scott, J.D., et al, "Design of the Devon Geogrid Test Fill," Proc. Geosynthetics '87 Conf. New Orleans, Louisiana, February, 1987.

62. Jaber, M., "Behavior of Reinforced Soil Walls in Centrifuge Model Tests", Dissertation submitted in partial satisfaction of the requirements for the degree of Doctor of Philosophy, University of California, Berkeley, Department of Civil Engineering, March, 1989.

63. Alimi, Bacot, J., Lareal, P., Long, N.T., and Schlosser, F., "Etude de l'Adherence Sols-armatures," Proc. 9th Int. Conf. on Soil Mechanics and Foundation Engineering, Vol. I, pp 11-14, Tokyo, 1977.

64. ASTM, "Soil and Rock; Building Stones," Annual Book of ASTM Standards, Section 4, Vol. 04.08, American Society for Testing and Materials, Philadelphia, PA, 1988.

65. Rowe, R.K., and Davis, E.H., "The Behavior of Anchor Plates in Sand," Geotechnique 32, No. 1, pp 25-41, 1982.

66. Bloomfield, R.A. "Proposed Design Modifications - VSL Retaining Earth," VSL Corporation, January, 1984.

67. Nielsen, M.R., "Pullout Resistance of Welded Wire Mats Embedded in Soil", Masters Thesis, Utah State University, Logan, UT, 1983.

68. Murray, R.T., "Studies of the Behavior of Reinforced and Anchored Earth," Ph.D. Thesis, Heriot-Watt University, Edinburgh, 1983.

69. Jewell, R.A., "Some Effects of Reinforcement on the Mechanical Behavior of Soils," Ph.D. Thesis, University of Cambridge, 1980.

70. Juran, I., and Chen, Ch.L., "Soil-Geotextile Pullout Interaction Properties: Testing and Interpretation", Transportation Research Board, 67th Annual Meeting, Paper No. 87-0159, 1988.

71. Littlejohn, G.S. and Bruce, D.A., "Rock Anchors State-of-the-Art," Part I: Design and Part II: Construction, Ground Engineering, May, 1975.

72. Peck, R.B., "A Study of the Comparative Behavior of Friction Piles", Highway Research Board Special Report No. 36, p 72, 1958.

73. Woodward, R.J., Lundgren, R., and Boitono, J.D., "Pile Loading Tests in Stiff Clays", Proc., 5th ICSMFE, Vol. 2, pp 177-184, 1961.

74. Louis, C., "Theory and Practice in Soil Nailing Temporary or Permanent Works," ASCE Annual Conference, Boston, Oct., 1986.

75. Louis, C., "Nouvelle Methode de Soutennement des Sols en Deblais," Revue Travaux No. 533, 1981.

76. Elias, V., and Juran, I., Draft Manual of Practice for Soil Nailing, Prepared for U.S. Department of Transportation, FHWA, Contract DTFH-61-85-C-00142, May, 1988.

77. LCPC-SETRA, "Reglis de Justification des Foundations err Pioux", 1985.

78. Singh, A., and Mitchell, J.K., "General Stress-Strain-Timi Function for Soils", 1968, J. SMFD., ASCE, Vol. 94, SMI, pp 21-46.

79. Bustamante, M., "Capacite de' Ancrage et Comportement des Tirants Injectes, Scelles dans une Angile Plastique," These' Docteur-Ingenieur ENPC, Paris.

80. Wilding, M.A. and Ward, I.M., "Tensile Creep and Recovery in Ultrahigh Modulus Linear Polyethylene", J. Polymer, 19, pp 969-976, 1978.

81. McGown, A., Andrawes, K.Z., and Kabir, M.H., "Load-Extention Testing of Geotextiles Confined in Soil", Proc. Second International Conference in Geotextiles, Vol. 3, pp 793-798, Las Vegas, Nevada, 1982.

82. John, N., Johnson, P., Ritson, R., Petley, D., "Behavior of Fabric Reinforced Soil Walls, Proceedings of the Second International Conference on Geotextiles, Las Vegas, Nevada, IFAI, St. Paul, MN, 1982.

83. Jarrett, P.M. and McGown, A., "The Application of Polymeric Reinforcement in Soil Retaining Structures," Proc. NATO Advanced Research Workshop, Kluwer Academic Publishers, Kingston, Ontario, Canada, 1987.

84. Adib, Mazen, E., "Internal Lateral Earth Pressure in Earth Walls", Dissertation Submitted in Partial Satisfaction of the Requirements of the Degree of Doctor of Philosophy, Department of Civil Engineering, University of California, Berkeley, 1988. Note: This research was supported primarily by the Institute for Transportation Studies, University of California, 1988.

85. Schmertmann, G., Chew, S.H., Mitchell, J., "Finite Element Modeling of Reinforced Soil Wall Behavior," Geotechnical Engineering Report No. UCB/GT/89-01, University of California, Berkeley, September, 1989.

86. Bastick, M., Schlosser, F., Amar, S., and Canepa, Y., "Instrumentation d'un Mur Experimental en Terre Armee a Armatures Courtes", Proc. 12th ICSMFE, 1988. To be published.
157

87. Bastick, M., and Schlosser, F., "Comportement et Dimensionnement Dynamique des Ouvrages en Terre Armee, ler Coll. Nat. de Genie Parasismique, Saint-Remy-les-Chevreuse France, January, 1986.

88. Tomlinson, M.J., "The Adhesion of Piles Driven in Clay Soils", Proc., 4th ICSMFE, Vol. 2, pp 61-71, 1957.

89. Ward, I.M., "The Orientatin of Polymers to Produce High Performance Materials," Proc. Symp. on Polymer Performance in Civil Engineering, London, 1984.

90. Juran, I., Shafiee, S., and Schlosser, F., "Numerical Study of Nailed Soil Retaining Structures," Proc., 11th ICSMFE, Vol. 4, pp 1713-1717, San Francisco, 1985.

91. Shafiee, S., "Simulation Numerique du Comportement des Sols Cloues: Interaction Sol-Renforcement et Comportement de L'ouvrage", Ph.D. Diss, ENPC, Paris, 1986.

92. Frank, R., Guenot, A., and Humbert, P., "Numerical Analysis of Contact in Geomechanics," Proc., 4th Int. Conf. on Numerical Methods in Geomechanics, Edmonton, 1982.

93. Zaman, M.M., Desai, C.S., and Brumm, E.C., "Interface Model for Dynamic Soil-Structure Interaction", Journal of Geotechnical Engineer Division, ASCE, Vol. 110, SM9, pp 1257-1273, September, 1984.